

FCC-ee Conceptual Machine Design - CDR Plan and Status

May 29, 2017 @ FCC Week 2017

K. Oide (KEK) for FCC-ee collaboration

Contributed by M. Aiba, A. Apyan, S. Aumon, E. Belli, M. Benedikt, A. Blondel, A. Bogomyagkov, M. Boscolo, O. Brunner, H. Burkhardt, D. El-Khechen, E. Gianfelice-Wendt, B. Goddard, B. Harer, B. Holzer, P. Janot, R. Kersevan, M. Koratzinos, E. Levichev, M. Migliorati, A. Milanese, A. Novokhatski, S. Ogur, K. Ohmi, G. Rumolo, D. Shatilov, P. Piminov, J. Seeman, S. Sinyatkin, H. Sugimoto, M. Sullivan, T. Tydecks, P. Vobly, J. Wenninger, D. Zhou, F. Zimmermann, M. Zobov

Special thanks to A. S. Langner and D. Schulte

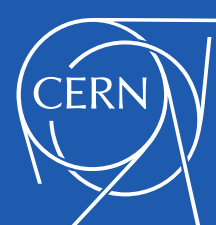
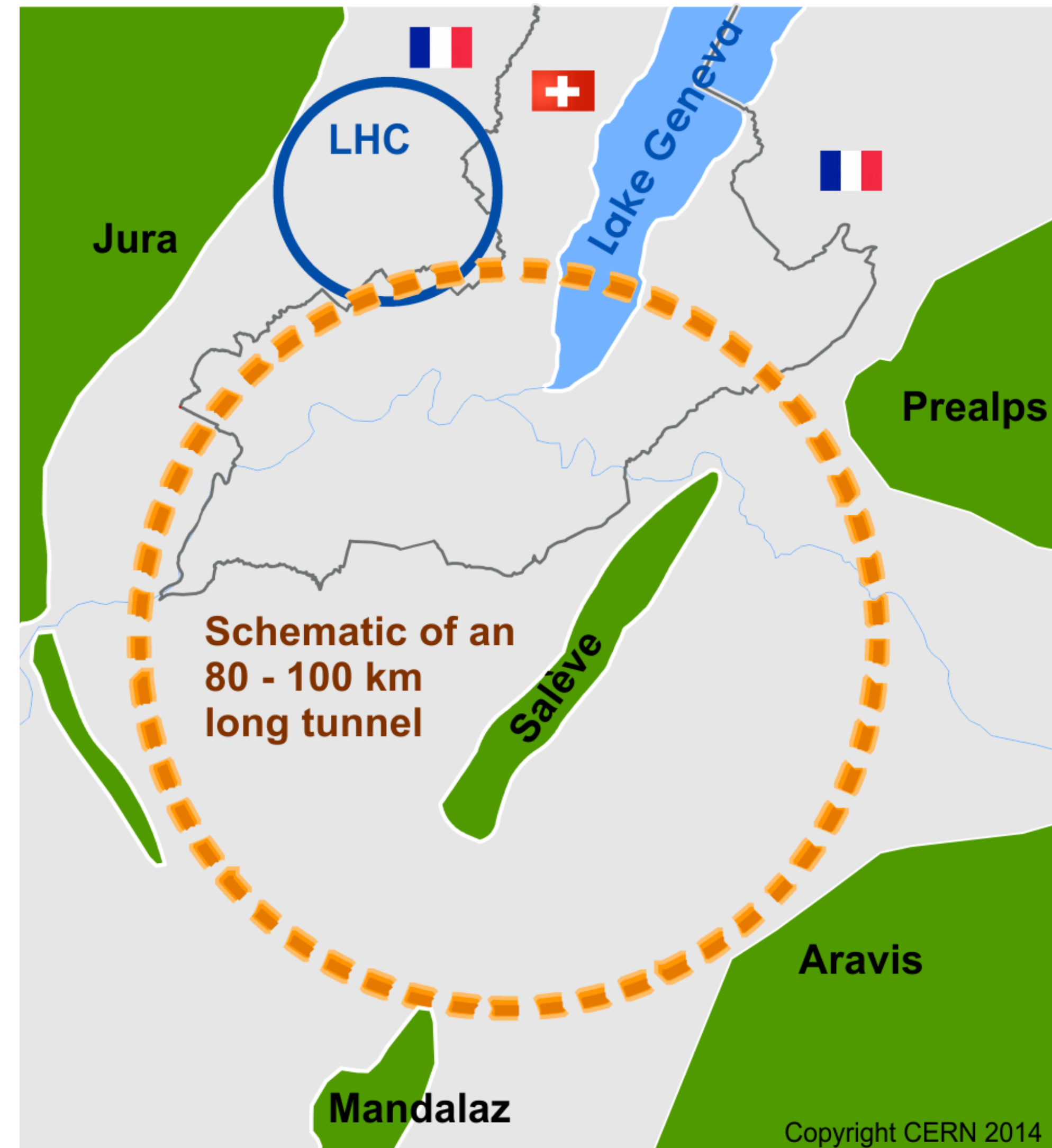
Work supported by the European Commission under Capacities 7th Framework Programme project EuCARD--2, grant agreement 312453, and under the Horizon 2020 Programme project CREMLIN, grant agreement 654166.

Future Circular Collider Study

GOAL: CDR and cost review for the next ESU (2018)

International FCC collaboration (CERN as host lab) to study:

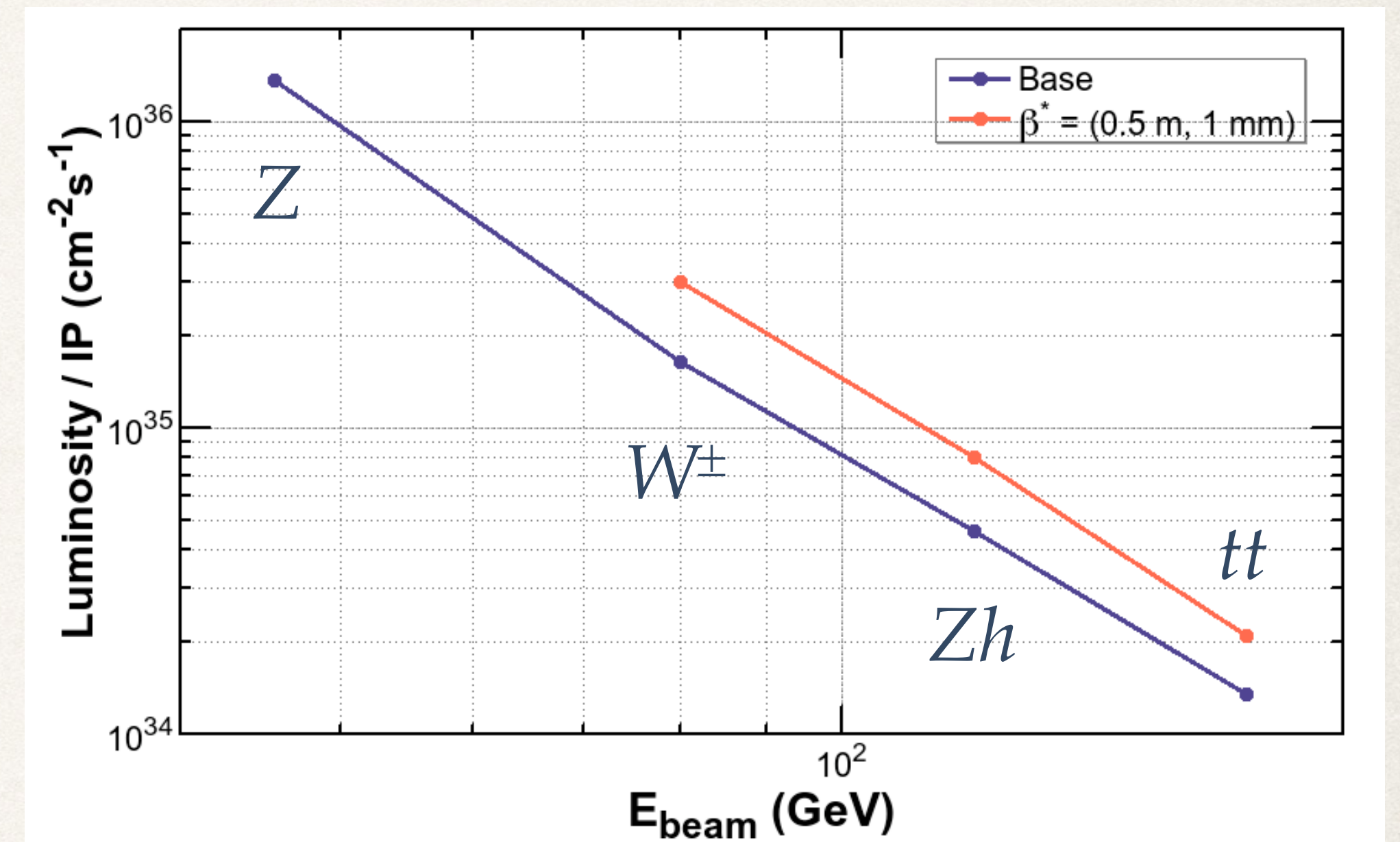
- *pp*-collider (*FCC-hh*)
→ main emphasis, defining infrastructure requirements
- ~ 16 T \Rightarrow 100 TeV *pp* in 100 km
- **80-100 km infrastructure in Geneva area**
- **e^+e^- collider (*FCC-ee*) as potential intermediate step / as a possible first step**
- *p-e* (*FCC-he*) option, HE-LHC ...



Parameters 2017 (Preliminary)



Design	2017			
Circumference [km]	97.750			
Arc quadrupole scheme	twin aperture			
Bend. rad. of arc dipoles [km]	10.747			
Number of IPs / ring	2			
Crossing angle at IP [mrad]	30			
Solenoid field at IP [T]	± 2			
ℓ^* [m]	2.2			
Local chrom. correction	<i>y</i> -plane with crab-sext. effect			
RF frequency [MHz]	400			
Total SR power [MW]	100			
Beam energy [GeV]	45.6	80	120	175
SR energy loss/turn [GeV]	0.036	0.34	1.72	7.80
Long. damping time [ms]	414	76.8	22.9	7.49
Current/beam [mA]	1390	147	29.0	6.4
Bunches/ring	70760	7280 (4540)	826 (614)	64 (50)
Particles/bunch [10^{10}]	4.0	4.1 (6.6)	7.1 (9.6)	20.4 (26.0)
Arc cell	60°/60°		90°/90°	
Mom. compaction α_p [10^{-6}]	14.79		7.31	
β -tron tunes ν_x / ν_y	269.14 / 267.22		389.08 / 389.18	
Arc sext. families	208		292	
Horizontal emittance ε_x [nm]	0.267	0.28	0.63	1.34
$\varepsilon_y/\varepsilon_x$ at collision [%]	0.38	0.36	0.2	0.2
β_x^* / β_y^* [m / mm]	0.15 / 1		1 / 2 (0.5 / 1)	
Energy spread by SR [%]	0.038	0.066	0.099	0.147
Energy spread SR+BS [%]	0.073	0.072 (0.091)	0.106 (0.122)	0.193 (0.212)
Hor. beam-beam ξ_x	0.008	0.080 (0.046)	0.081 (0.053)	0.082 (0.049)
Ver. beam-beam ξ_y	0.106	0.141 (0.141)	0.140 (0.140)	0.140 (0.138)
RF Voltage [MV]	255	696	2620	9500
Bunch length by SR [mm]	2.1	2.1	2.0	2.4
Bunch length SR+BS [mm]	4.1	2.3 (2.9)	2.2 (2.5)	2.9 (3.5)
Synchrotron tune ν_z	-0.0413	-0.0340	-0.0499	-0.0684
RF bucket height [%]	3.8	3.7	2.2	10.3
Luminosity/IP [$10^{34}/\text{cm}^2\text{s}$]	137	16.4 (30.0)	4.6 (8.0)	1.35 (2.09)

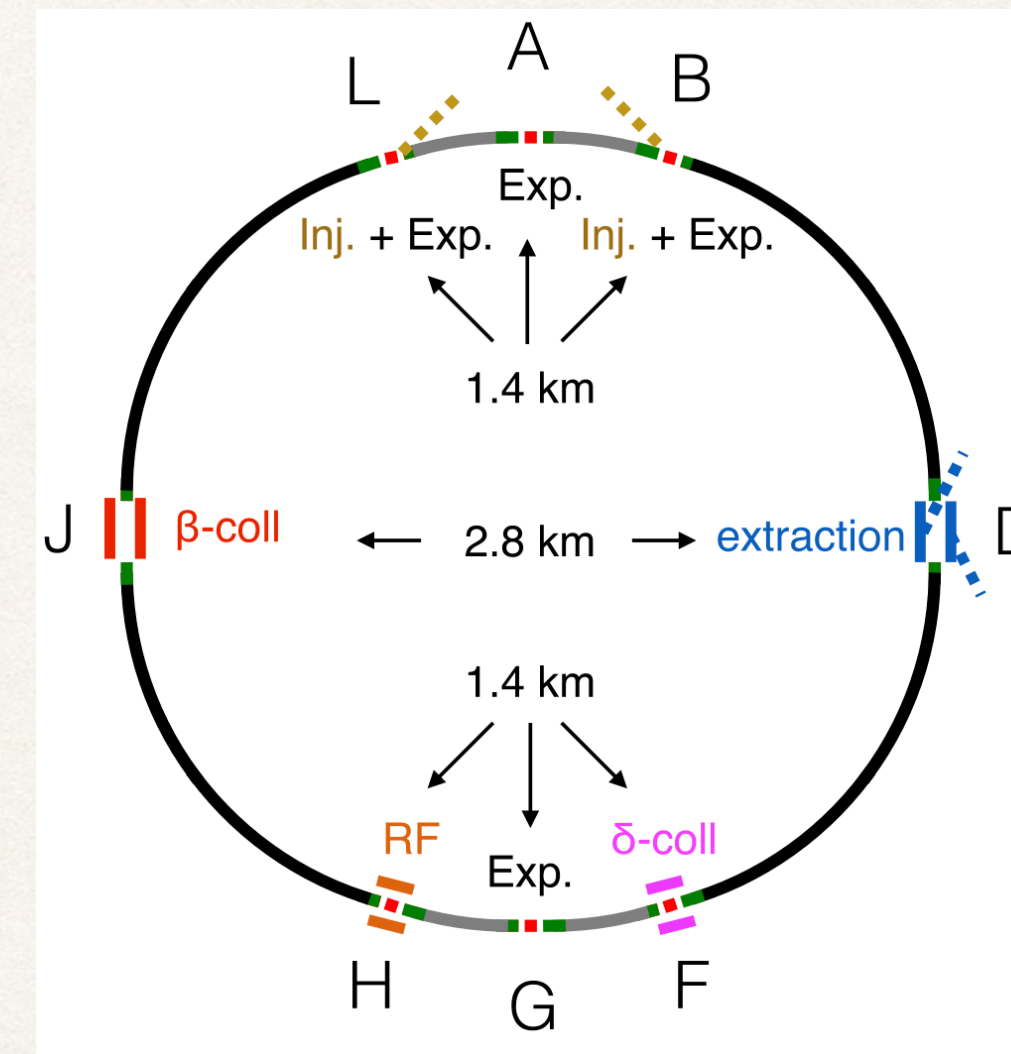
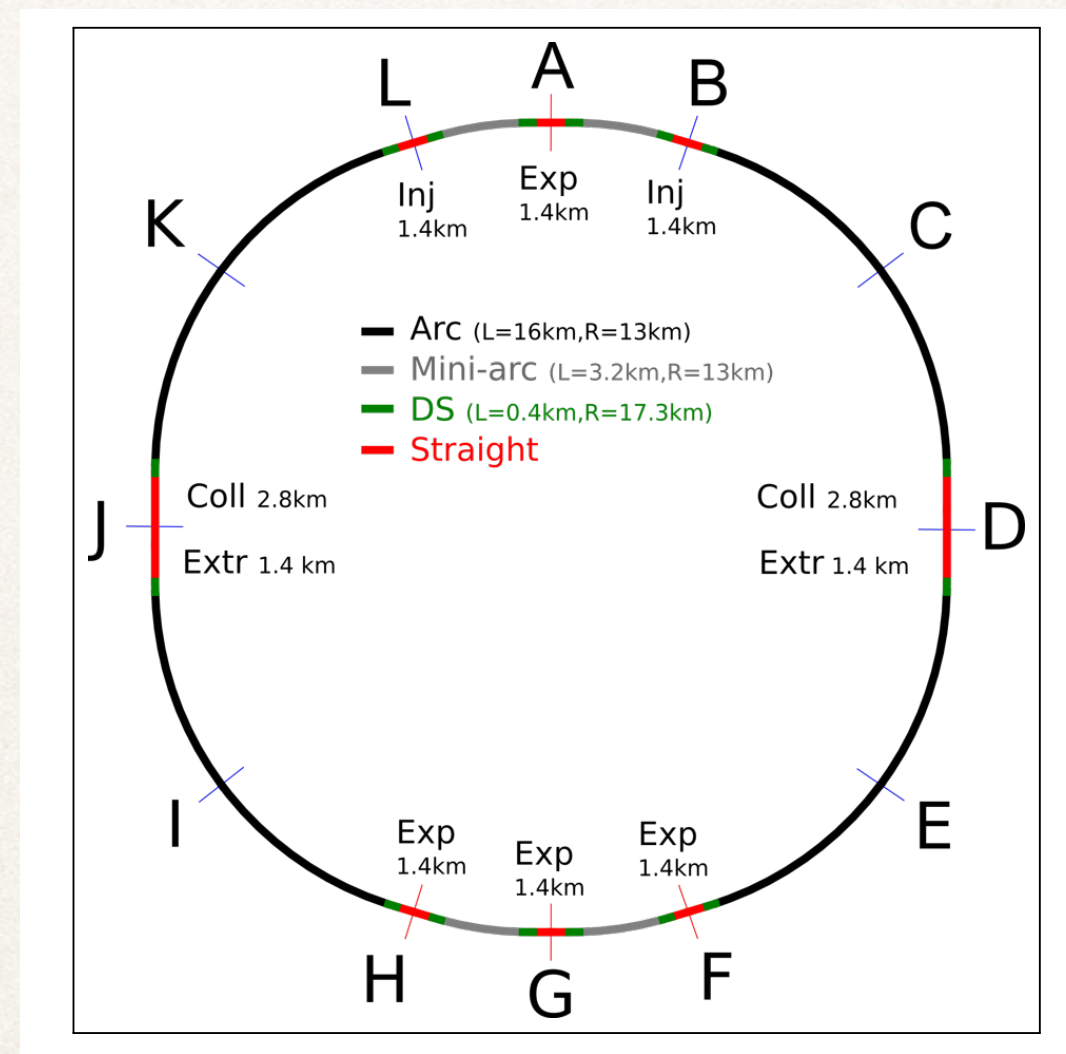


- ✦ The numbers in () correspond to “high-lumi” option.
- ✦ The luminosities are geometrical ones, no dynamics involved.

- ❖ A baseline optics* for FCC-ee was once established in Oct. 2016 characterized by:
 - ❖ 100 km circumference, 2 IP / ring.
 - ❖ Follow the footprint of FCC-hh, except for around the IPs.
 - ❖ common lattice for all energies, except for the detector solenoid (2T).
 - ❖ $\varepsilon_x \cong 1.3 \text{ nm @ } 175 \text{ GeV}$, basically scaling with energy.
 - ❖ $\beta_{x,y}^* = (1 \text{ m}, 2 \text{ mm})$ at 175 GeV, (0.5 m, 1 mm) at 45.6 GeV
 - ❖ $90^\circ / 90^\circ$ FODO cell in the arc with non-interleaved sextupole pairs.
- ❖ 30 mrad crossing angle at the IP, with the crab-waist scheme.
- ❖ local chromaticity correction for y -plane, incorporated with crab sextupoles .
- ❖ Suppress the critical energy of SR toward the IP below 100 keV at 175 GeV, up to 450 m upstream.
- ❖ 100 MW total SR power for all energies.
 - ❖ Tapering of magnets along the ring to compensate the effects of SR on orbit / optics.
 - ❖ Common RF cavities for e^+e^- at tt .
- ❖ Sufficient dynamic aperture for beamstrahlung and top-up injection.

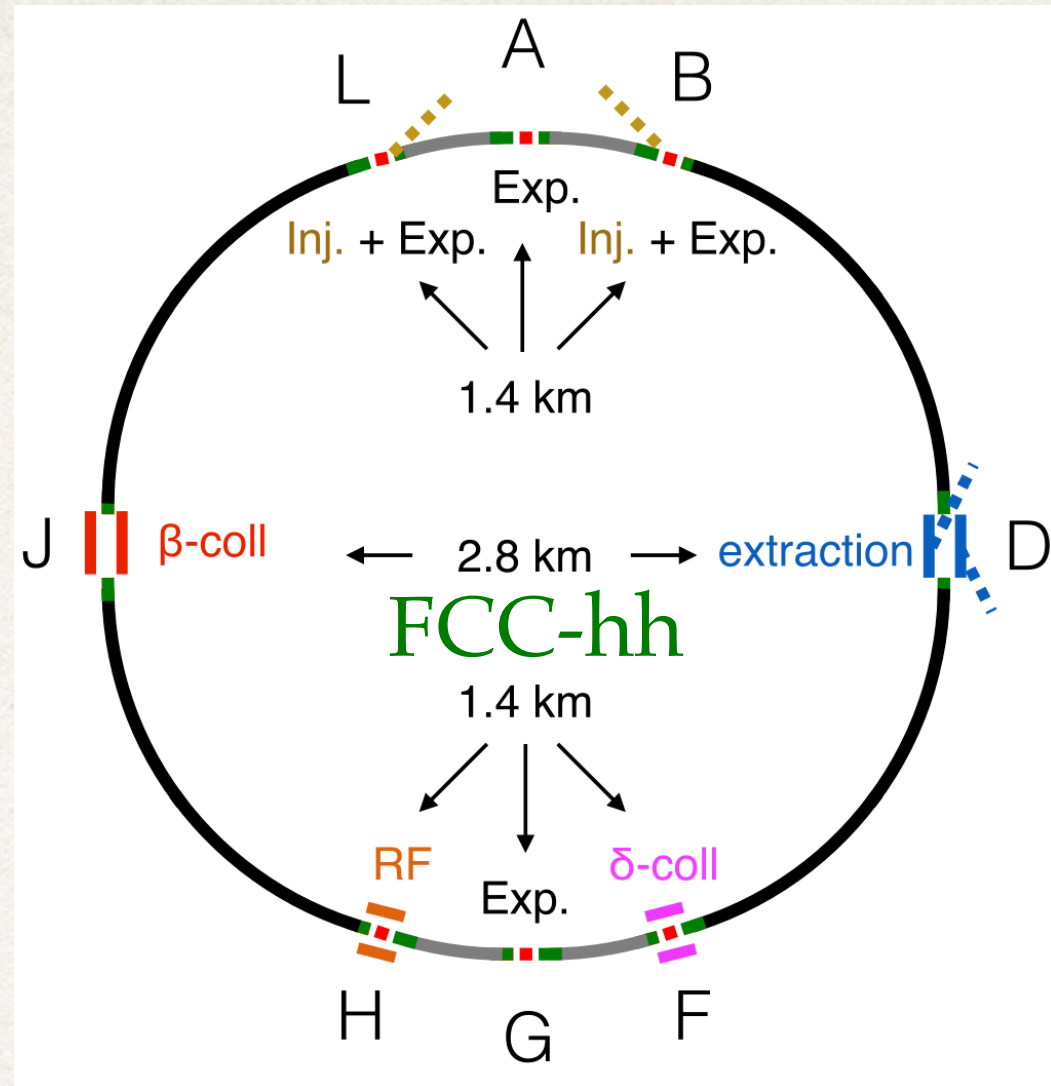
Changes in 2017

- ❖ Motivations for change in 2017*:
 - ❖ Mitigation of the coherent beam-beam instability at Z:
 - ❖ *Smaller β_x^**
 - ❖ *60°/60° cell in the arc, only at Z*
 - ❖ Adopt the “Twin Aperture Quadrupole” scheme for arc quadrupoles.
 - ❖ Fit the footprint to a new FCC-hh layout.



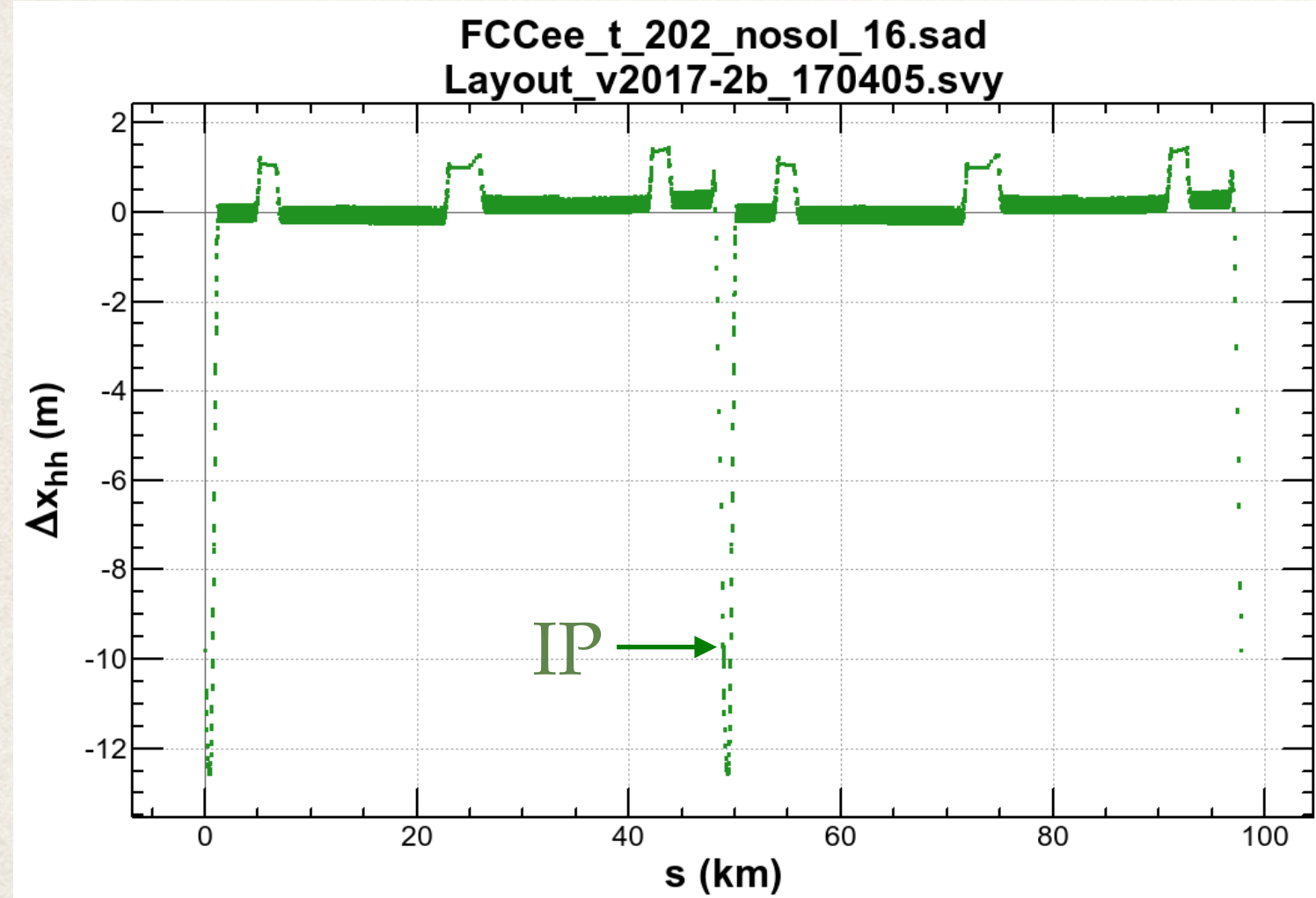
- ❖ The straight sections D&J have been shortened from 4.2 km to 2.8 km each.
- ❖ The circumference has shortened by 2.2 km.
- ❖ The location of sections B, F, H, L are slightly changed.

Layout of FCC-ee

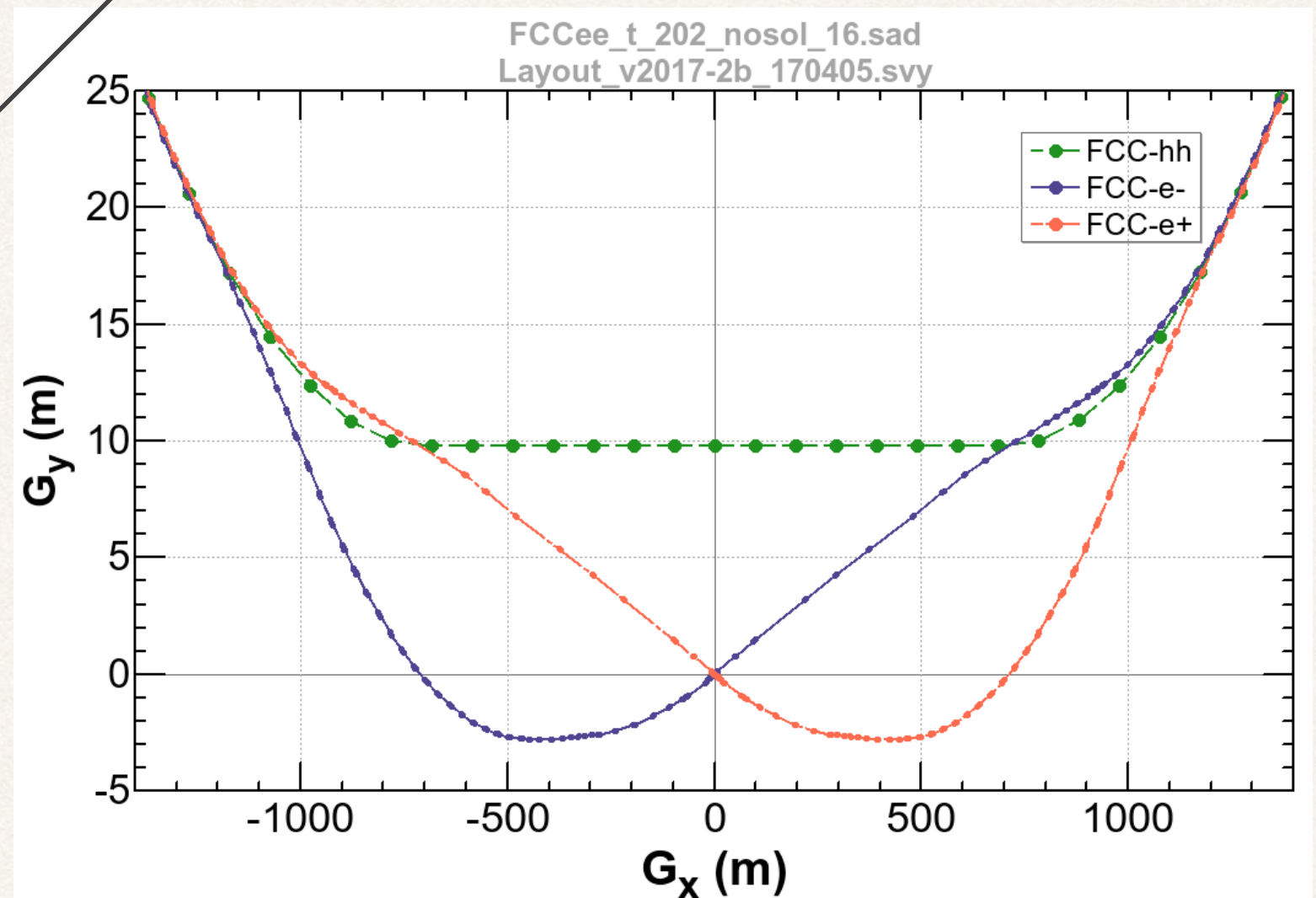
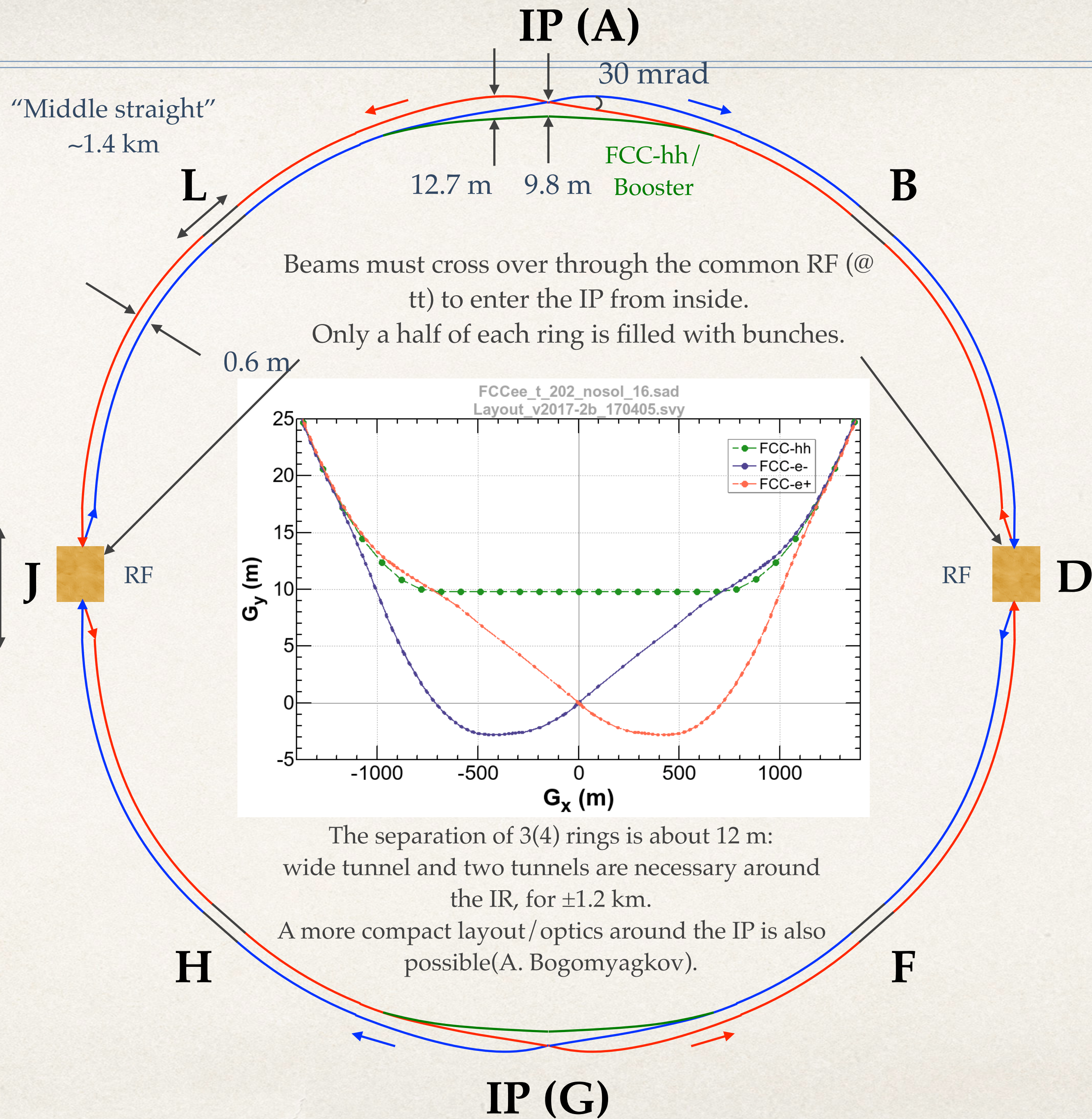


"Middle straight" ~1.4 km

"90/270 straight" ~2.8 km

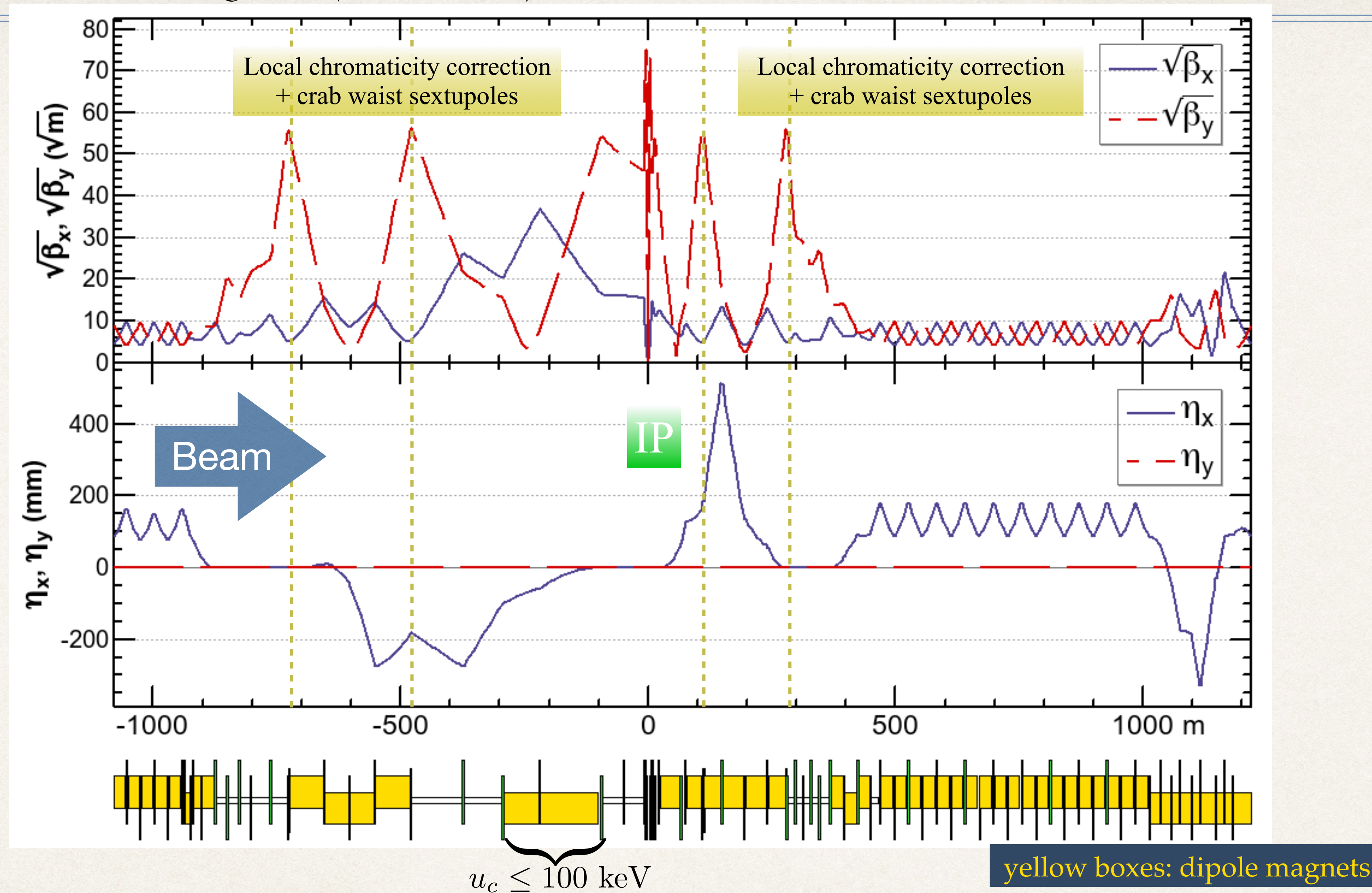


Relative distance to FCC-hh



The separation of 3(4) rings is about 12 m: wide tunnel and two tunnels are necessary around the IR, for ± 1.2 km.
A more compact layout/optics around the IP is also possible (A. Bogomyagkov).

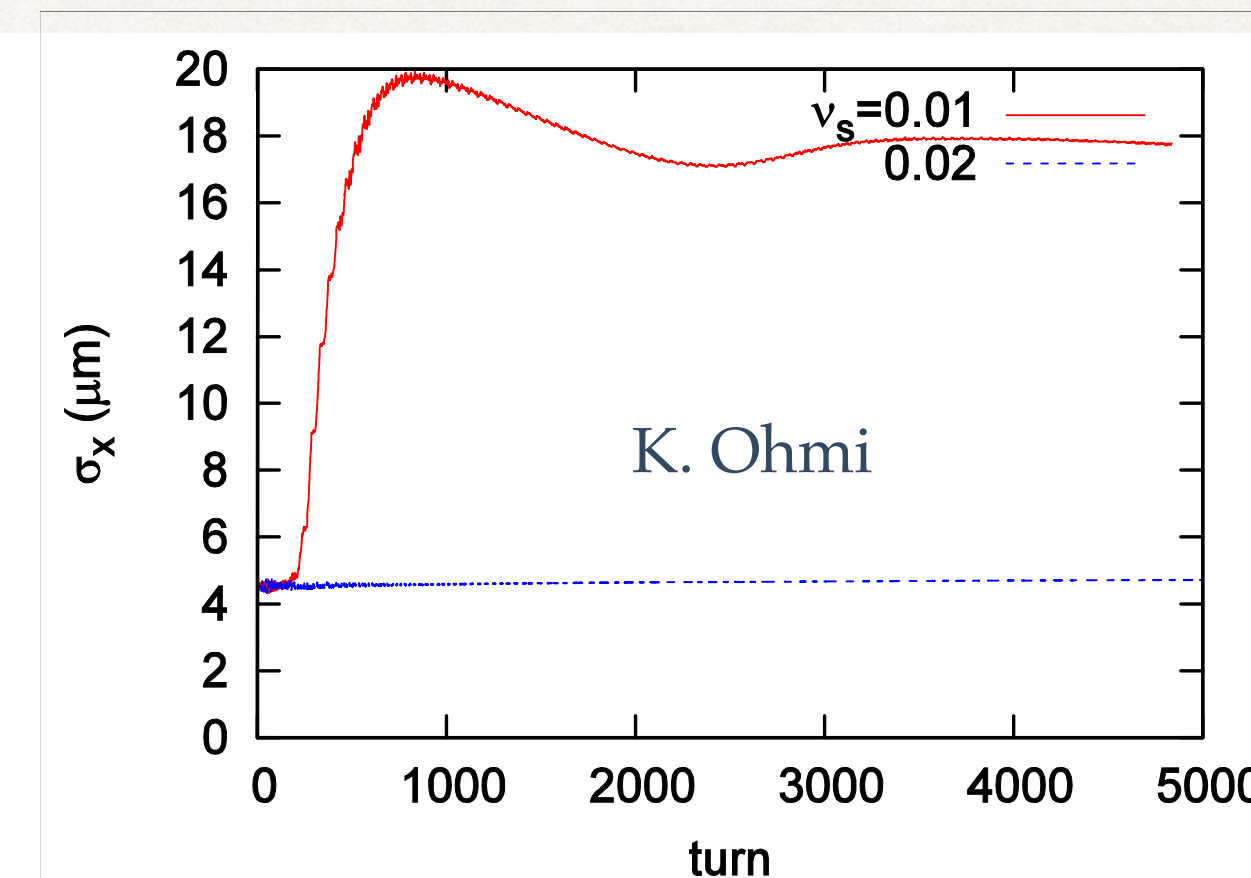
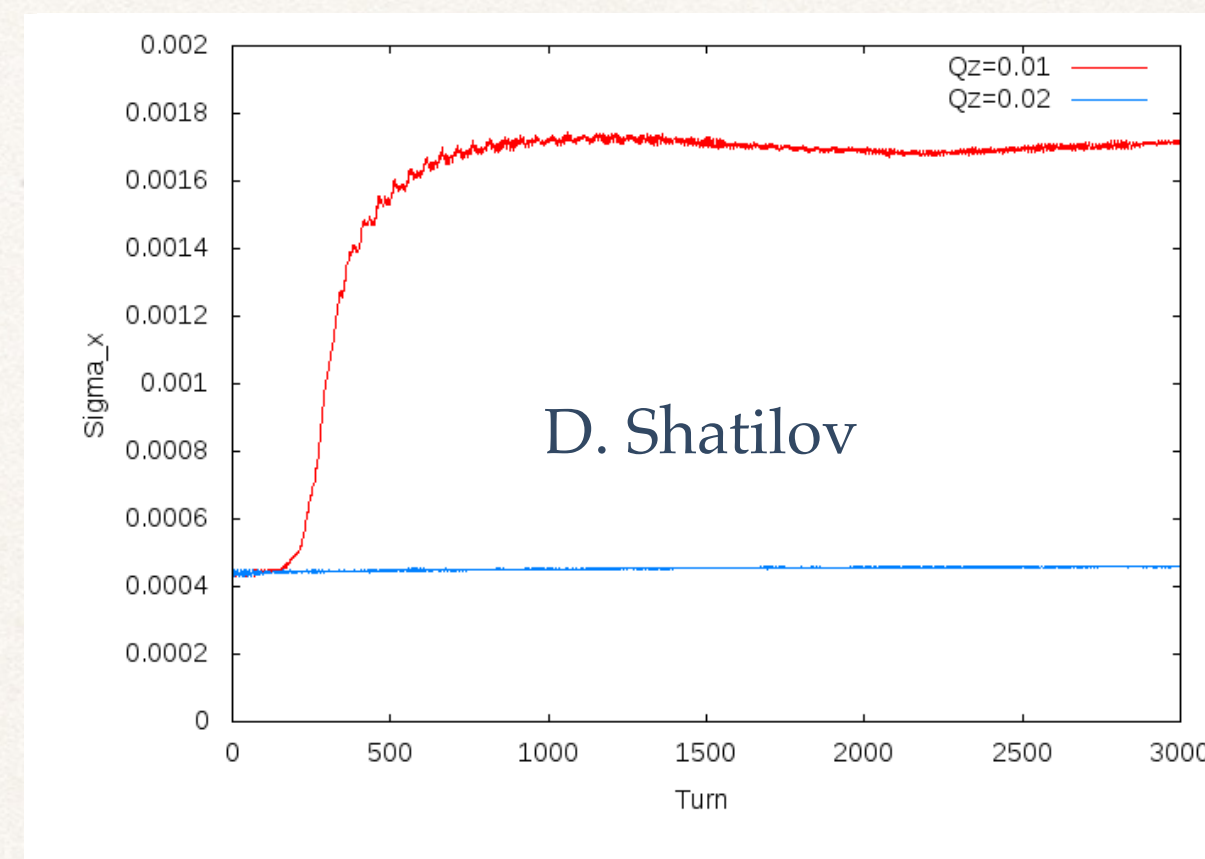
Interaction Region (tt, Zh, W)



- The optics in the interaction region are asymmetric.
- The synchrotron radiation from the upstream dipoles are below 100 keV up to 470 m from the IP.
- The crab sextupoles are integrated in the local chromaticity correction system in the vertical plane.

Mitigation of Coherent Beam-Beam Instability at Z

- ❖ A new coherent instability in x-z plane was first found by K. Ohmi by FCC Week 2016 with a strong-strong beam-beam simulation.
- ❖ D. Shatilov confirmed their phenomenon by a completely independent simulation, with a turn-by-turn alternating quasi-strong-strong method. The results of these two agree to each other very well.

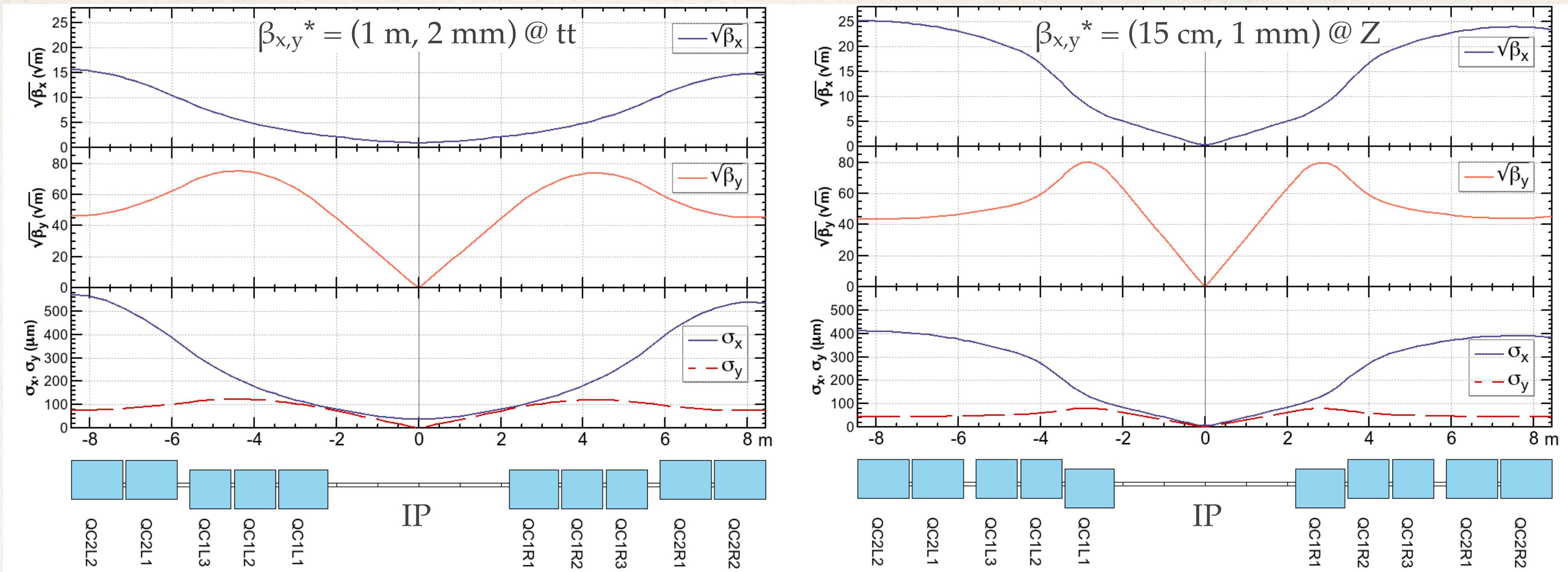


- ❖ A semi-analytic scaling the threshold bunch intensity has been derived by K. Ohmi:

$$N_{th} \propto \frac{\alpha_p \sigma_\delta \sigma_z}{\beta_x^*}$$

- ❖ Thus a smaller β_x^* and a larger momentum compaction α_p are favorable. The latter can be achieved by changing the phase advances of the arc at Z.
- ❖ We have reduced β_x^* to about 1/3, and increased α_p by a factor of 2 compared to the baseline 2016.

Reduce $\beta_{x,y}^*$, from 50 cm to 15 cm



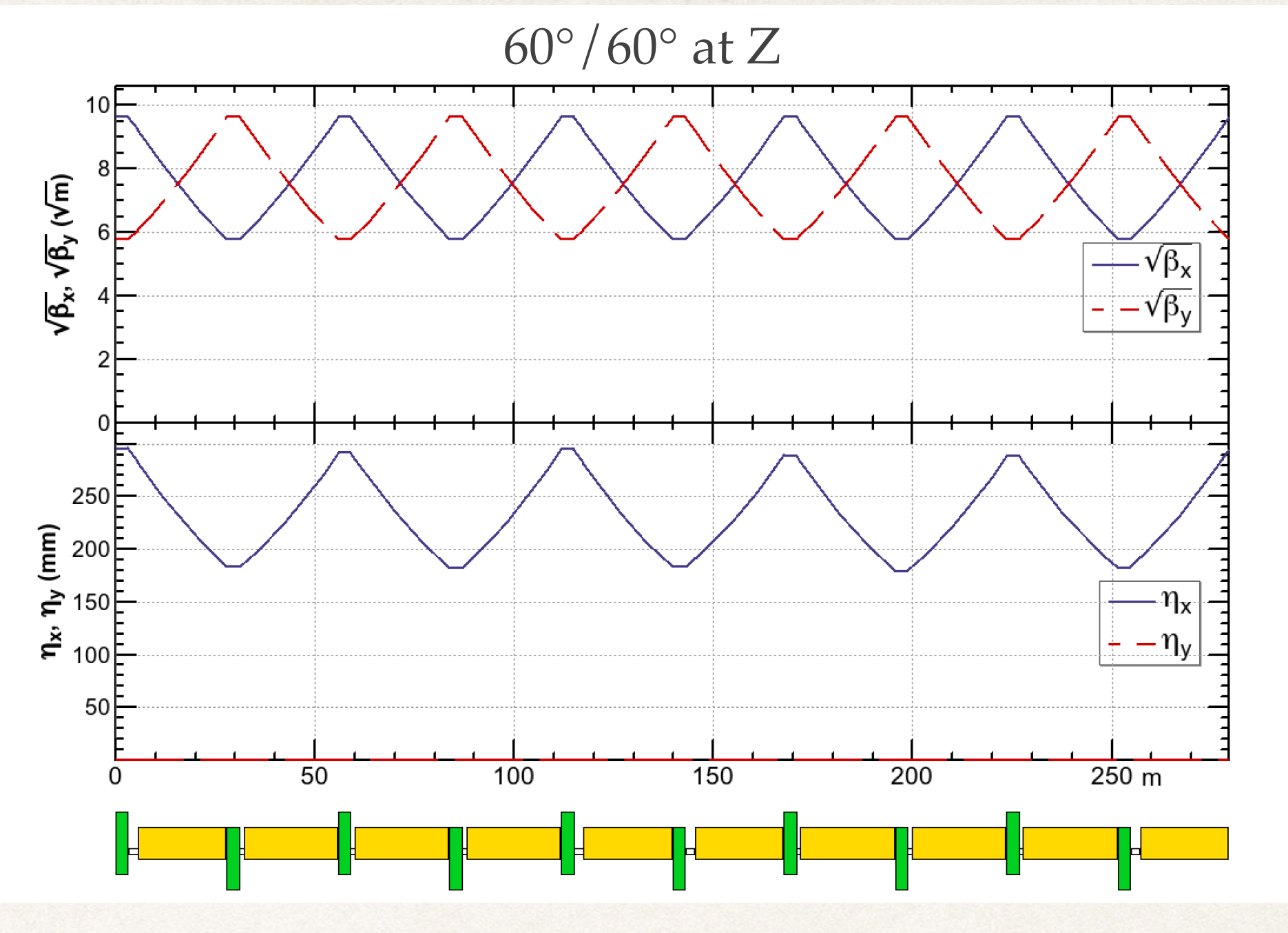
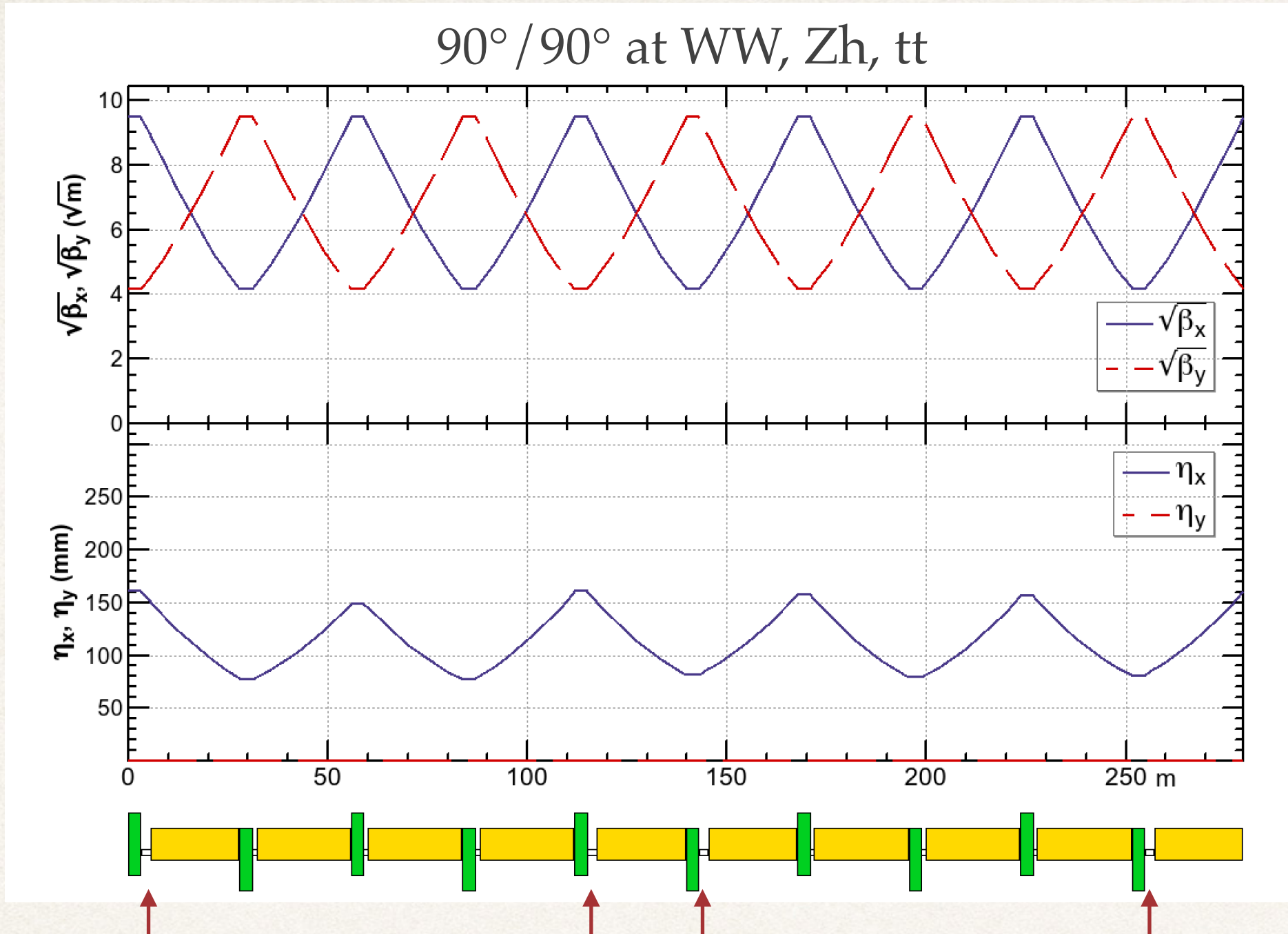
❖ Divide QC1 into three independent pieces, reverse the polarity at Z.

	L (m)	B' @ tt (T/m)	B' @ Z (T/m)
QC1L1	1.2	-94.4	-96.3
QC1L2	1	-92.6	+50.3
QC1L3	1	-96.7	+9.8
QC2L1	1.25	+45.8	+6.7
QC2L2	1.25	+74.0	+3.2

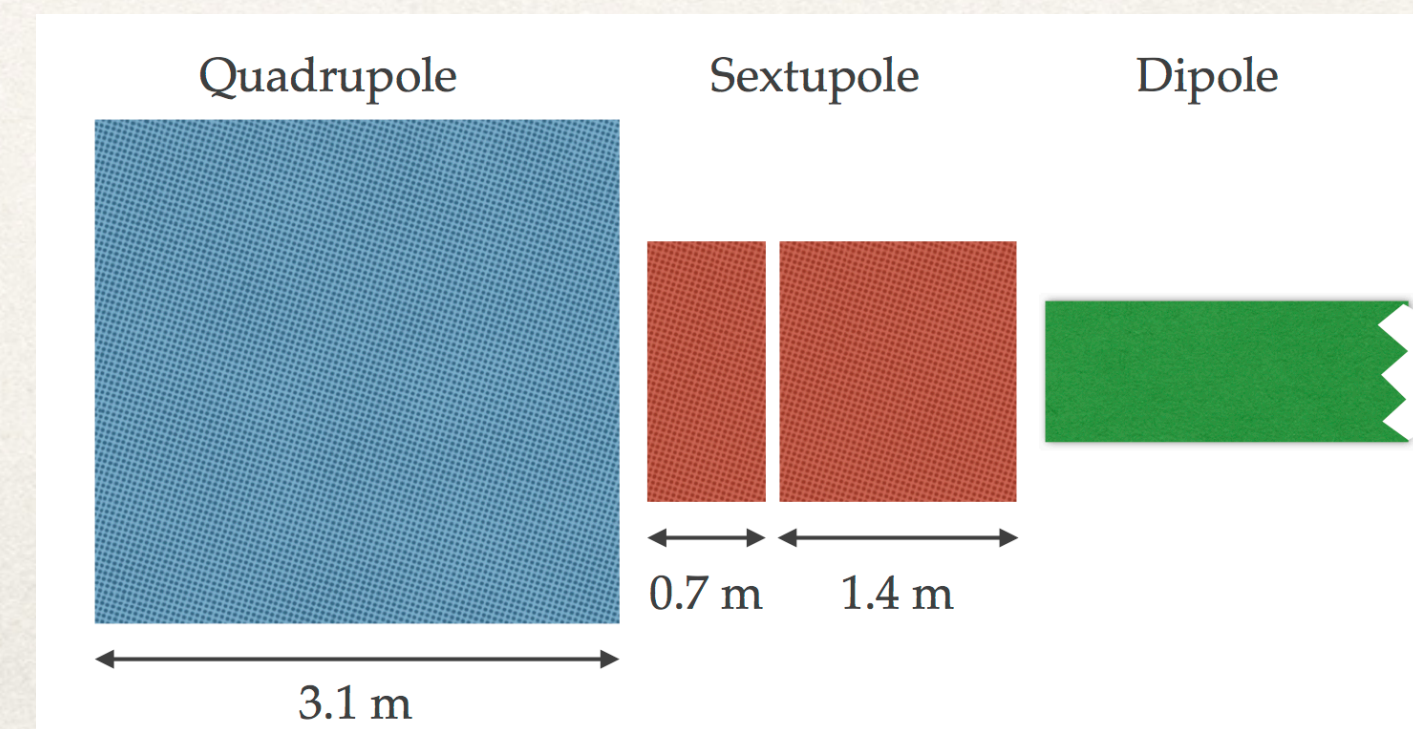
	L (m)	B' @ tt (T/m)	B' @ Z (T/m)
QC1R1	1.2	-99.9	-97.2
QC1R2	1	-99.9	+51.2
QC1R3	1	-99.9	+12.0
QC2R1	1.25	+78.6	+7.3
QC2R2	1.25	+76.2	+7.2

❖ By this split the chromaticity and the peaks of $\beta_{x,y}$ around the IP are suppressed for the reduction of $\beta_{x,y}^*$ at Z to (1/7, 1/2) at tt.

60°/60° Arc FODO Cell at Z

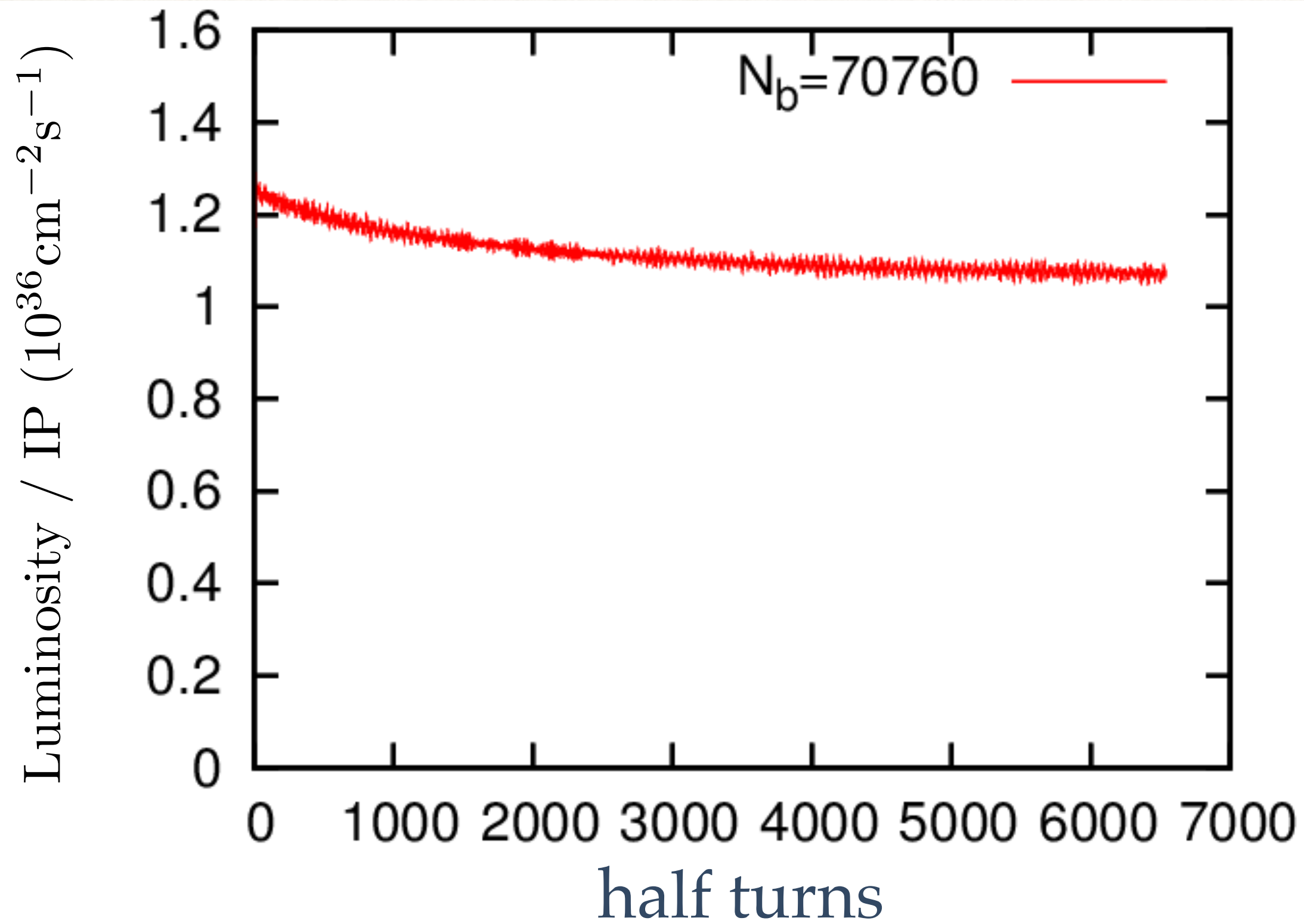


- ❖ There are two lengths for the space for sextupoles between quads and dipoles.
- ❖ The longer ones \uparrow are used for sexts in the case of 90°/90° cell. Some of shorter ones are used in the 60°/60° cell, making $-I$ transformation between a pair of sextupole.
- ❖ There are two lengths for the dipole, with the same field strength, thus a small irregularity is seen in the dispersion.
- ❖ The sextupole at the longer space consists of two slices.
- ❖ Only the shorter one is used/inserted at Z.



The mitigation for the beam-beam instability looks OK

Strong-strong simulation (K. Ohmi)



$$E = 45.6 \text{ GeV}$$

$$\beta_{x,y}^* = (0.15 \text{ m}, 1 \text{ mm})$$

$$\varepsilon_{x,y} = (0.267 \text{ nm}, 1 \text{ pm})$$

$$\sigma_{z,SR} = 2.1 \text{ mm}$$

$$N = 4 \times 10^{10}$$

Luminosity / IP ($10^{34} \text{ cm}^{-2} \text{ s}^{-1}$)

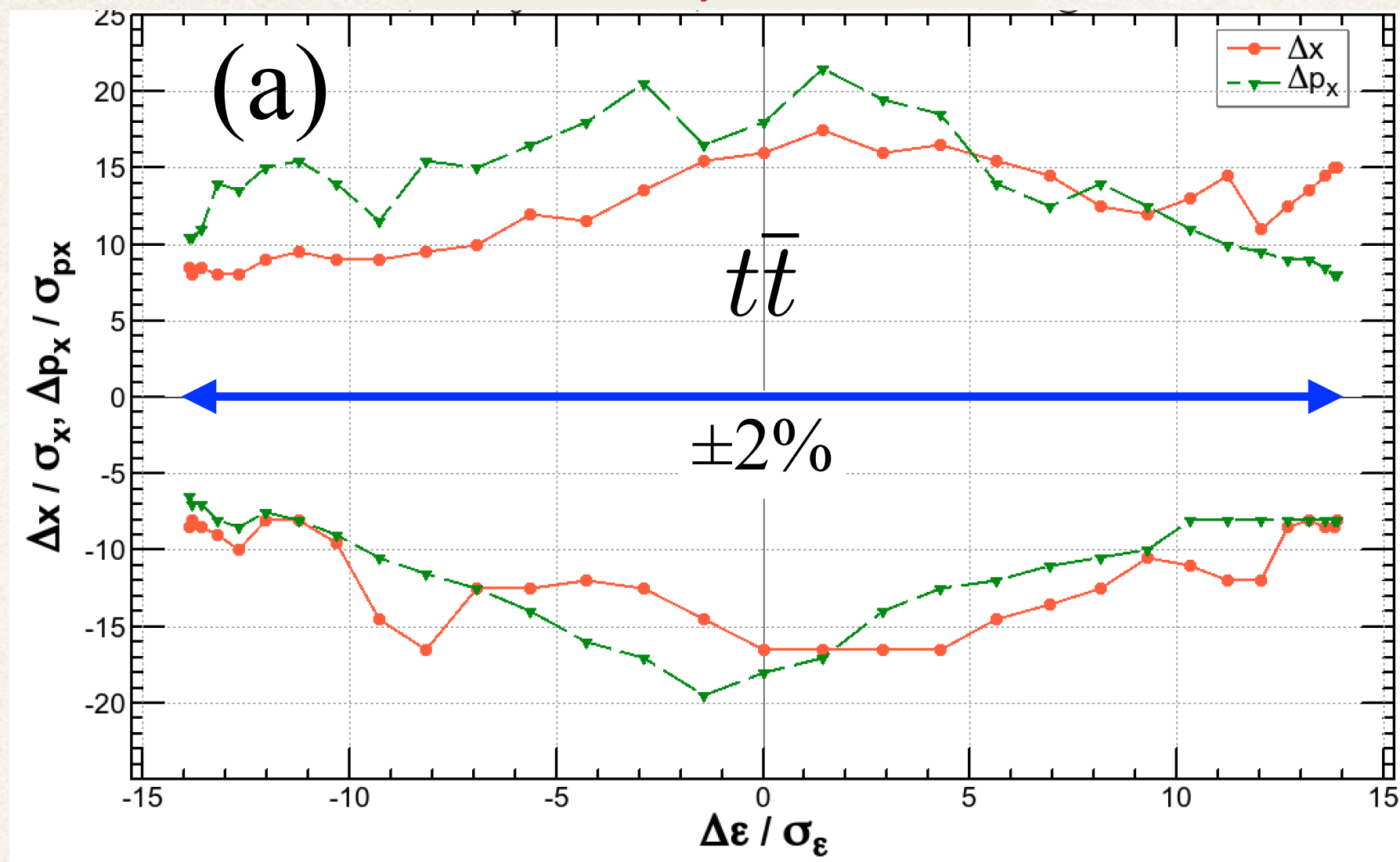
Energy	Geometrical	Strong-Strong (K. Ohmi)	Remarks
Z	137	107	a small blowup
W [±]	16.4	18	remaining coherent oscillation
Zh	4.6	5.3	
tt	1.35	1.15	

- ❖ The luminosity by the strong-strong beam-beam simulation agrees with the geometrical ones within $\pm 20\%$ differences.
- ❖ This means the blowup due to beam-beam effect is not large.
- ❖ Further tuning of the bunch charge, β -tron tunes, bunch length, etc., will improve the luminosity further.
- ❖ More, independent results with quasi-strong-strong model will be presented by D. Shatilov in this workshop.

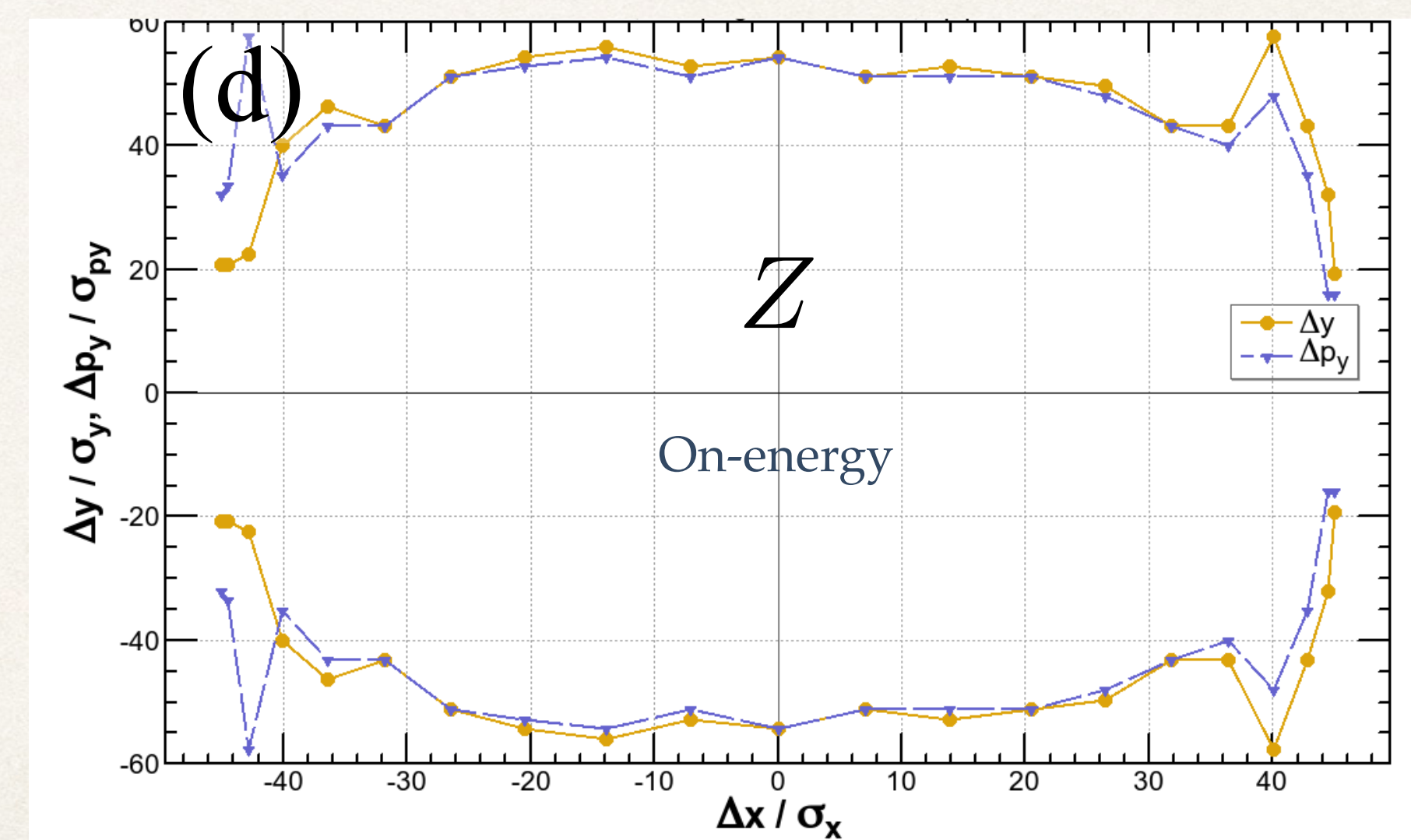
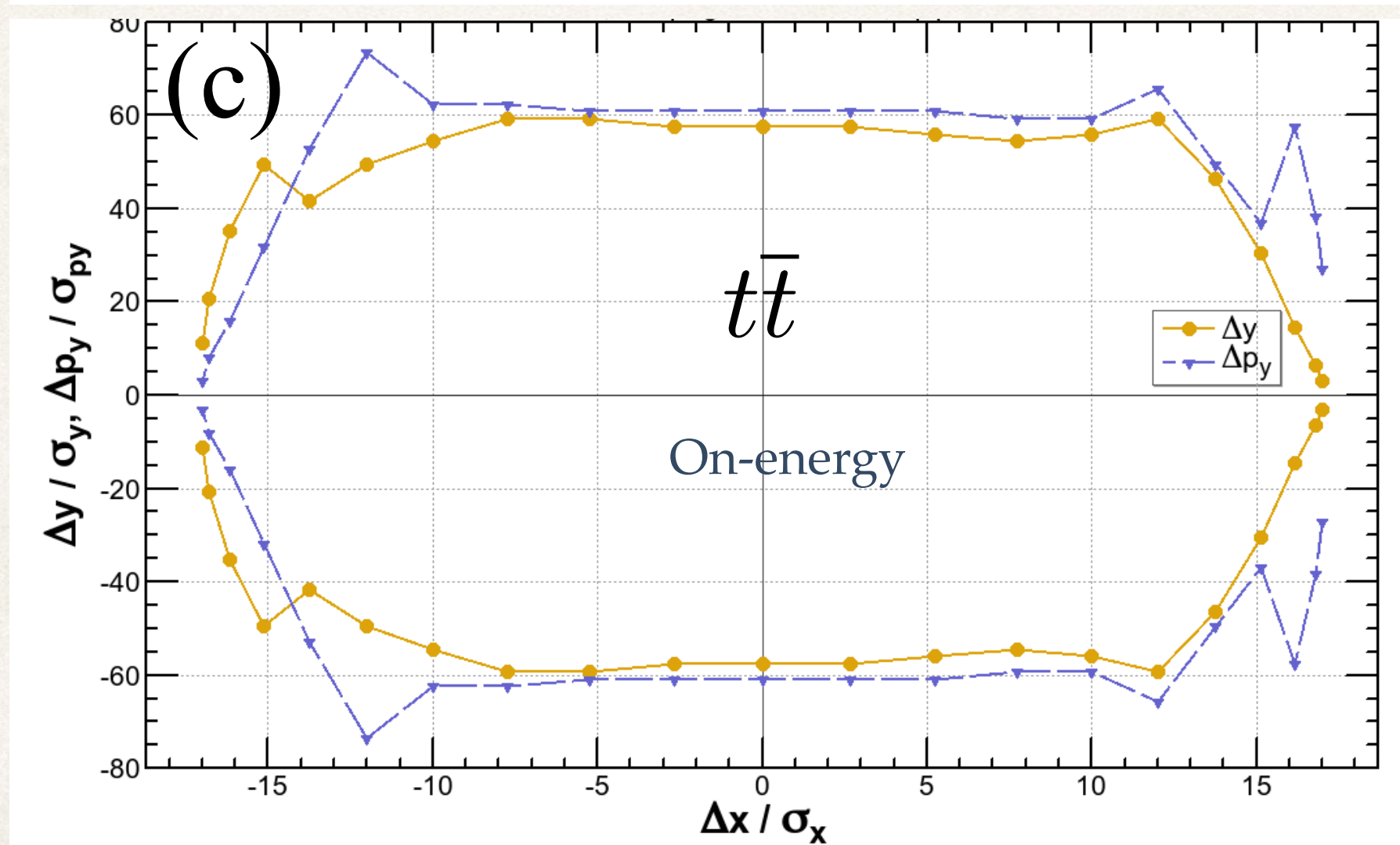
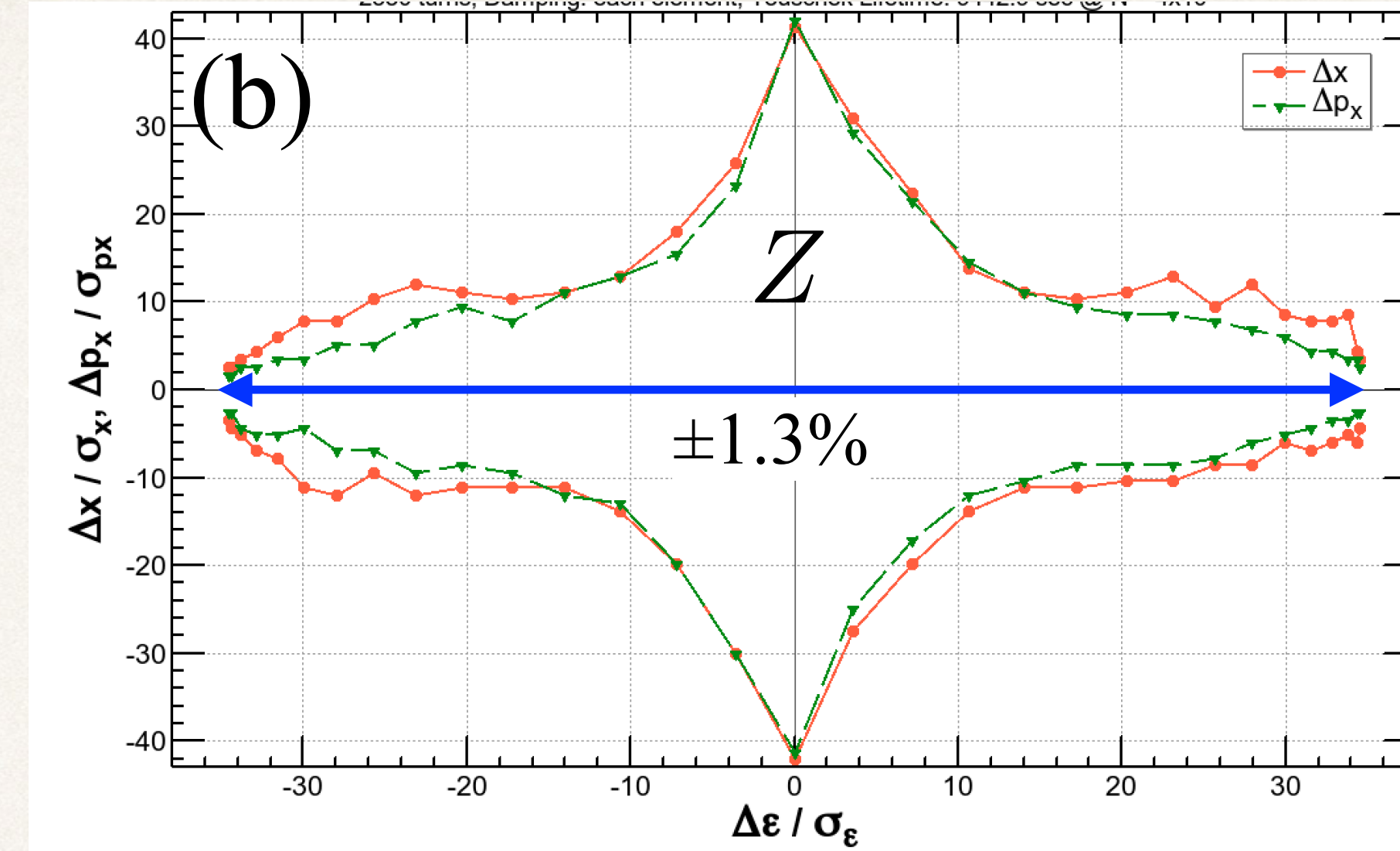
Dynamic Aperture satisfies the requirements



175 GeV, $\beta^*_{x,y} = (1 \text{ m}, 2 \text{ mm})$



45.6 GeV, $\beta^*_{x,y} = (0.15 \text{ m}, 1 \text{ mm})$

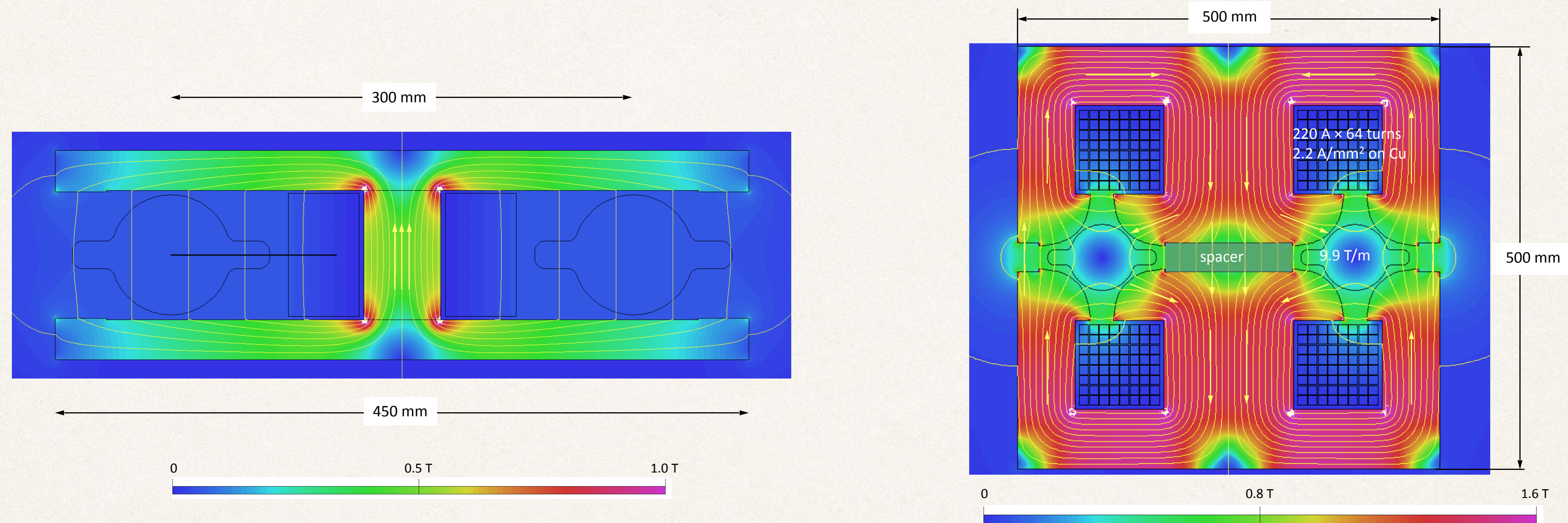


Momentum acceptances: $\pm 2\% = 10.4\sigma_\delta$ @ $t\bar{t}$, $\pm 1.3\% = \pm 17.8\sigma_\delta$ @ Z , including beamstrahlung.

Tracking 50 turns @ $t\bar{t}$, 2550 turns at Z . Synchrotron motion, synchrotron radiation damping in dipoles & quads, tapering, Maxwellian fringes, kinematical terms, crab waist are included.

Twin Aperture Arc Magnets (A. Milanese)

- ❖ An idea of “twin aperture quadrupole” has been developed by A. Milanese to save the power consumption of quadrupole magnets.
- ❖ The currents in the magnet are always surrounded by iron to maximize the usage.



An example of the cross section of a twin aperture dipole and quadrupole for FCC-ee (A. Milanese).

The separation between two beams is 30 cm.

- ❖ The power consumption of the twin aperture quad: 22 MW at 175 GeV with Cu coil = half of single-aperture quads.
- ❖ Dipoles are also “twin”: power consumption = 17 MW at 175 GeV with Al bus bar.

Interaction Region Arrangement

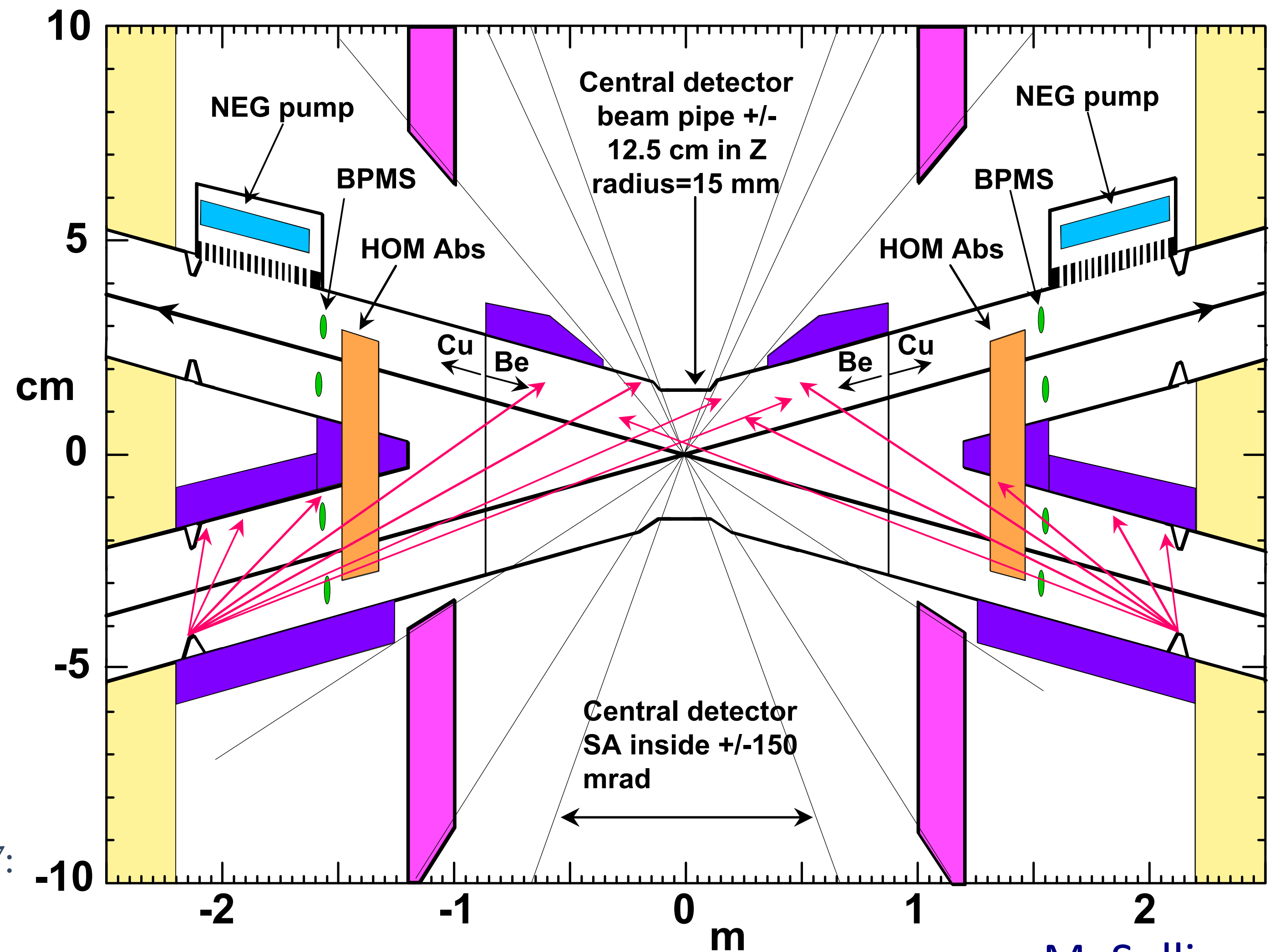
(@ top energy)

- central Be beam pipe (0.8 mm thick and $|s| < 0.9\text{m}$ from IP)
- **luminometers**
- **Ta (or Pb) shieldings**
- 5 μm Au coating in the central chamber

warm pipe:

- water cooling ($\sim 2\text{mm}$)

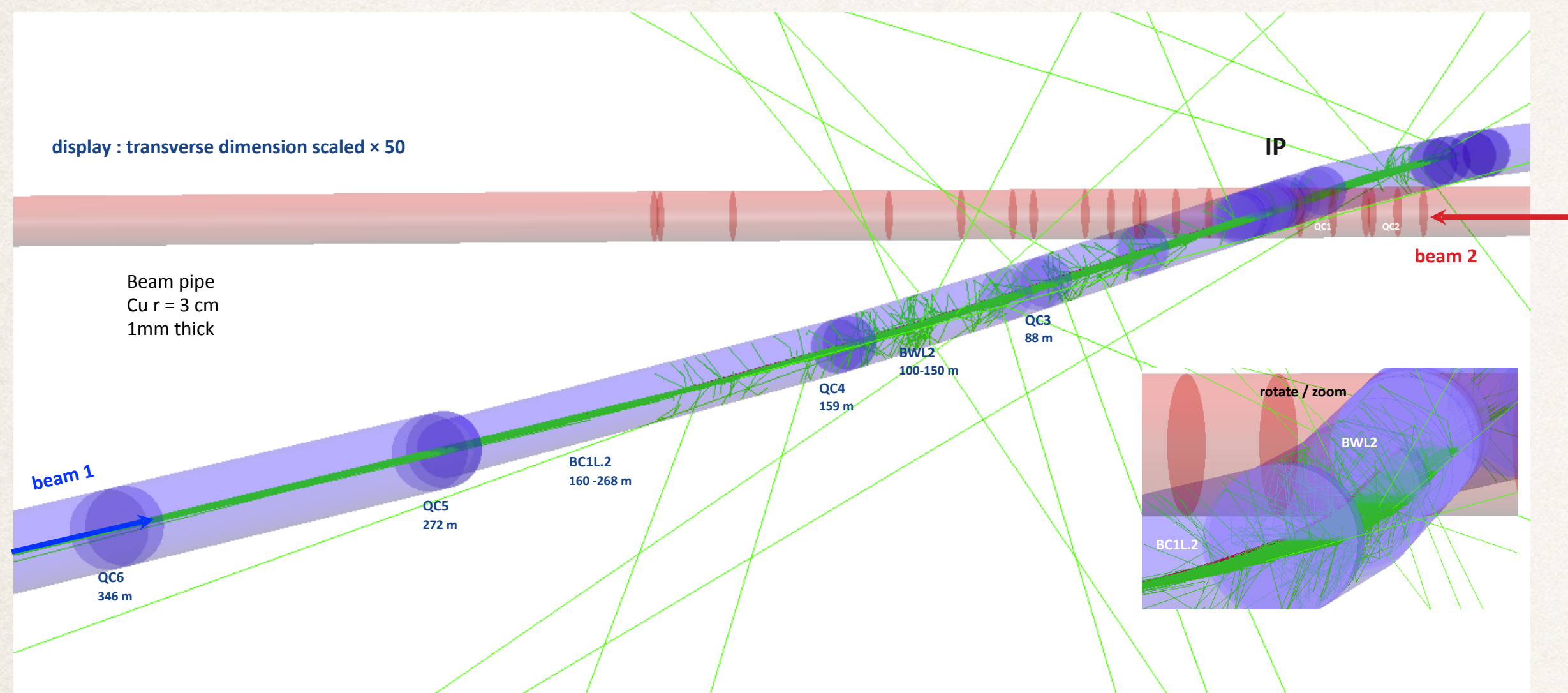
The basic arrangement around the IP has been converged through an MDI workshop in Jan. 2017:
<https://indico.cern.ch/event/596695/>



M. Sullivan

Synchrotron Radiation hitting the IP

3d display - SR MDISim - Geant4 simulation



(Gaussian) beam 1, 5000 e+ 175 GeV

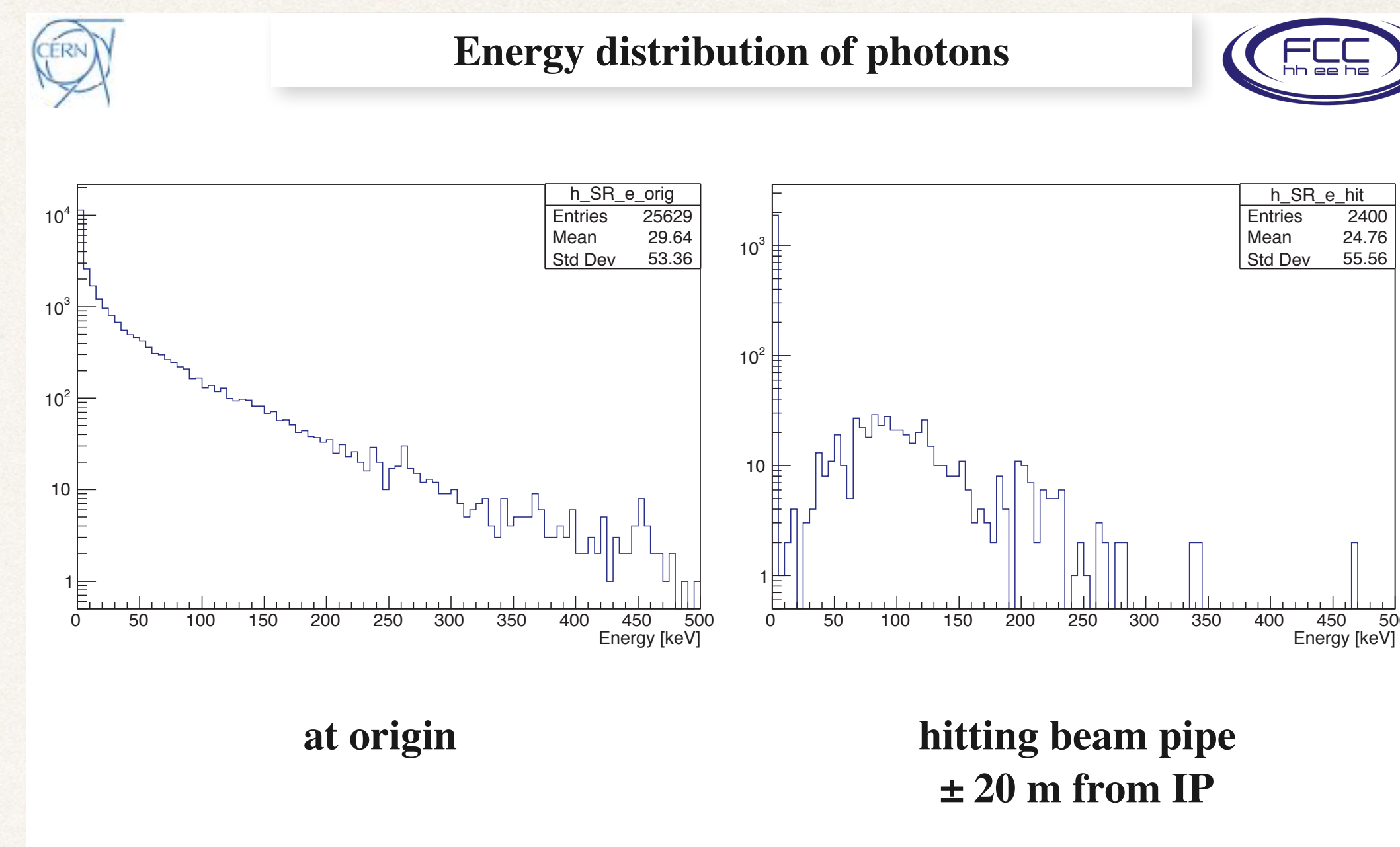
tracked 510 m to IP (just after BC3 to Q2)

with SR and standard G4 em processes eloni, eBrem, annihil, phot, compt, conv, Rayl

28300 SR γ 's generated, first 1000 γ 's shown here

rather fast, < 1 min (MacMini i7)

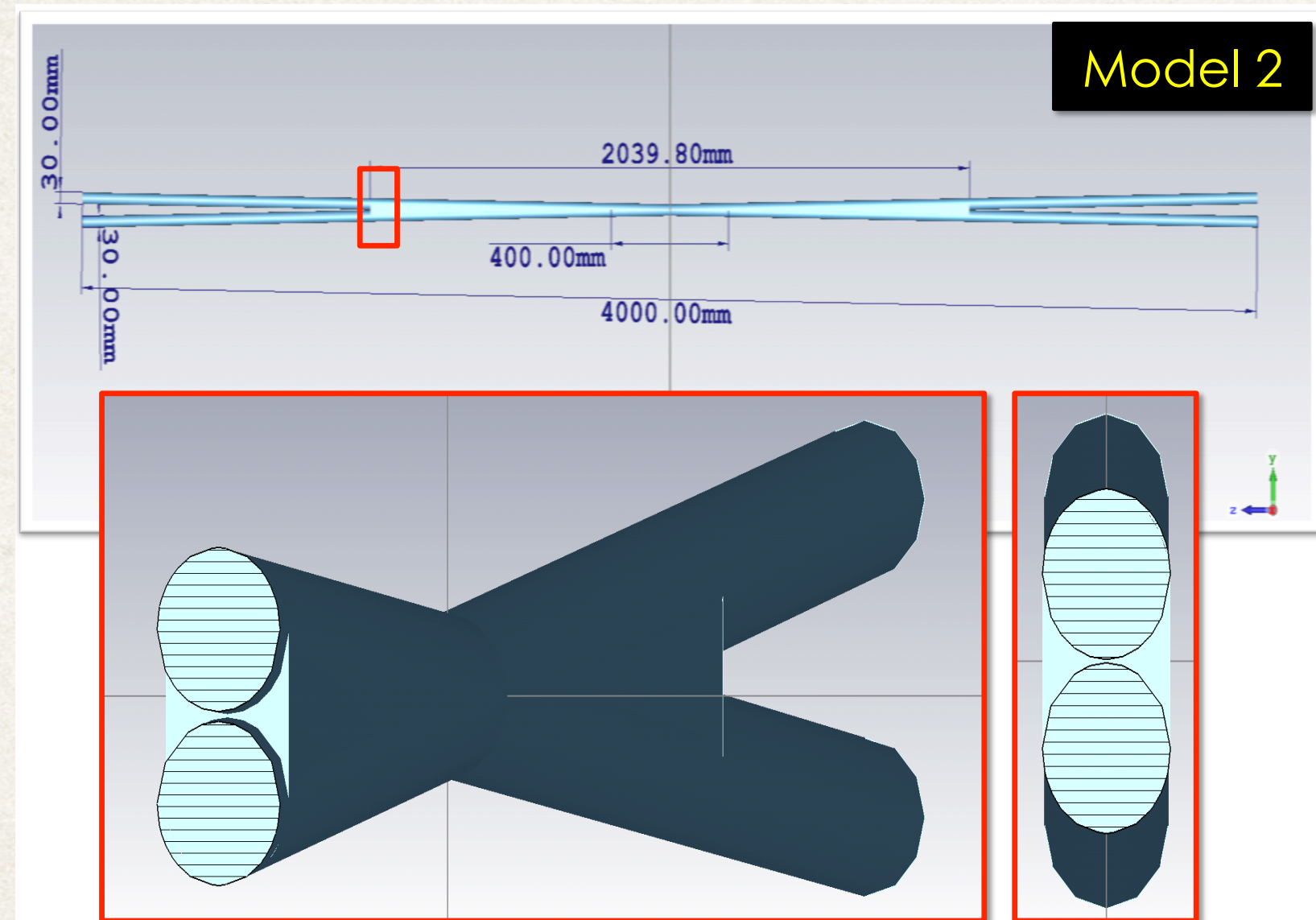
multiply with
 $2.3e+11/5000 = 4.6e7$
 to get statistics of 1 bunch
 $1.3e12$ SR γ 's



at origin

hitting beam pipe
 ± 20 m from IP

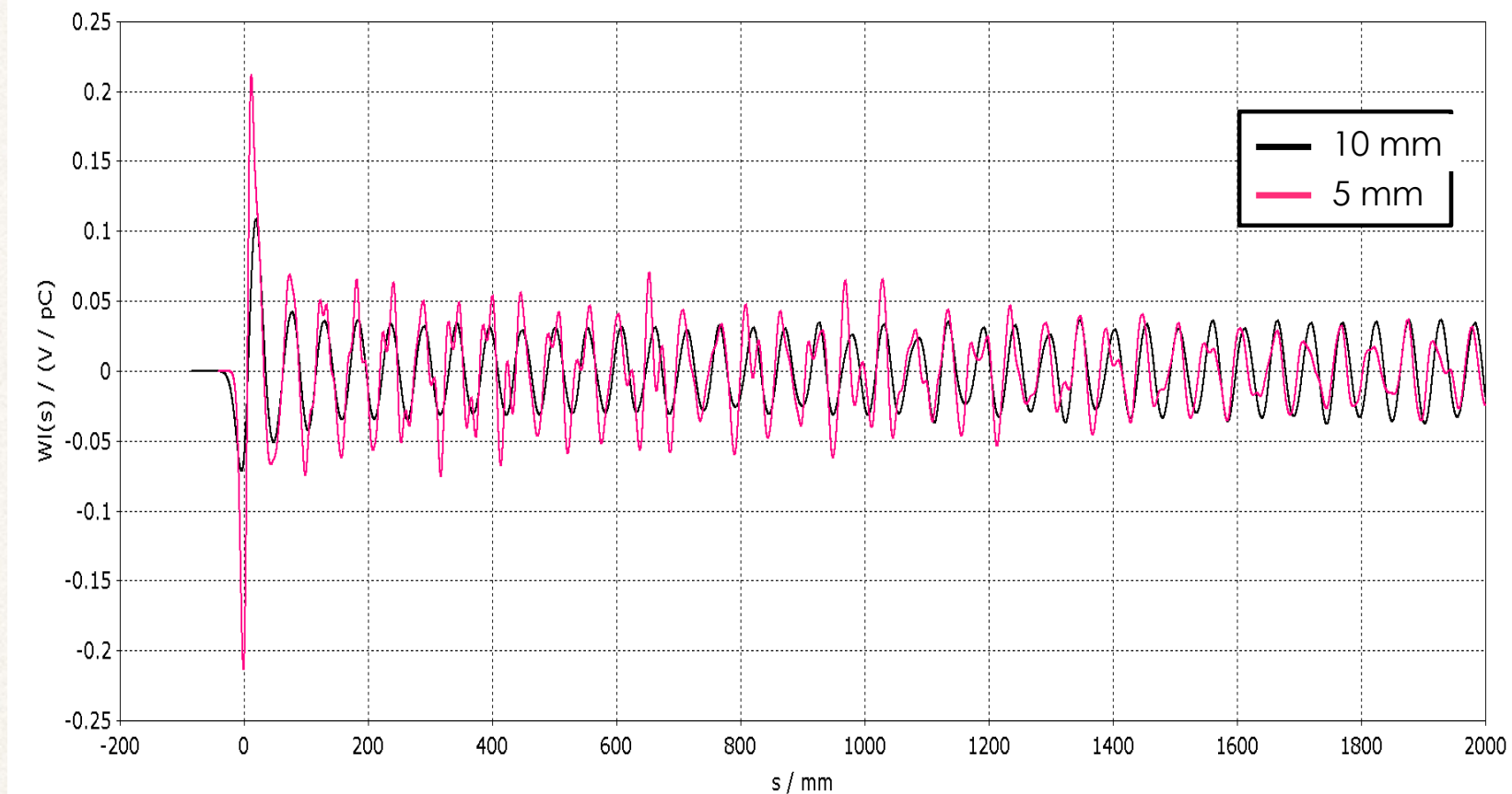
- ❖ Several methods have been applied to analyze the SR hitting the IP. Above is an example with MDISim/Geant4 (H. Burkhardt and M. Lückhof).
- ❖ No show stopper has been found.
- ❖ Optimization of shields, masks, sawtooth surfaces of the beam pipe are in progress.



25/01/2017 – FCCee MDI Workshop

E. Belli

We managed to do only wake field simulation, but failed to do eigen mode simulations.

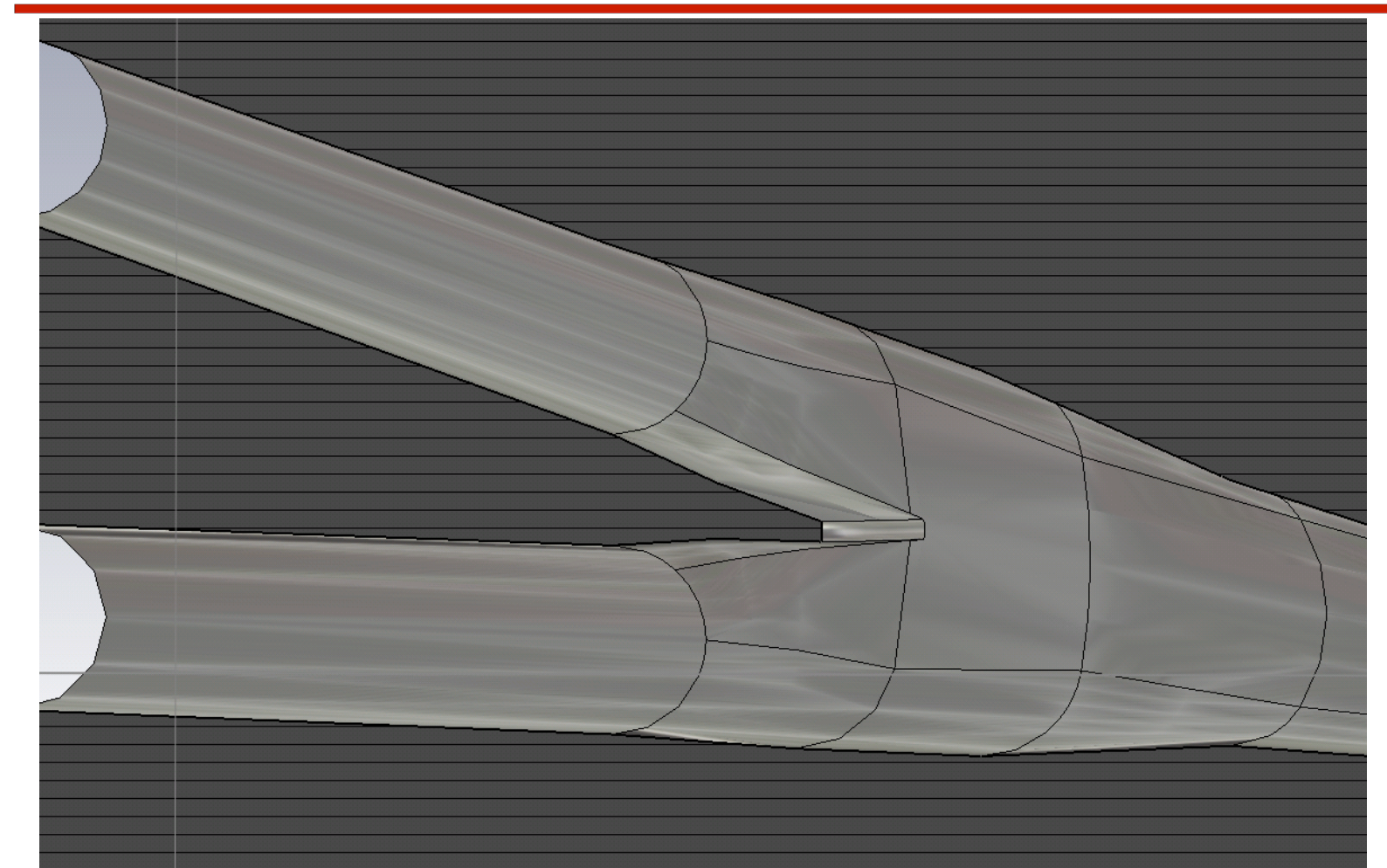


25/01/2017 – FCCee MDI Workshop

Alexander Novokhatski, Eleonora Belli, Miguel Gil Costa, Michael K. Sullivan and Roberto Kersevan

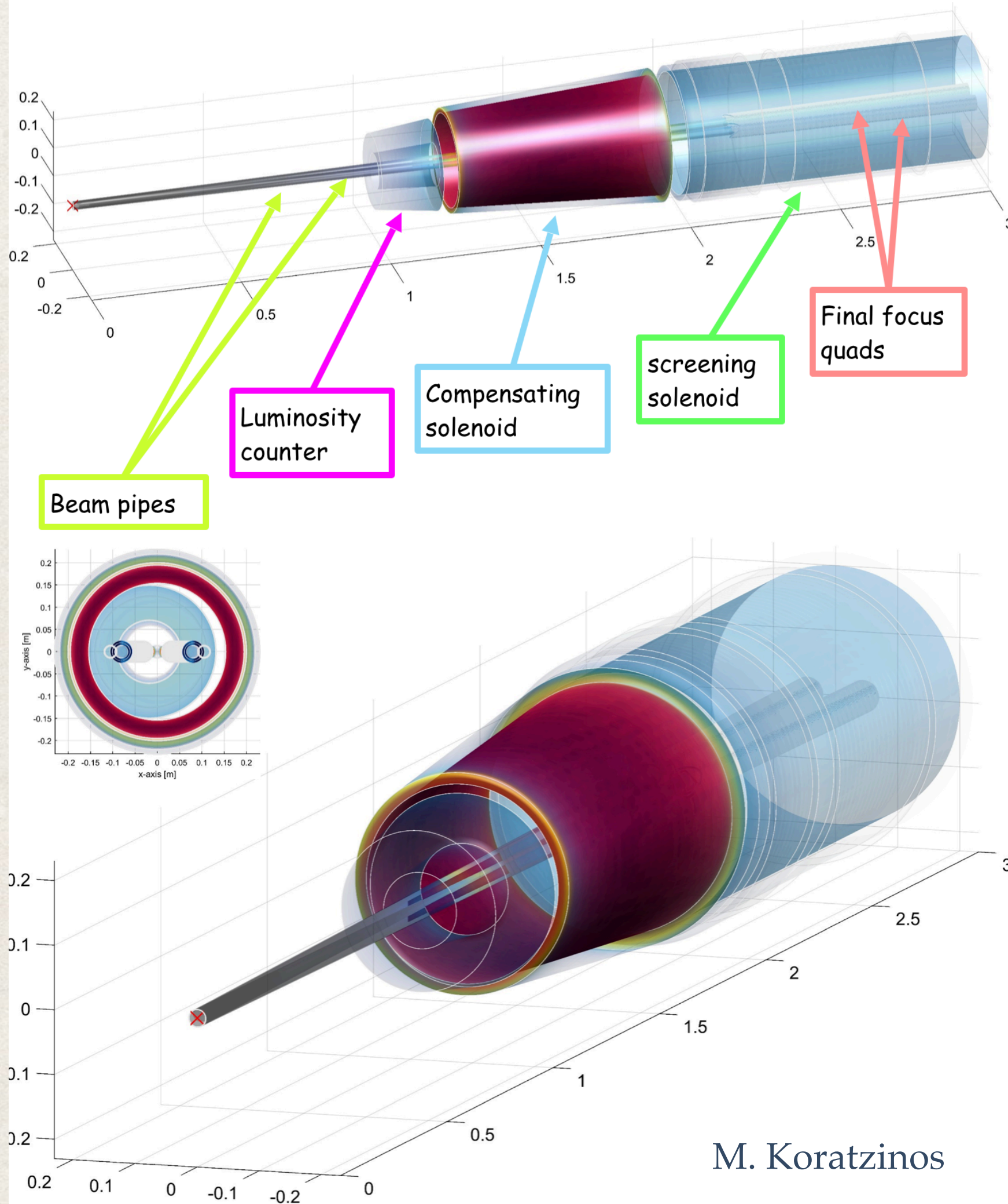
- ❖ The generation of HOM and heating in the IP beam pipe will be an issue, esp. with the very high beam current at Z.
- ❖ Detailed 3D calculation of the EM field has been carried out.
- ❖ The beam pipe with $d \cong 30$ mm everywhere seems OK.
- ❖ More realistic modeling is on going.

More details. All smooth geometrical transitions.



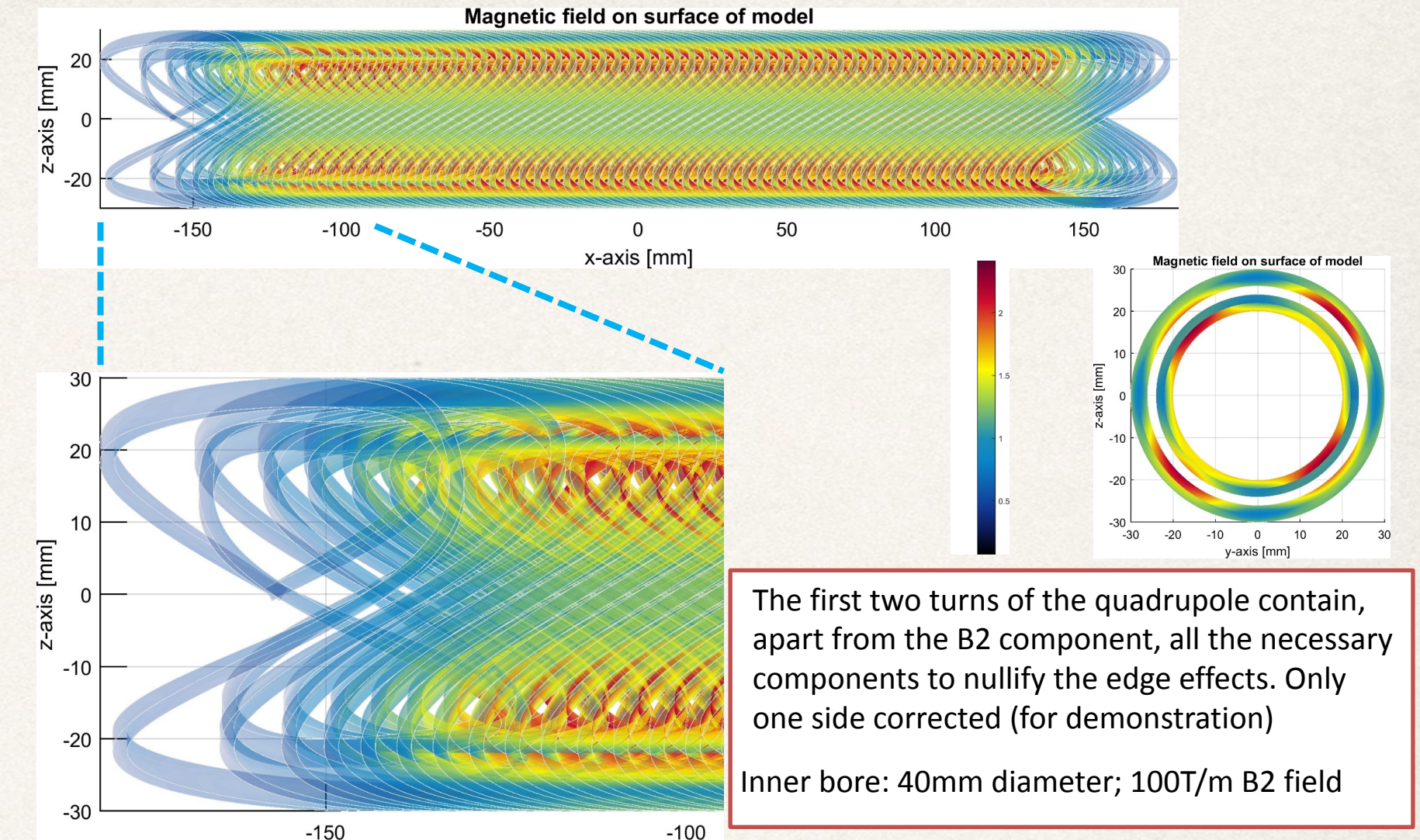
Final Focus Magnet Complex

View of magnetic elements, beampipe and luminometer

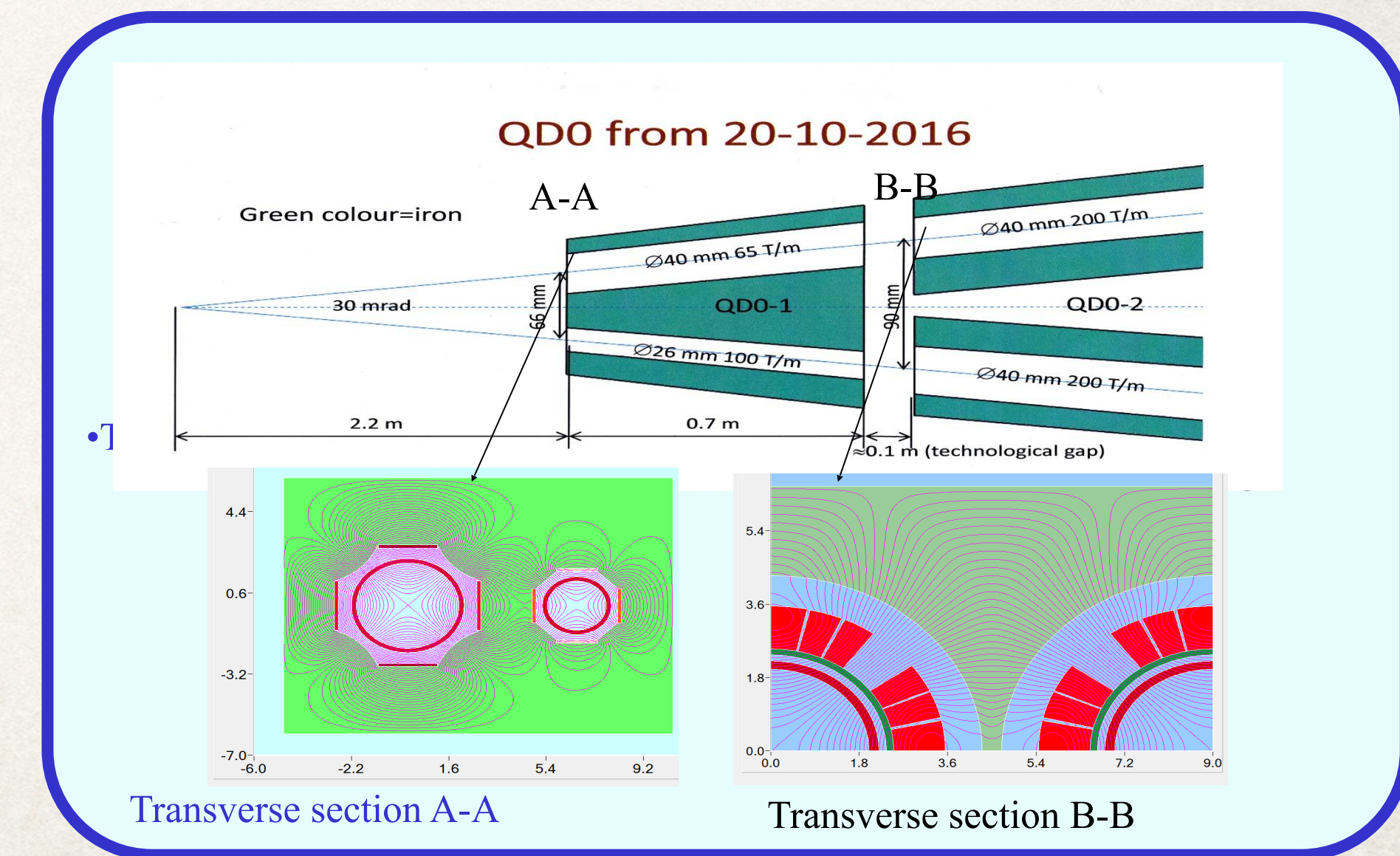


- ❖ The Final Focus magnets consists of
 - final focus quadrupole doublet
 - compensation solenoids between the final quad to the IP
 - shielding solenoids to make $B_z = 0$ at the quadrupoles.
- ❖ A few design choices have been proposed.

- ❖ Prototyping for a double aperture quadrupole has been going on at BINP.



CCT Quadrupole (M. Koratzinos)



Double Aperture Quadrupole (P. Vobly)

Quadrupoles of the arcs (no FF)

$$\Delta x = 100\mu m, \Delta y = 100\mu m, \theta = 100\mu rad$$

Sextupoles

$$\Delta x = 100\mu m, \Delta y = 100\mu m, \theta = 0\mu rad$$

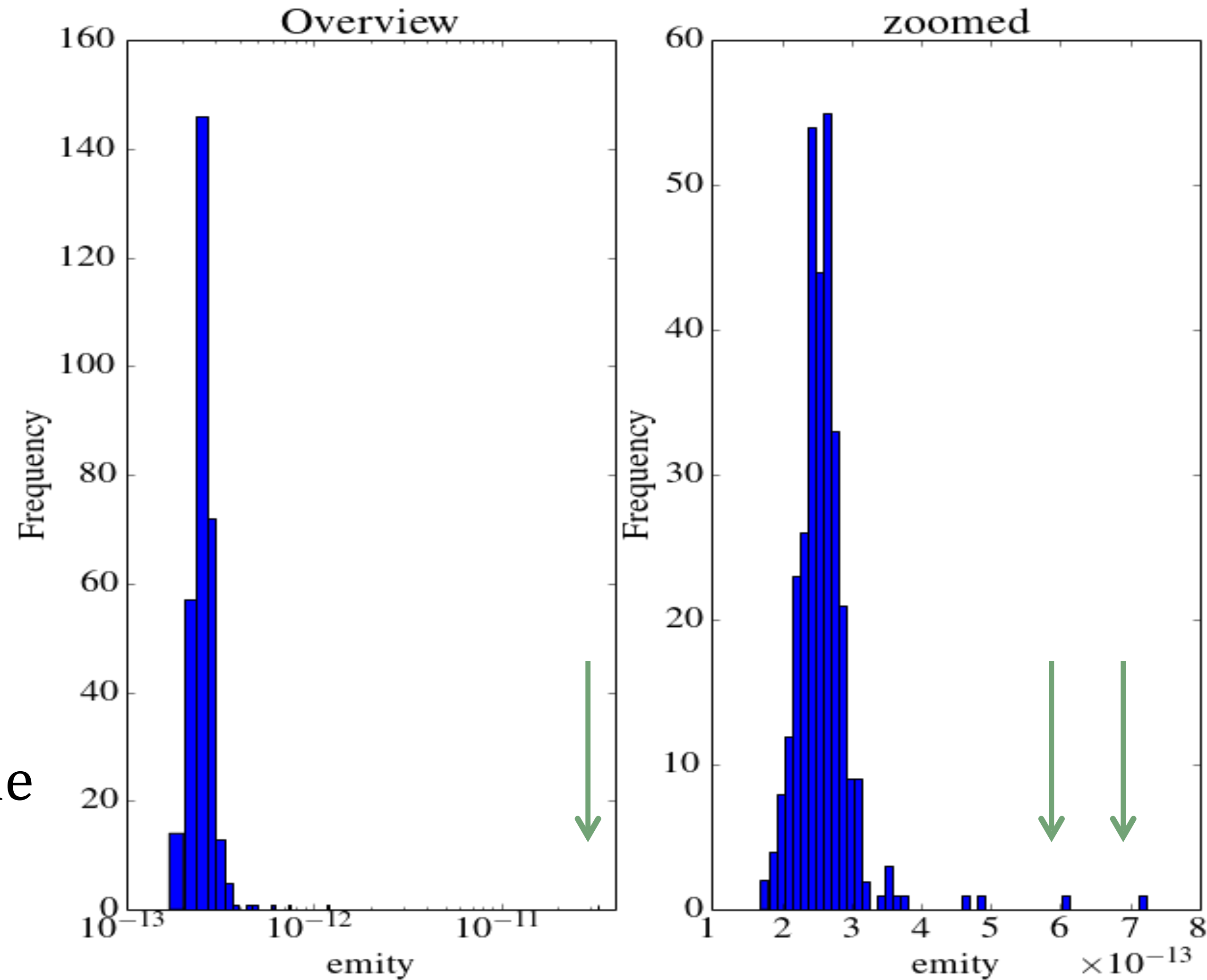
$$\varepsilon_y = 0.36 \text{ pm}$$

$$\varepsilon_x = 1.25 \text{ nm}$$

$$\varepsilon_y / \varepsilon_x = 0.0003$$

→ Sextupole misalignments dominate the source of vertical emittance

Larger vertical dispersion > millimeters



- Vertical dispersion and coupling are successfully corrected.
- Arc quadrupoles and sextupoles do not need special care, so far.
- The sextupole misalignments contribute the most to the vertical emittance budget with $\epsilon_y=0.3 \text{ pm}$
- Introduction of misalignments in the FF quadrupoles:
 - The treatment of the FF roll angle need a special treatment with a local correction.
 - Work on going for more statistics for H&V displacement of the FF quadrupoles.
- Packed multi-coil H&V kicker, corrector skew + FF quadrupoles will be a condition sine qua none !!
- Next steps:
 - Treatment of the FF quadrupoles, BPM errors.
 - Relax the tapering, move kicker after sextupoles (less correctors)
 - DA studies on going.

Quadrupoles of the arcs (no FF)

$$\Delta x = 100\mu m, \Delta y = 100\mu m, \theta = 100\mu rad$$

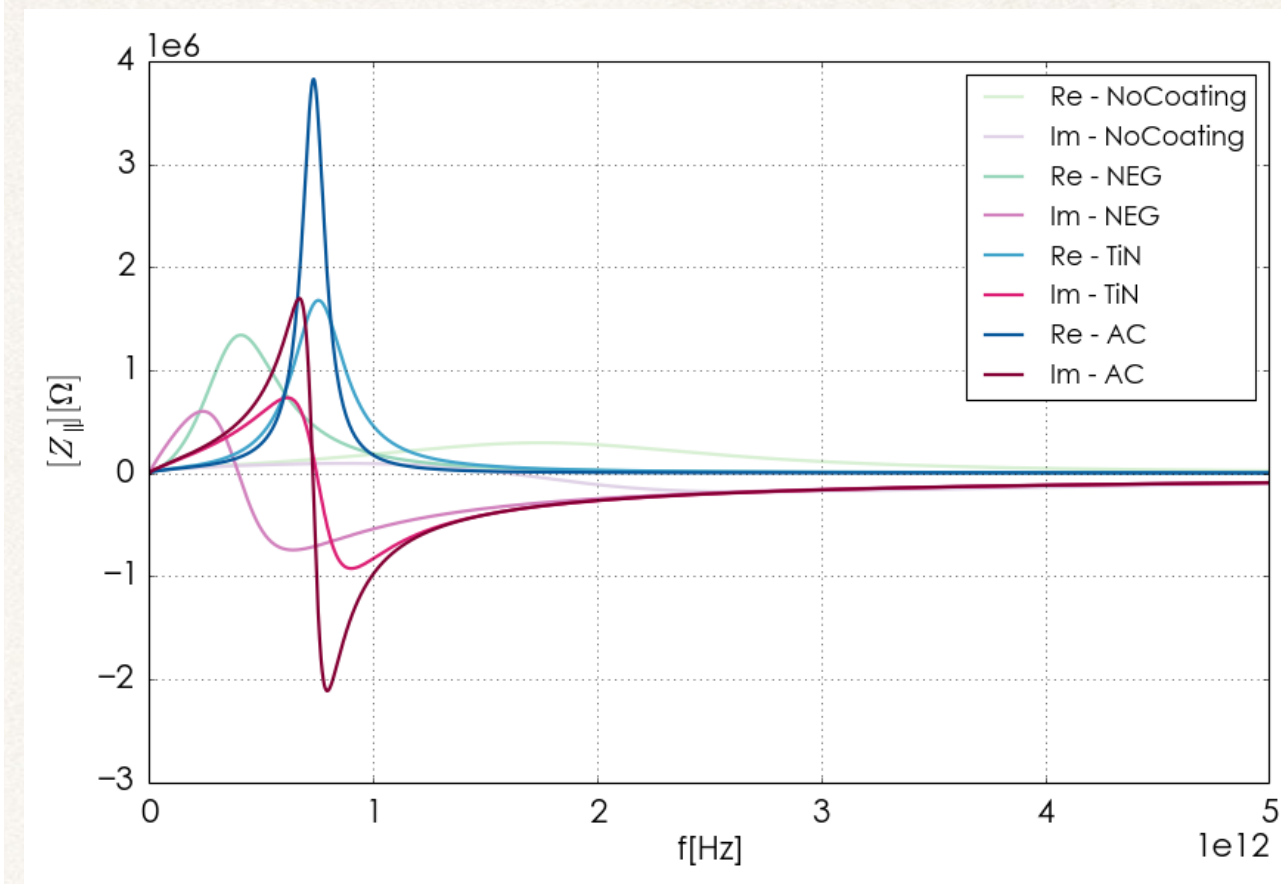
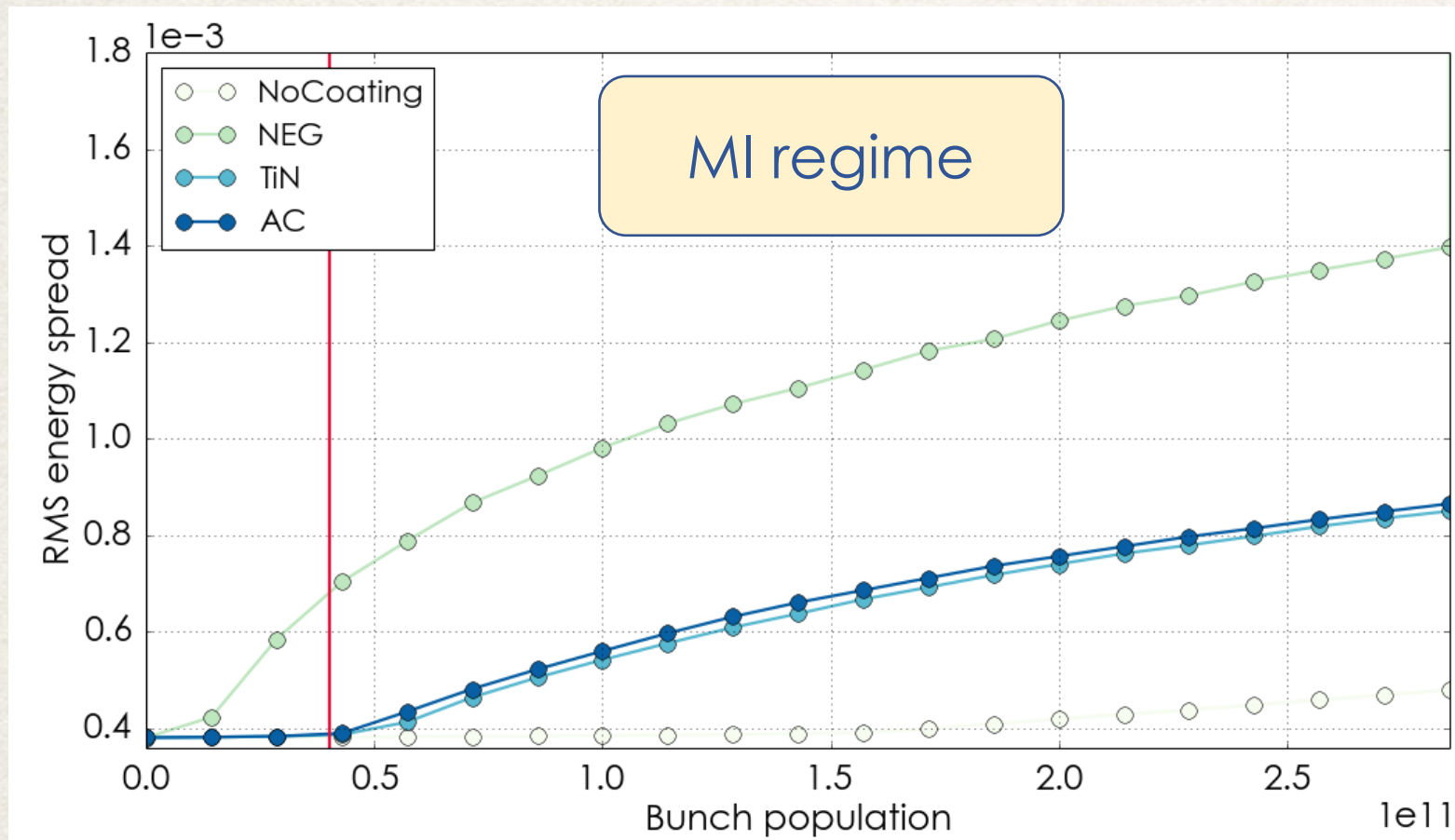
Sextupoles

$$\Delta x = 100\mu m, \Delta y = 100\mu m, \theta = 0\mu rad$$

BPMs < 100μm in x&y planes

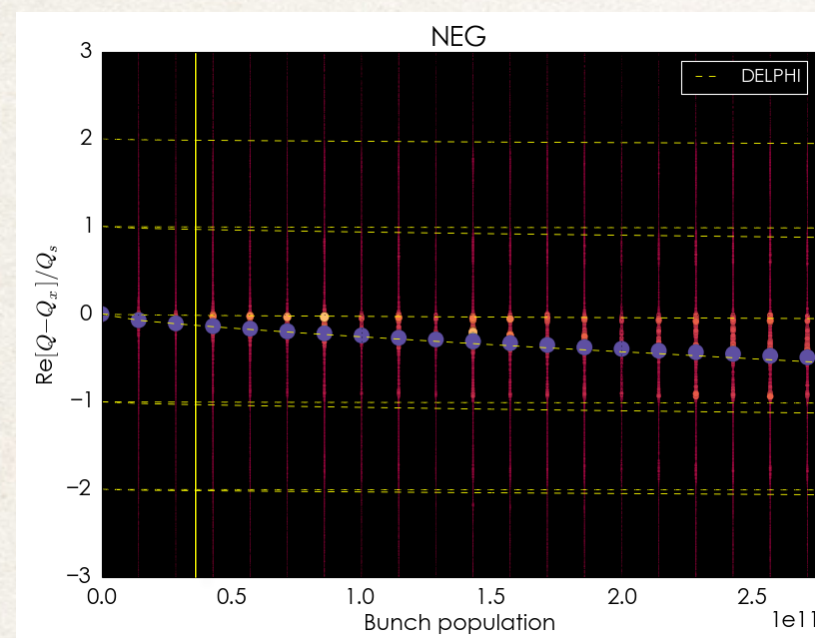
Independent simulations by E. Gianfelice-Wendt, E. S. Sinyatki, and H. Sugimoto also show similar levels of the tolerances.

Long. Microwave Instability



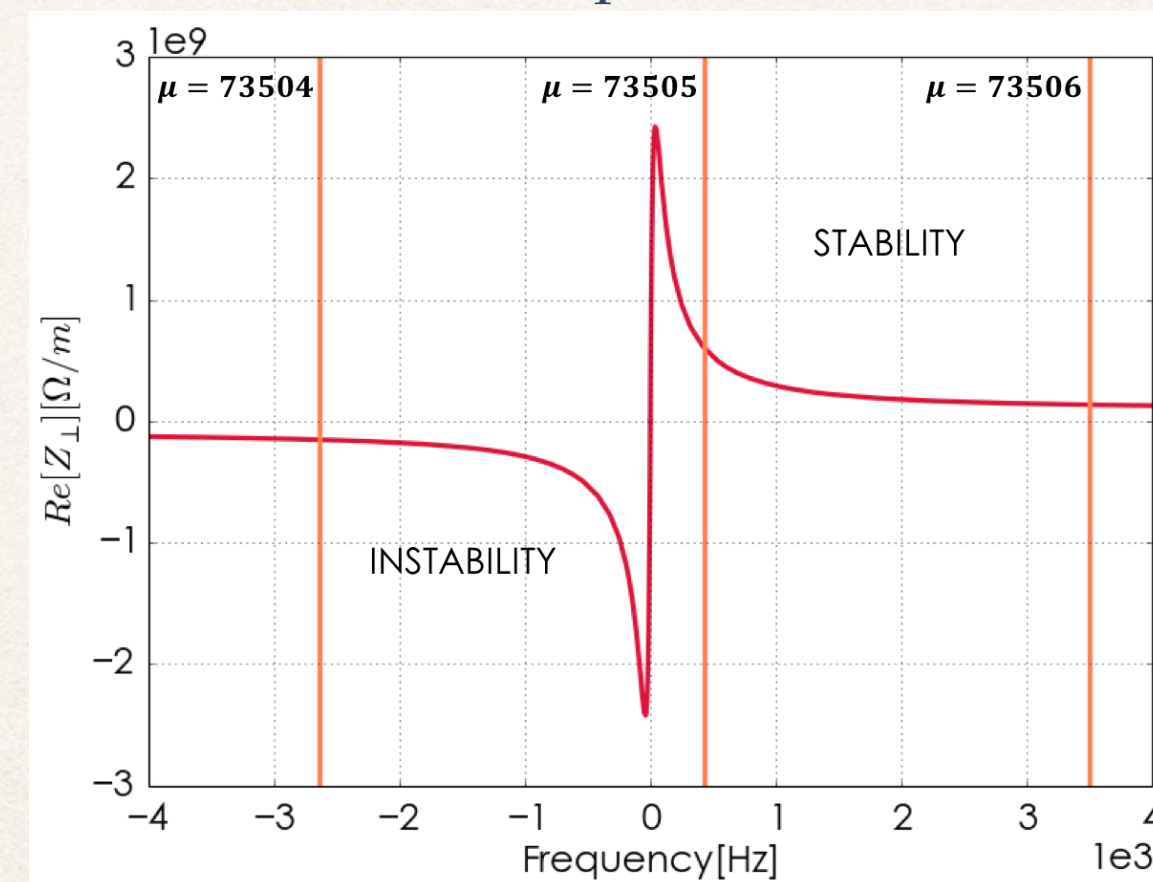
- The effects of the resistive wall on the beam dynamics have been analyzed
 - ❖ No Beamstrahlung: MI regime, i.e. the beam would be unstable (for NEG MI threshold is below the nominal bunch intensity)
 - ❖ Beamstrahlung allows to have stable beams
 - injection with alternating beams would allow a good margin of safety
 - ❖ TMCI not dangerous: threshold far beyond the nominal bunch intensity
 - ❖ Robust feedback system required for the fast (6 turns) transverse instability suppression
 - ❖ Maximum allowed shunt impedance of a HOM as a function of its resonant frequency estimated

TMCI (w/ NEG)



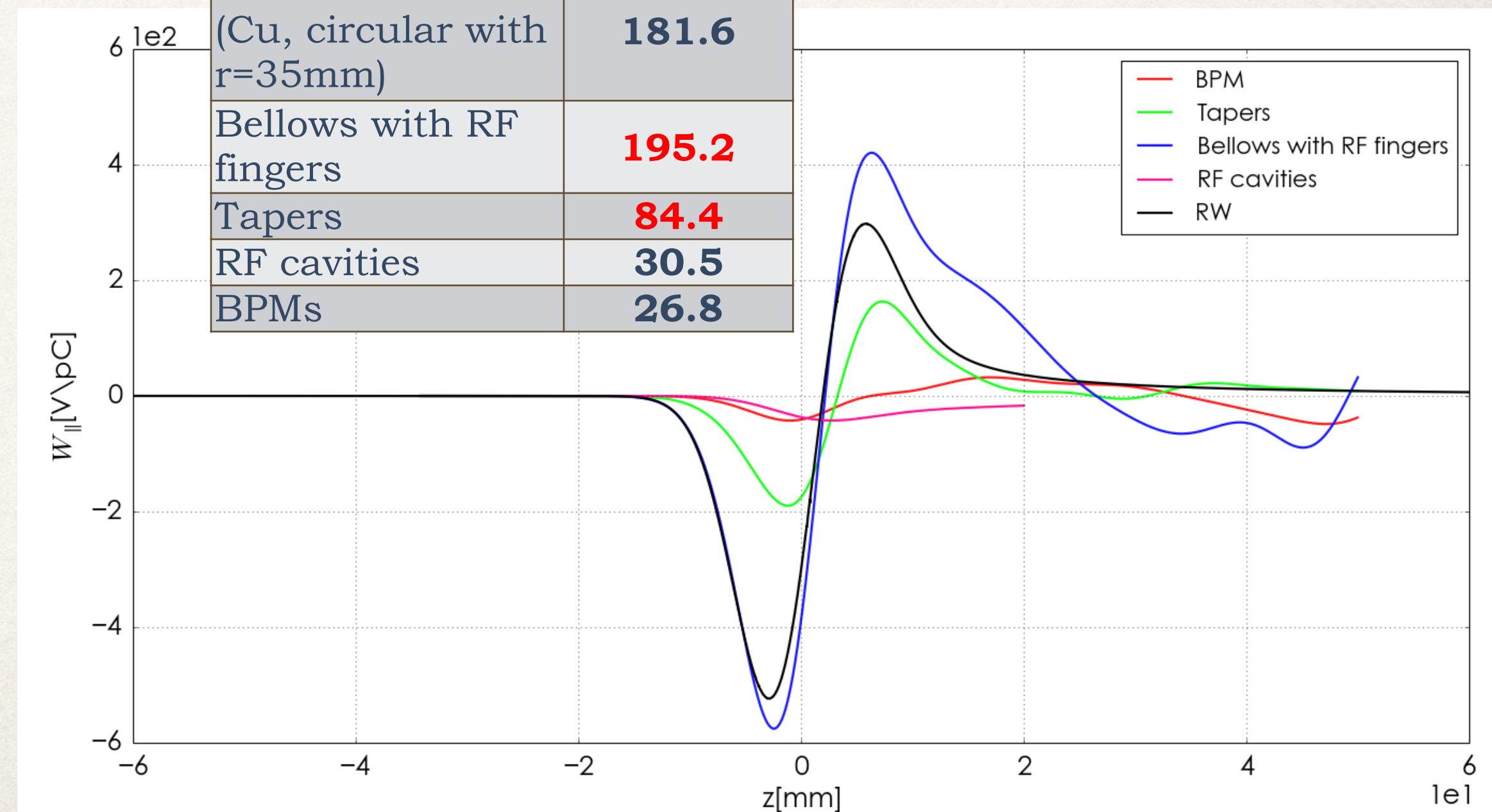
TMCI seems to be not dangerous

Trans. coupled bunch

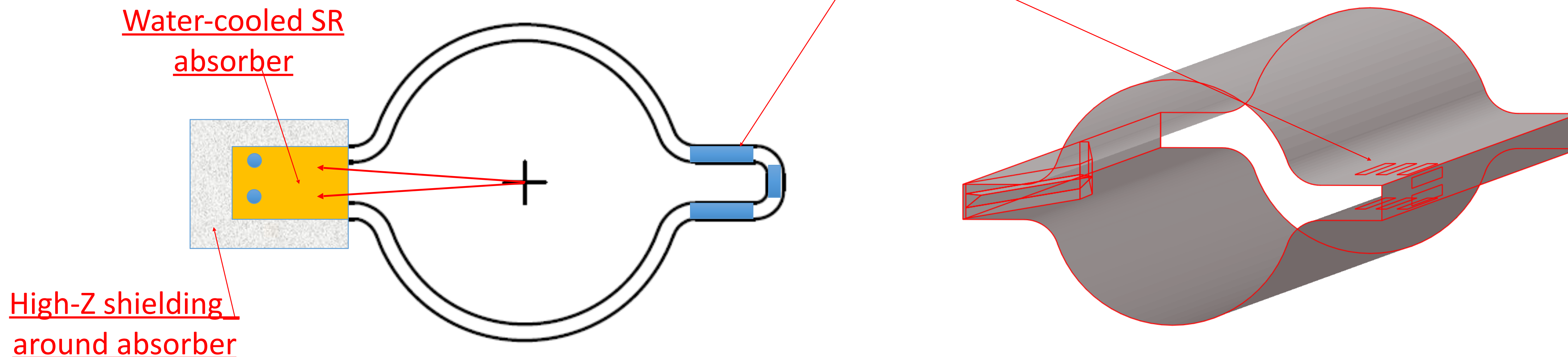


Robust feedback for instability suppression

	k_loss [V/pC]
Resistive Wall (Cu, circular with r=35mm)	181.6
Bellows with RF fingers	195.2
Tapers	84.4
RF cavities	30.5
BPMs	26.8



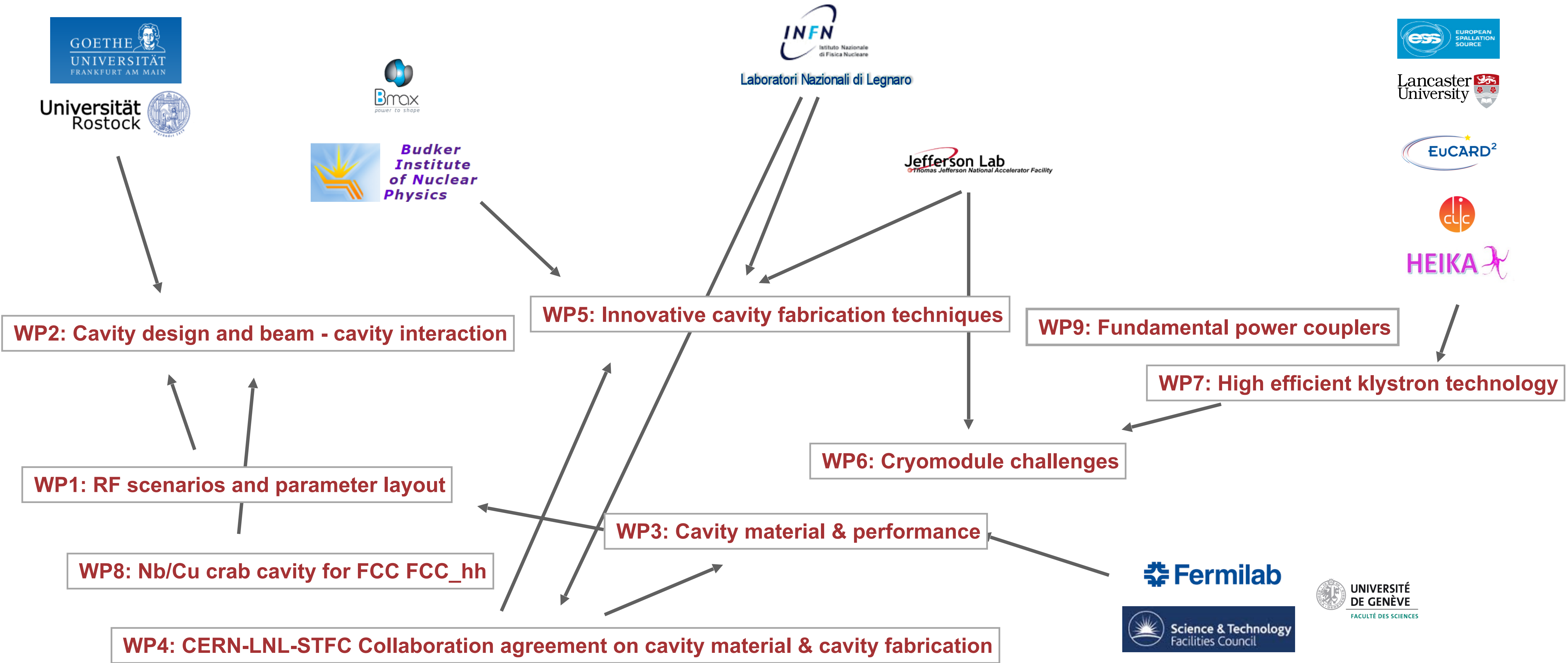
- The integration of the vacuum system with the design of the arc magnets has lead us to the decision to adopt a **SuperKEKB-like vacuum chamber (VC) cross-section**;
- The cross section looks like this:



- It has a 70 mm diameter (internal) circular shape with two 25x10 mm² (HxV) rectangular “winglets” on both sides of it, in the plane of the orbit;
- The winglet on the external side is used to host a number of **lumped synchrotron radiation (SR) absorbers**, so that all of the primary SR fan generated along the arc dipoles is collected on them;
- Careful **ray-tracing** tells us that we would need on average **one SR absorber every 5 meters or so**;
- The absorbers have a **tapered shape**, taking into account the need to minimize their impact on the geometric impedance of the machine. Each absorber has to deal with between 3 and 4 kW of SR power, a value similar to present-day light sources or B-factories;

- The winglet on the internal side is used to machine **pumping slots** in front of the absorbers: this allows an optimized pumping configuration, which minimizes the impact of the residual gas pressure on the stored beams;
- **Monte carlo simulations of the pressure profiles** have shown that, especially for the low-energy, high-current Z-pole machine, using lumped pumps installed in front of each absorber would not be sufficient to guarantee a reasonably fast **vacuum conditioning**. On the other hand, if **distributed pumping** of some sort could be envisaged, like it was done in LEP, then the pressure profiles could be greatly improved, and the conditioning time shortened;
- The internal winglet can also be used to install **distributed NEG pumps** based on a “stacked” design, i.e. 3 layers of NEG strips laying one on top of each other with small spacers in between them and integrated heaters for NEG activation: this solution has been successfully developed for the SuperKEKB rings;
- Finally, after some optimization, **we propose an arc vacuum pumping system based on distributed NEG strips and one lumped pump per 25 m arc length**;
- **Material for the vacuum chamber**: the higher-energy versions of the machine, W-, H-, and T-pole, have critical energies at or above the Compton edge (~ 100 keV photon energy), and therefore **copper is preferred to aluminium** in order to minimize radiation leakage and the related radioprotection and material damage issues;
- A small fraction of the SR fan is finally absorbed on the walls of the vacuum chamber (VC), due to the non-zero reflectivity of the absorbers’ copper surfaces. This inevitable “stray” photon flux, about 5% for the Z-pole machine, is potentially capable of generating a large amount of photo-electrons, which in turn can trigger the e-cloud effect;
- We are therefore proposing to integrate into the arc vacuum system design also some **e-cloud mitigation features**, such as **grooved surfaces** (see SuperKEKB developments) and/or **thin-films, like titanium nitride or amorphous carbon**;
- **Other vacuum components**: the developments carried out at SuperKEKB, such as comb-type RF contacts for bellows and gate valves, seem to guarantee low-impedance component design, and therefore its adoption is suggested;

Work Package structure and collaborations for FCC RF system

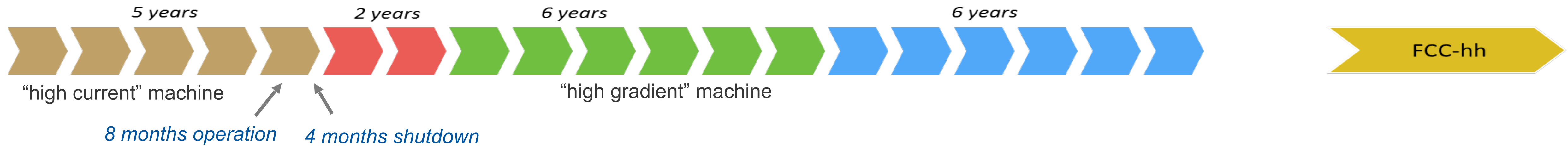


Framework of the study of the RF system

“high current” machine

	<u>V_tot (GV)</u>	<u>n_bunch</u>	<u>I_beam (mA)</u>	σ (mm)	<u>E_turnloss (GeV)</u>
FCC-hh	0.032		500		
Z	0.4 / 0.2	30180 / 91500	1450	0.9/1.6	0.03
W	0.8	5260	152	2	0.33
H	3	780	30	2	1.67
t	10	81	6.6	2.1	7.55

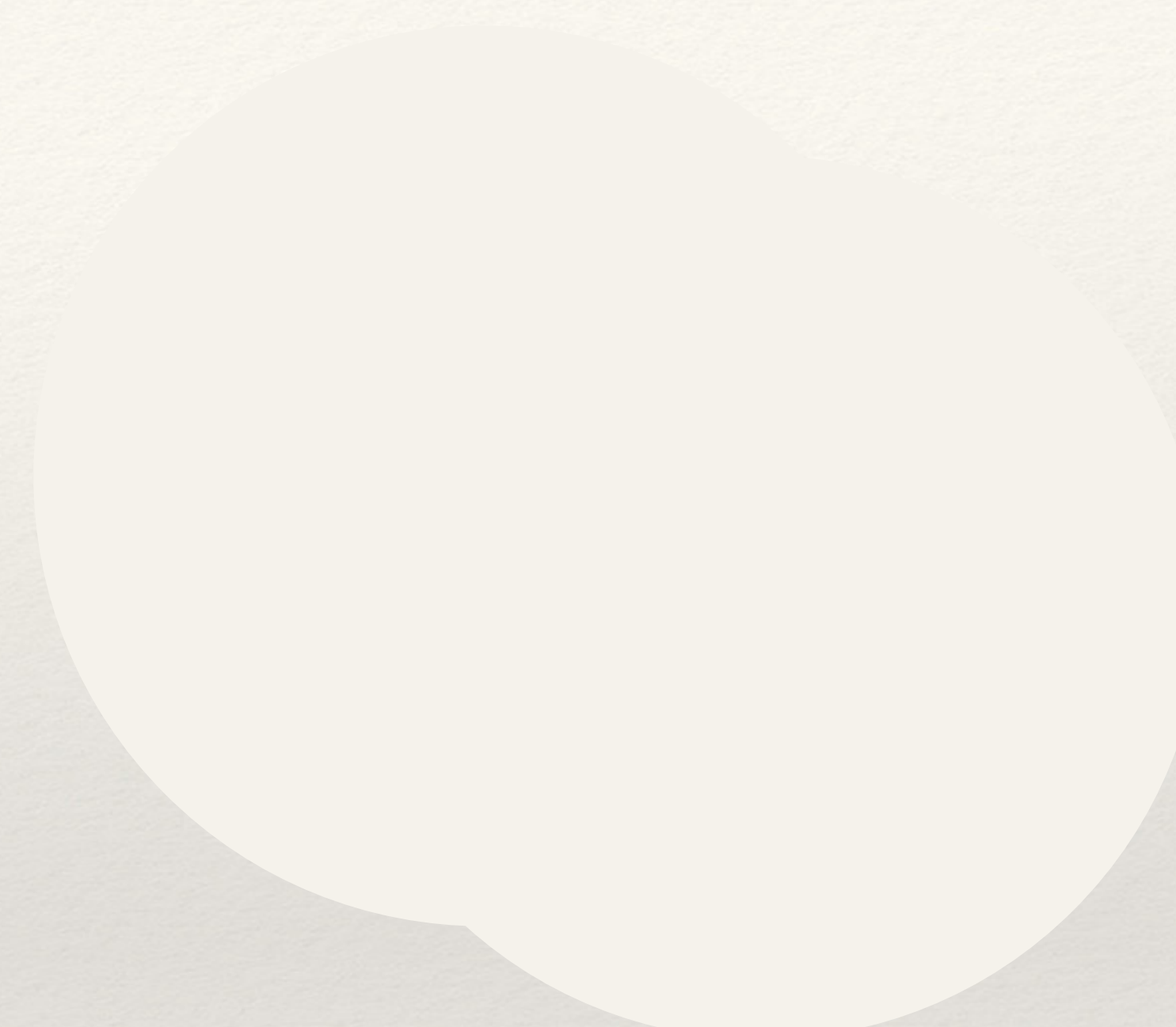
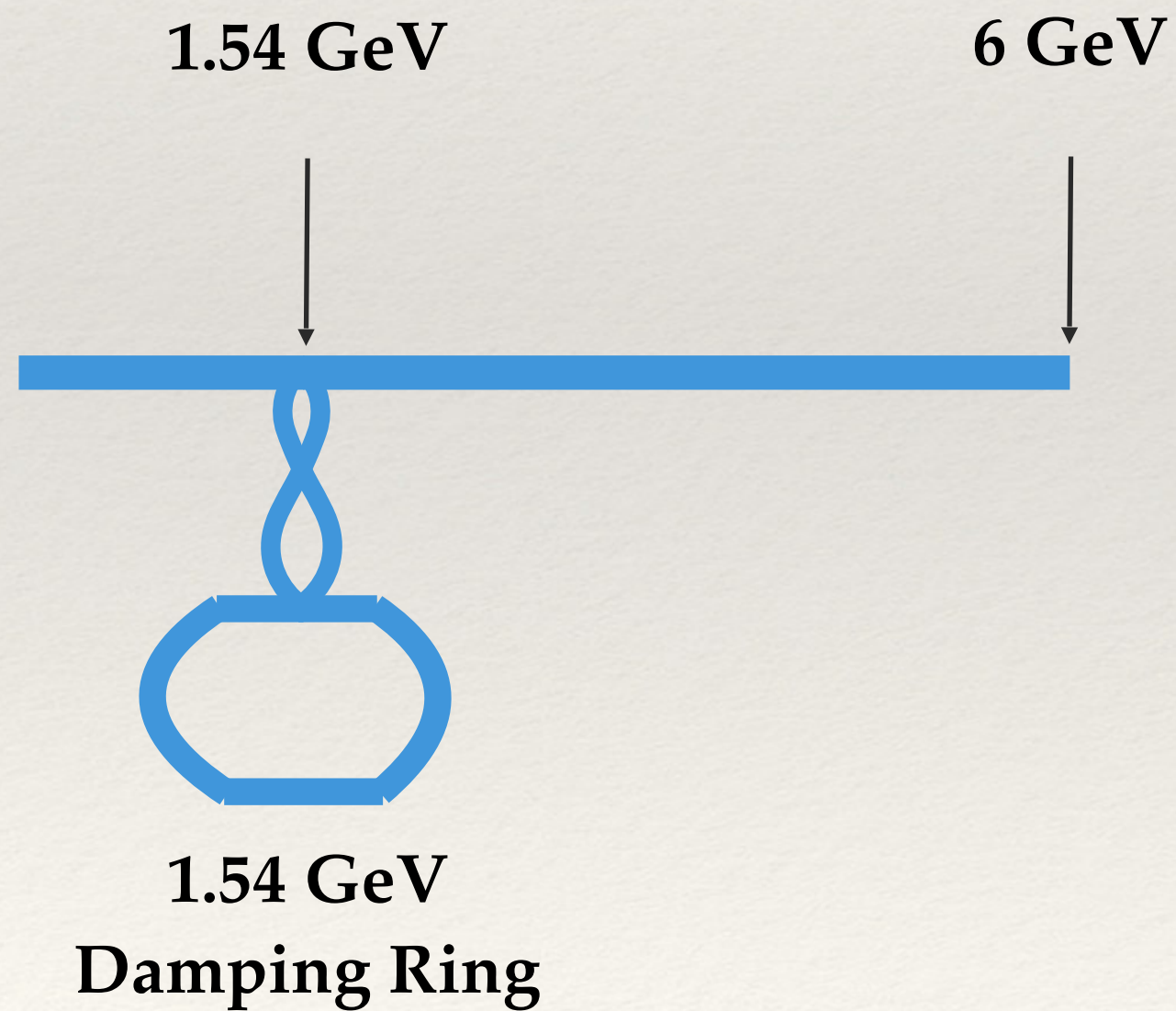
“high gradient” machine



- Define “ideal” RF system for each machine
- Identify technology choices and R&D perspectives
- Propose optimum baseline scenario (fabrication, installation, cost)



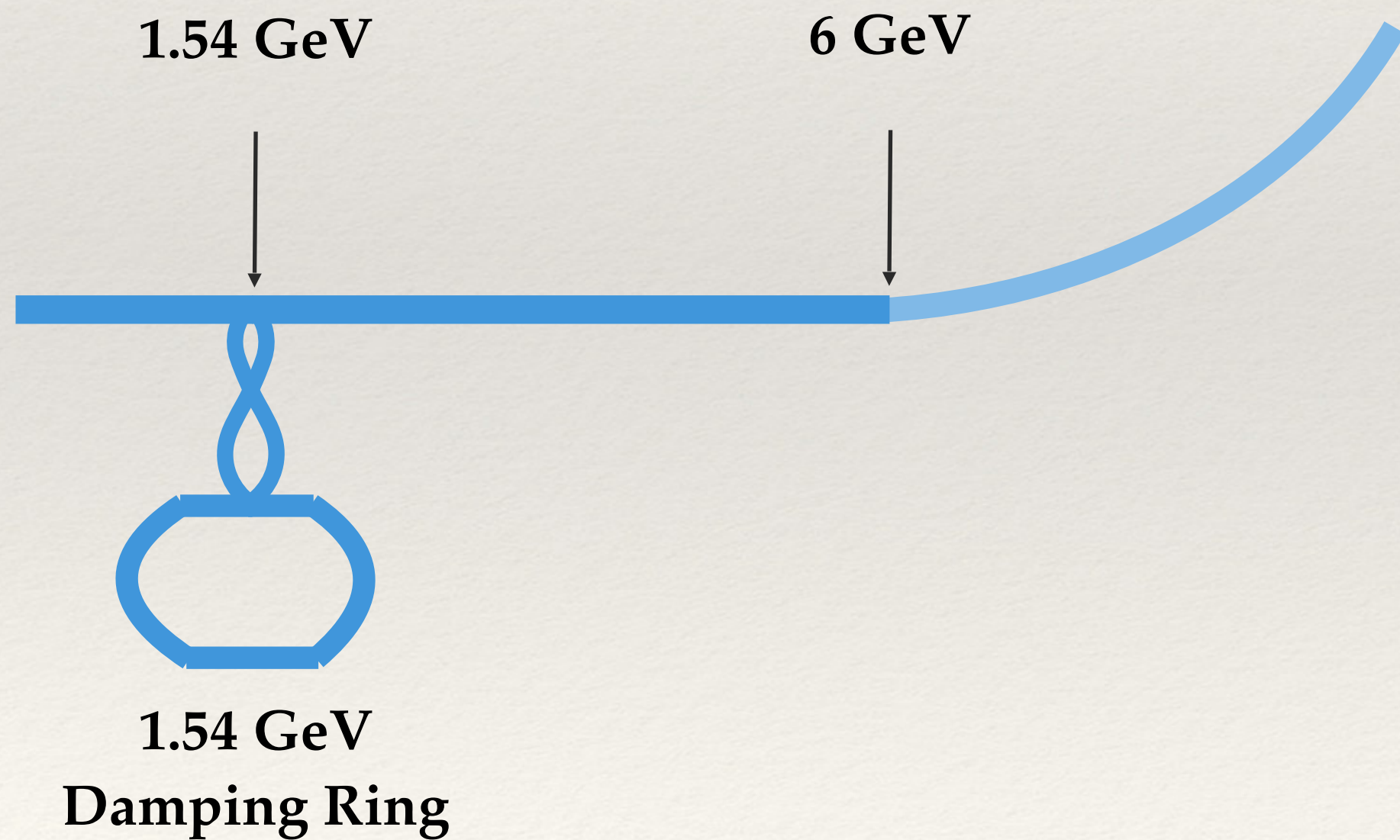
1. Electron Flow Scheme



not to scale!



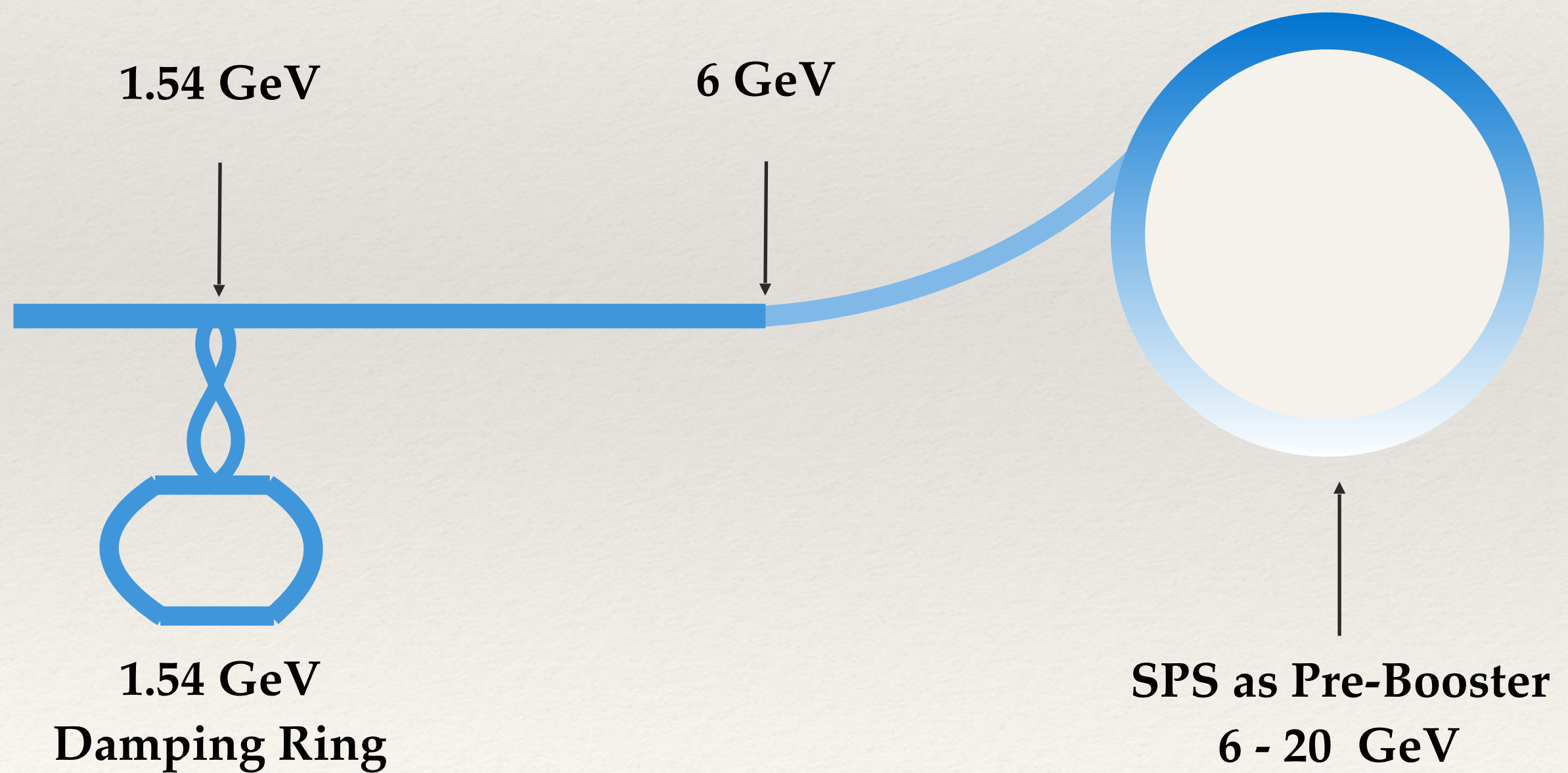
1. Electron Flow Scheme



not to scale!



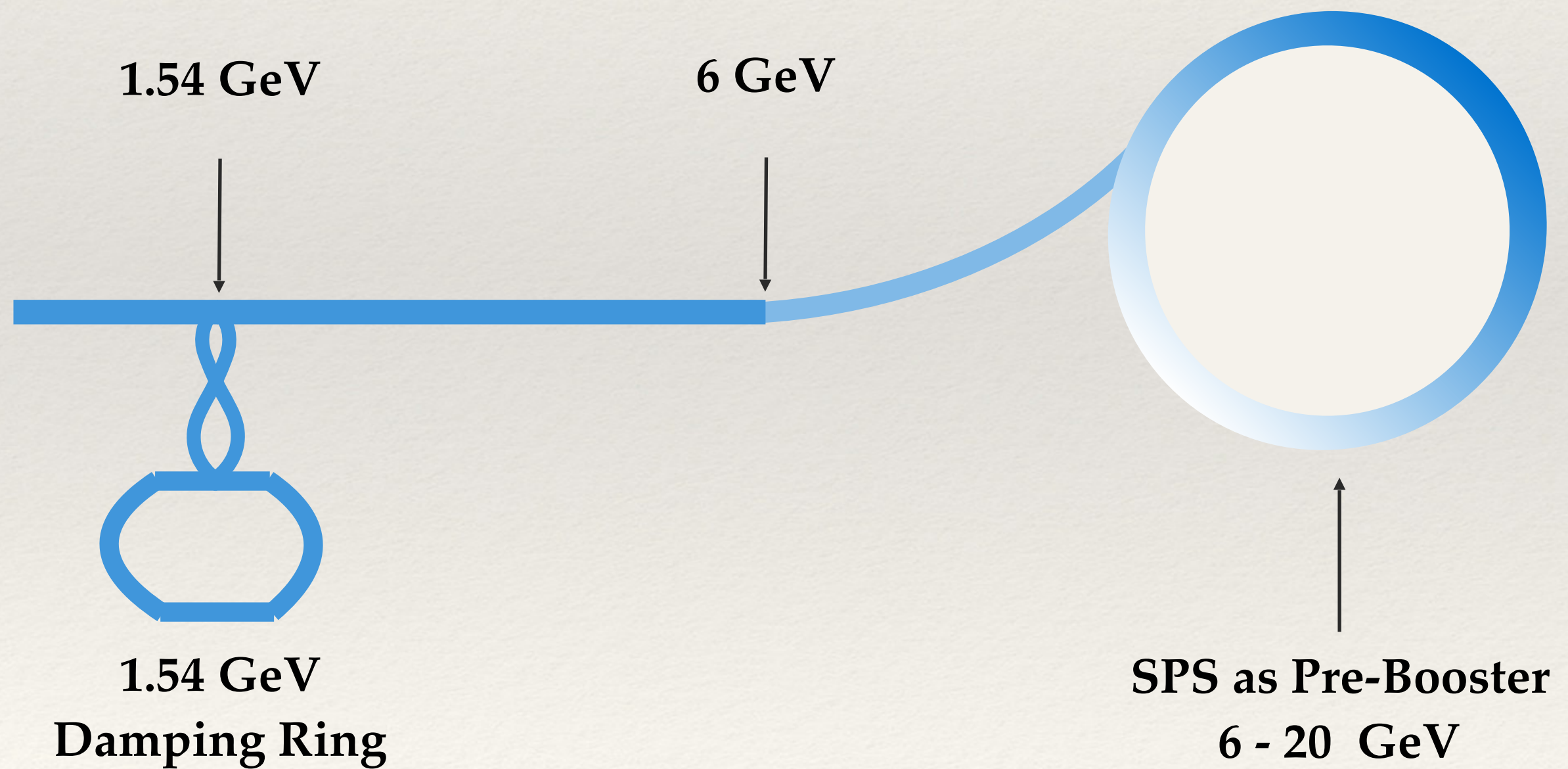
1. Electron Flow Scheme



not to scale!



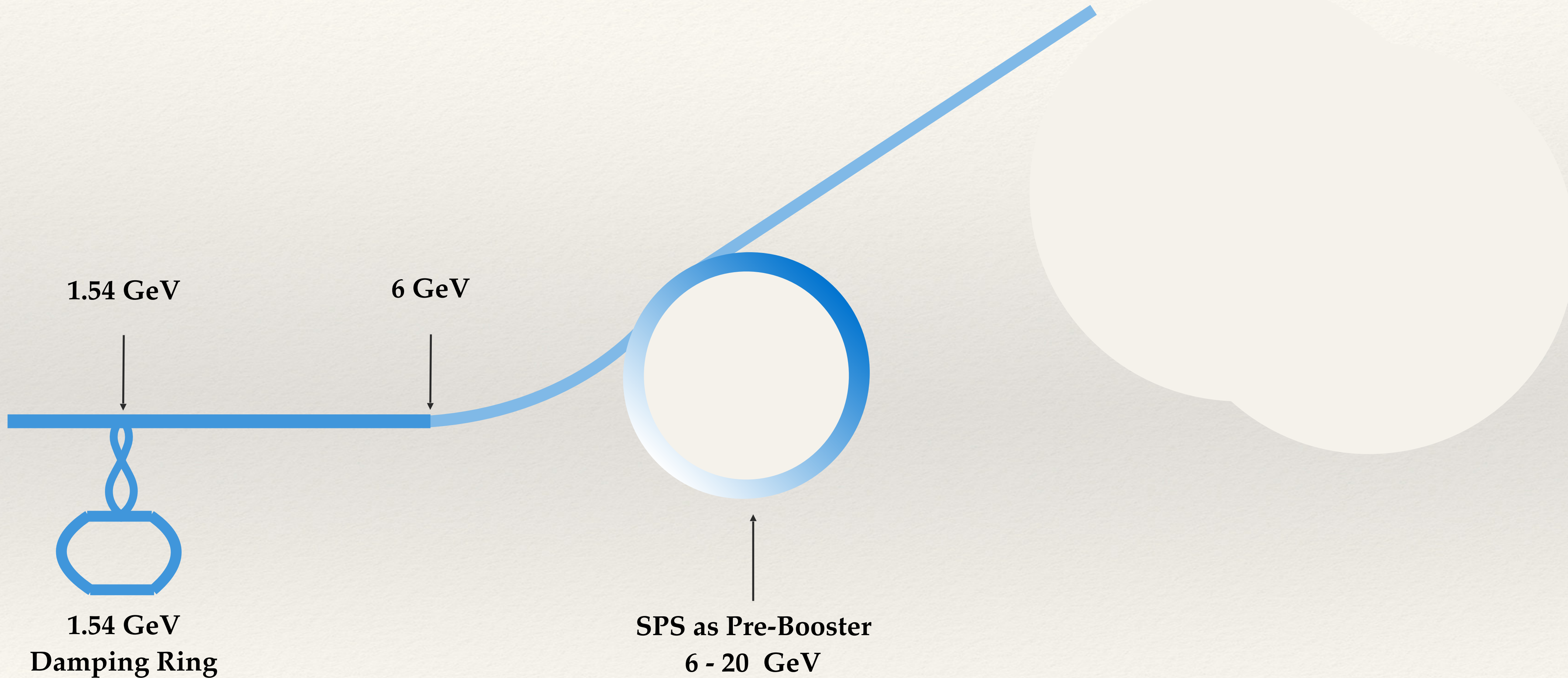
1. Electron Flow Scheme



not to scale!



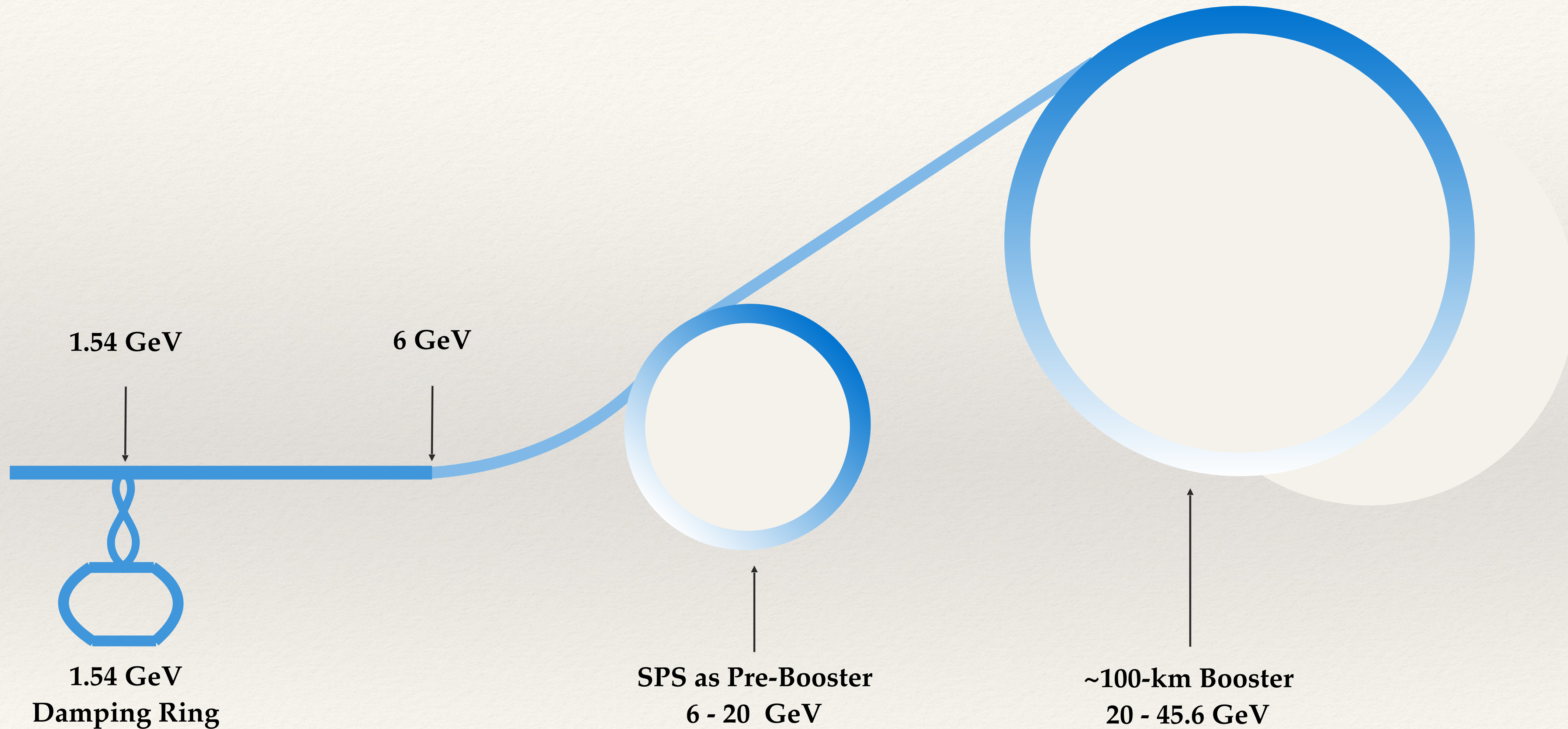
1. Electron Flow Scheme



not to scale!



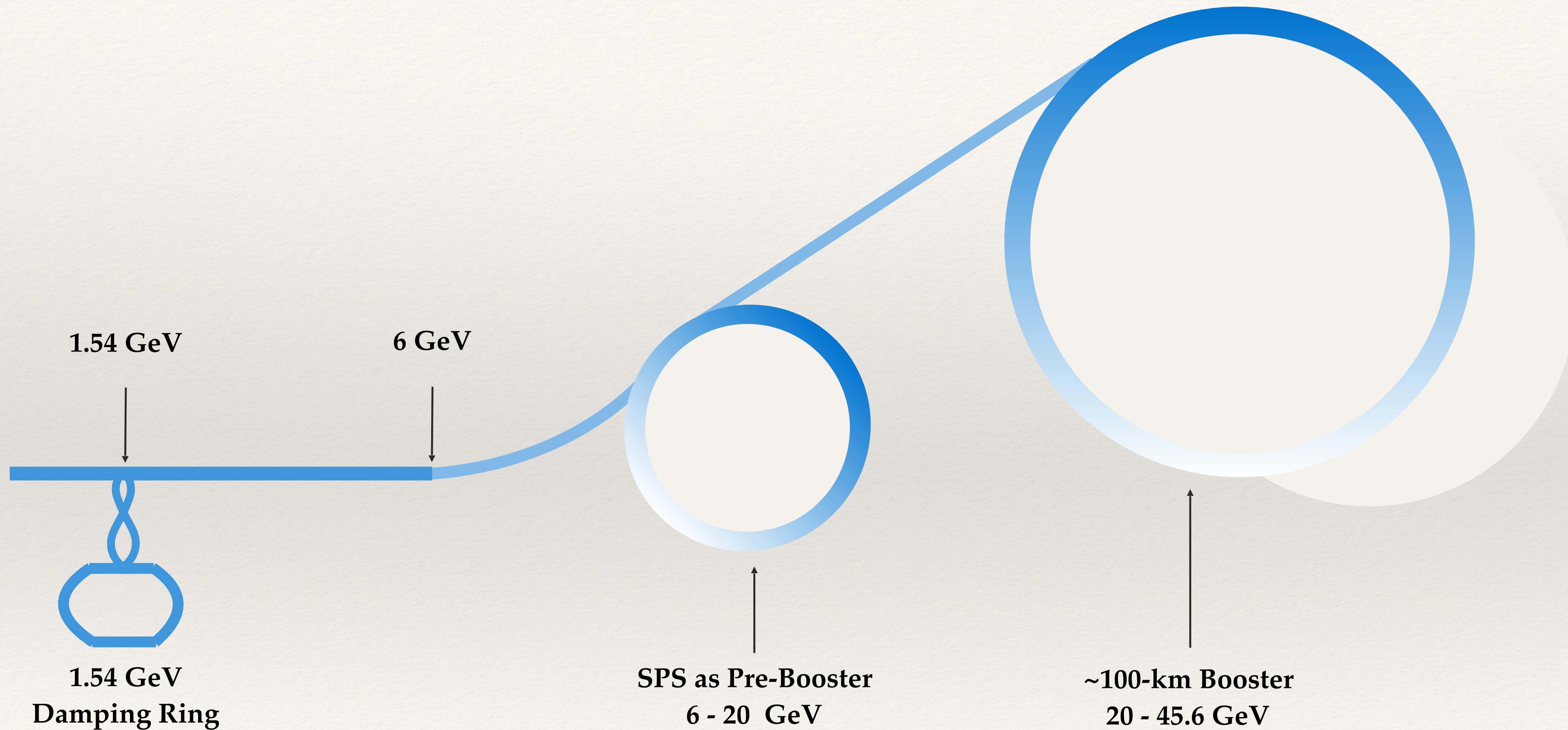
1. Electron Flow Scheme



not to scale!



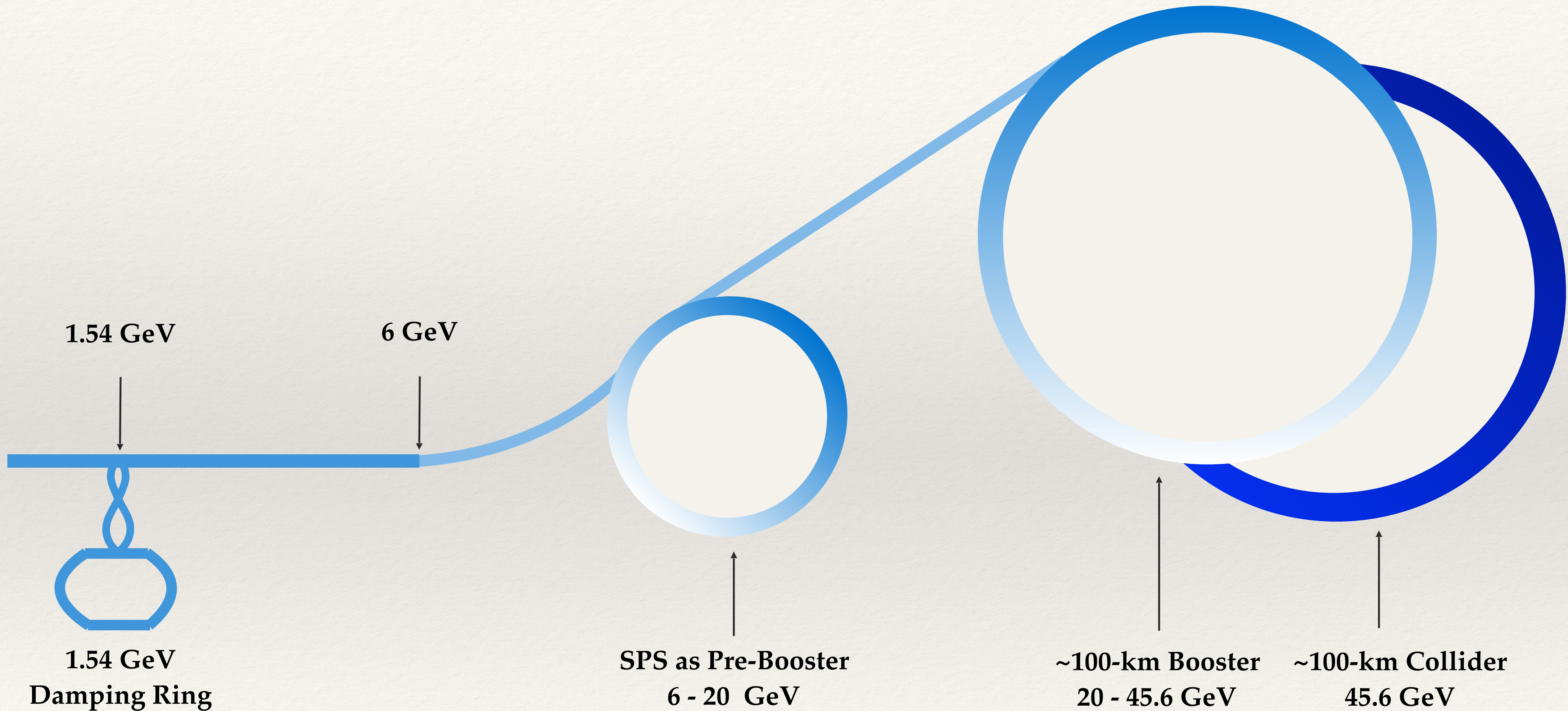
1. Electron Flow Scheme



not to scale!



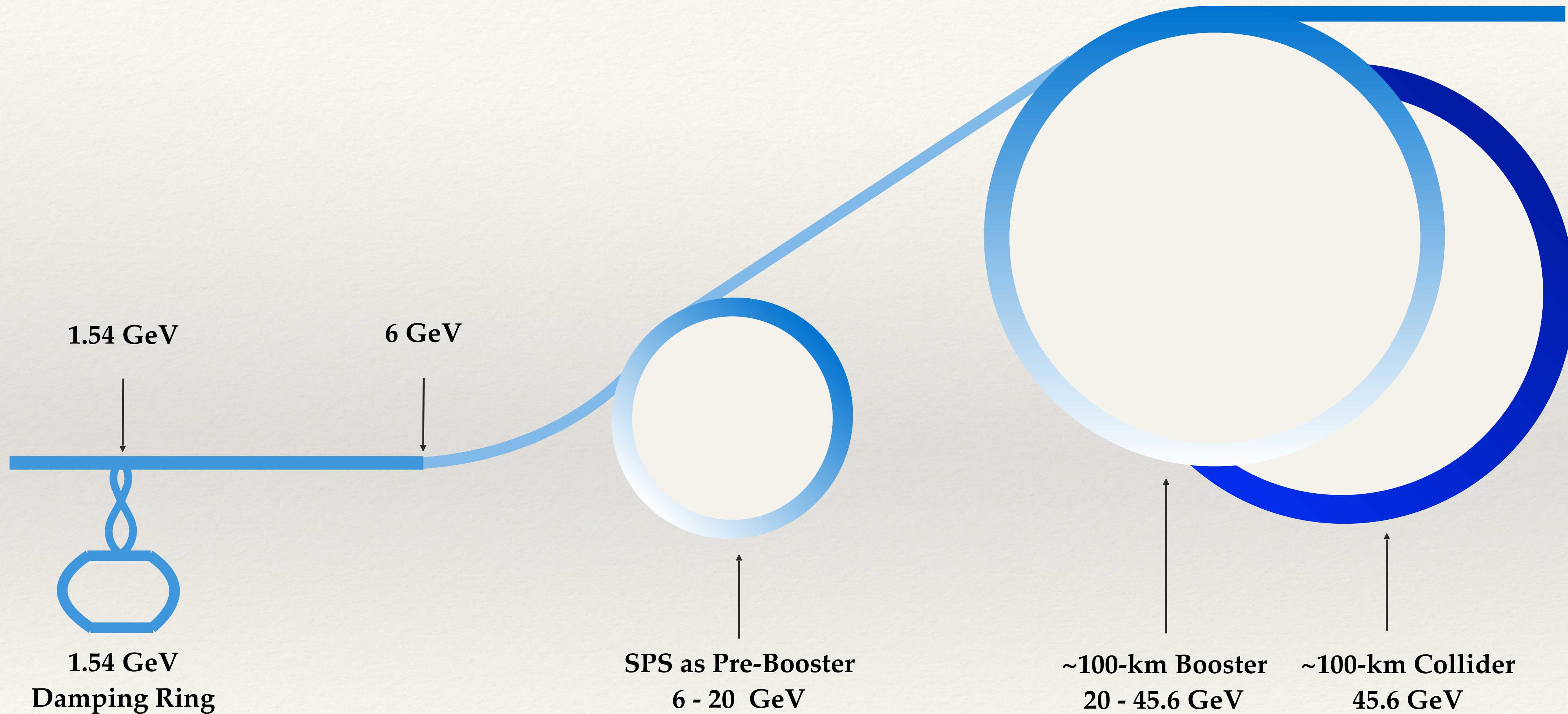
1. Electron Flow Scheme



not to scale!



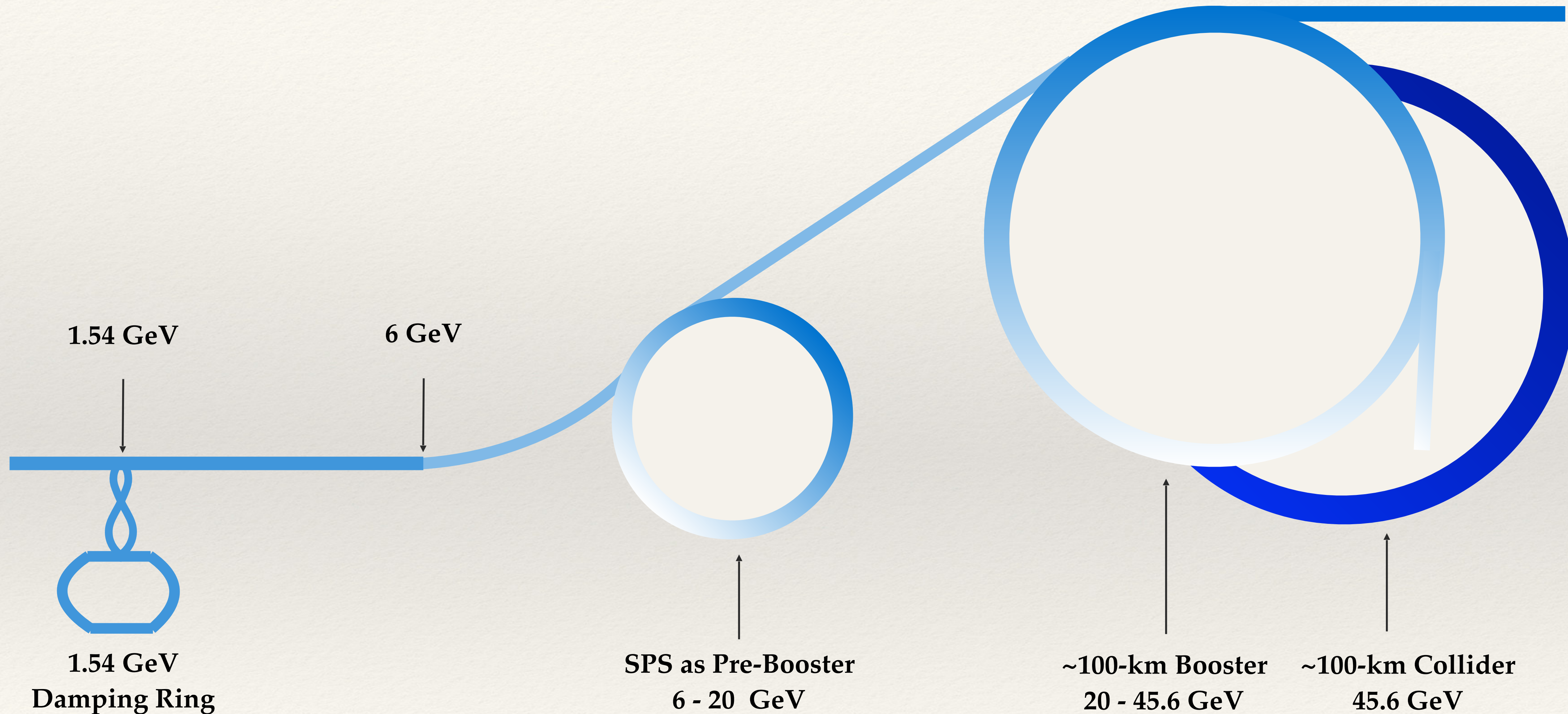
1. Electron Flow Scheme



not to scale!



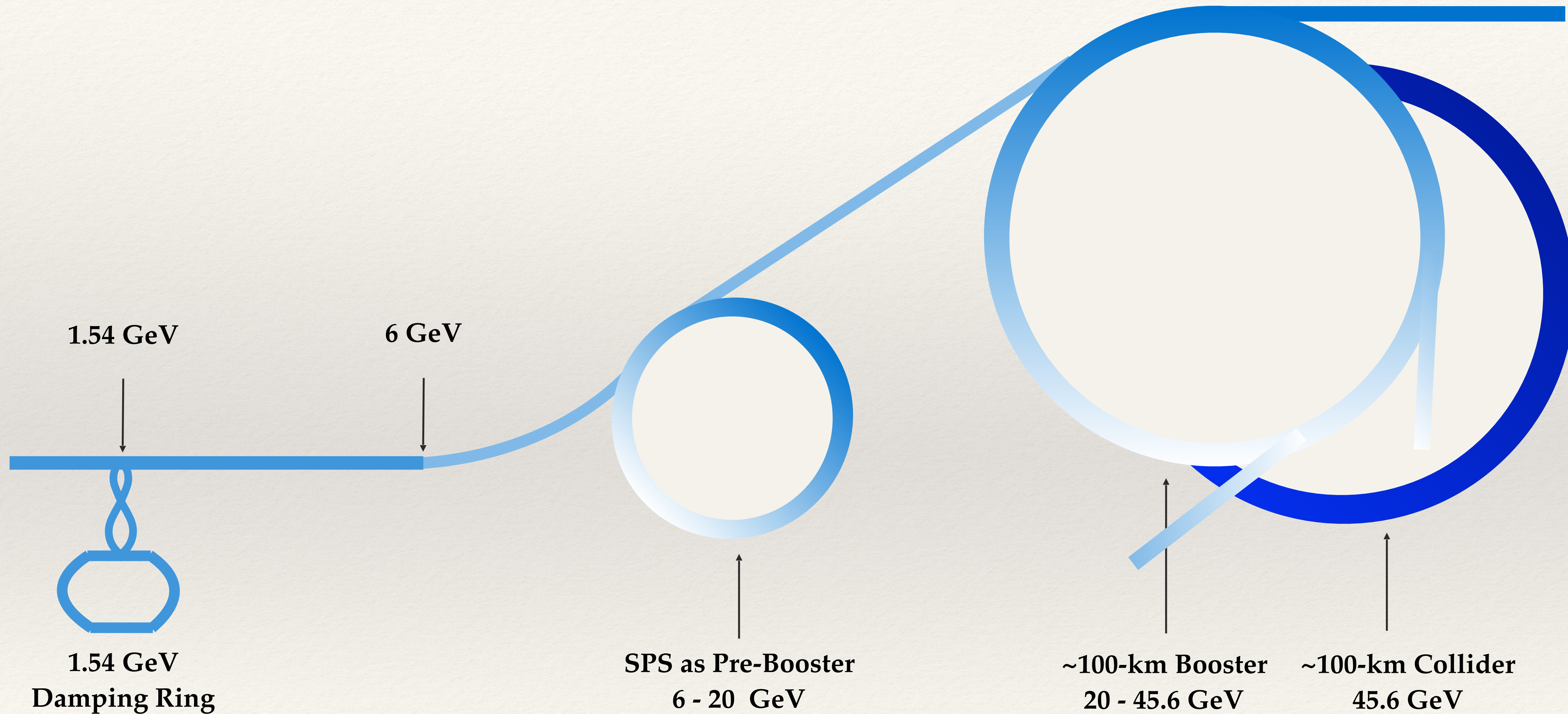
1. Electron Flow Scheme



not to scale!



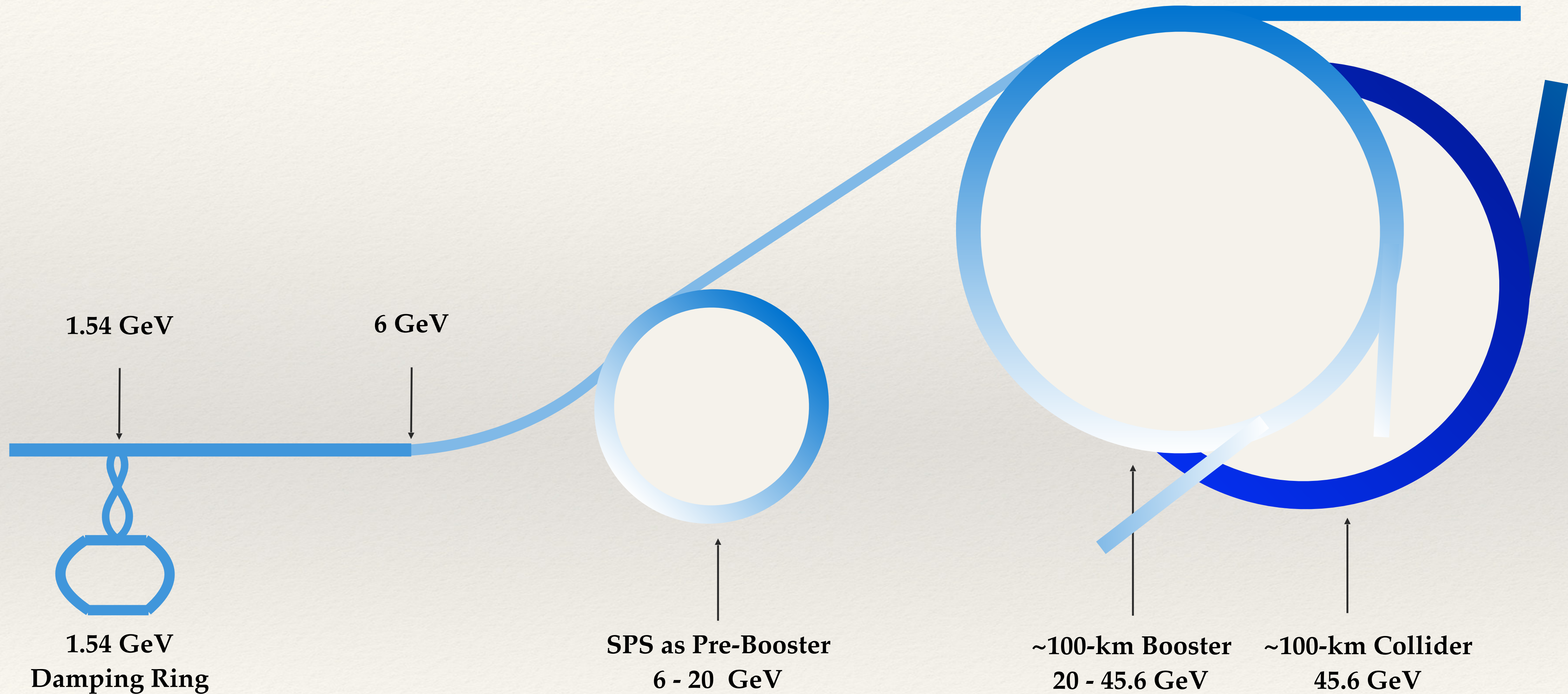
1. Electron Flow Scheme



not to scale!



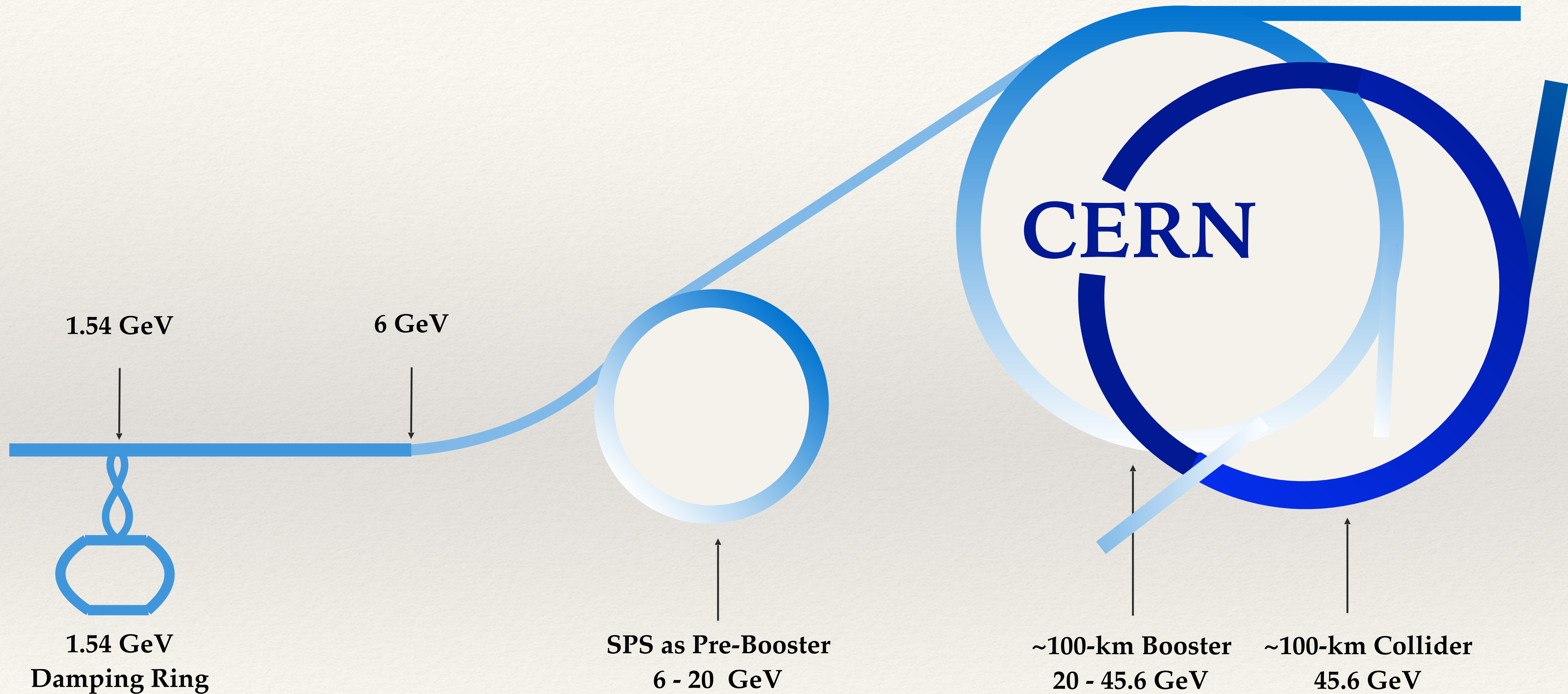
1. Electron Flow Scheme



not to scale!



1. Electron Flow Scheme



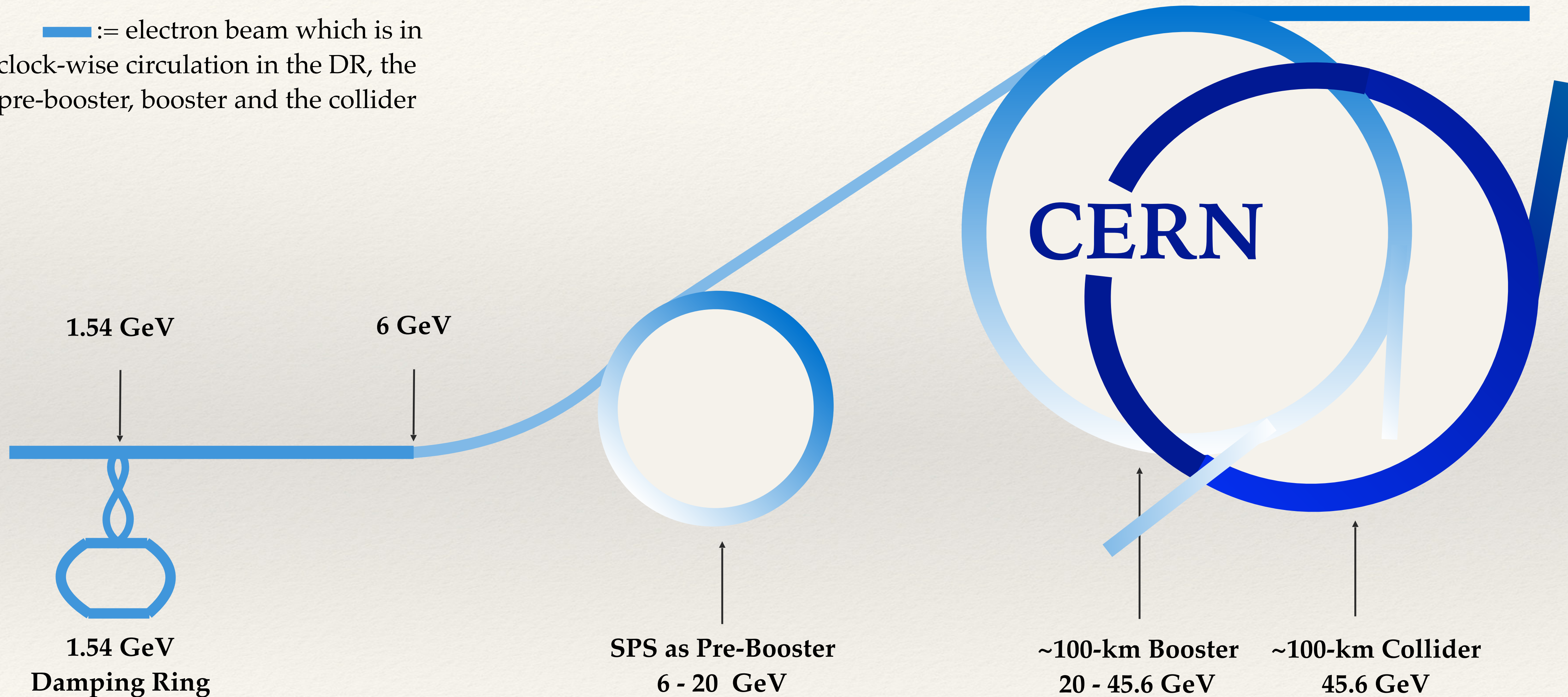
not to scale!



1. Electron Flow Scheme



— := electron beam which is in clock-wise circulation in the DR, the pre-booster, booster and the collider



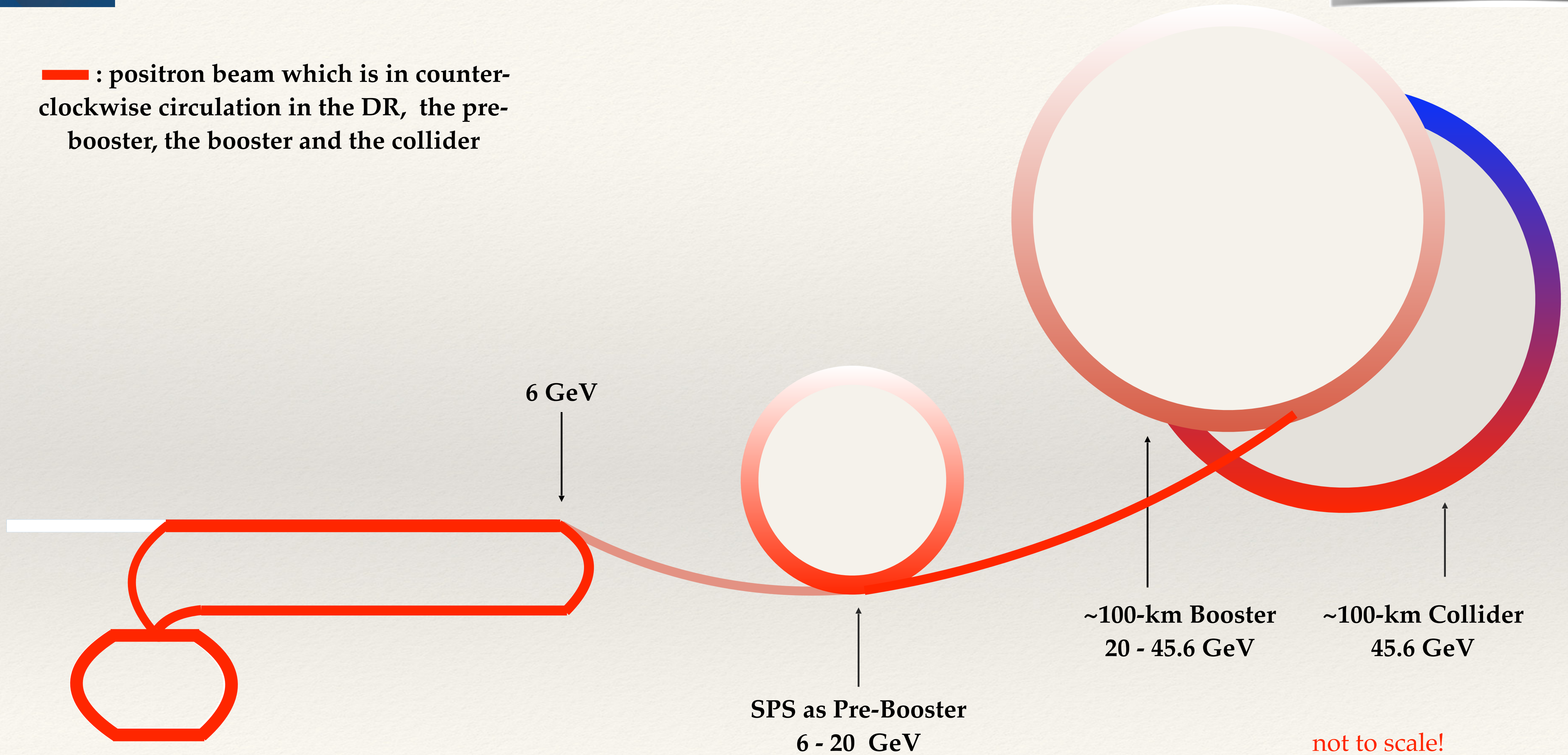
not to scale!



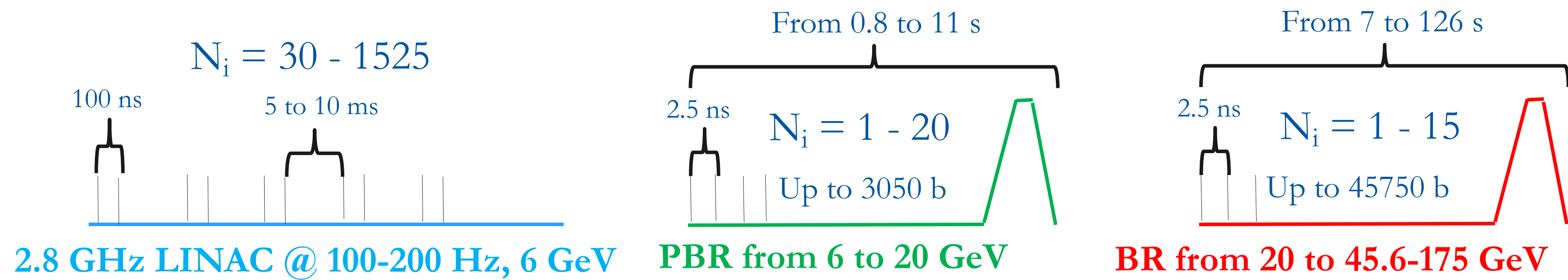
Positron Flow Scheme



— : positron beam which is in counter-clockwise circulation in the DR, the pre-booster, the booster and the collider



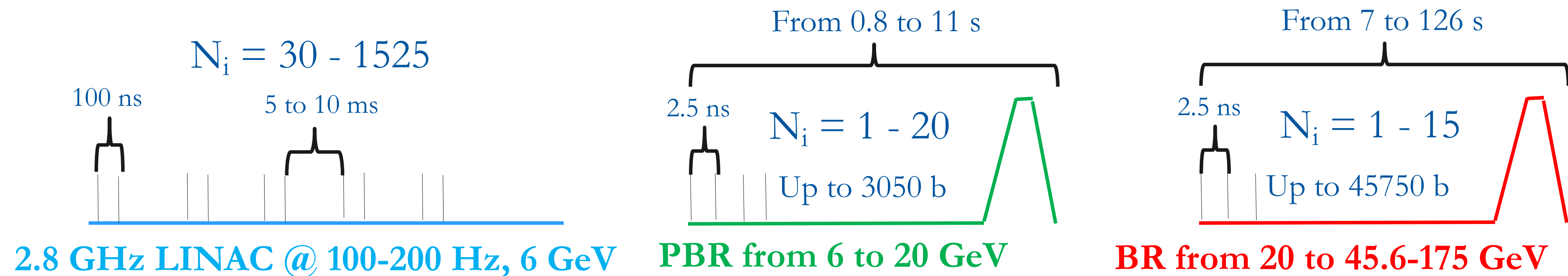
FCC-ee injector baseline scheme



FCC-ee injector baseline scheme



- **Baseline** established based on SLC/SUPERKEKB-like linac (higher gradient)
 - Longer pulses with **1 or 2** bunches with repetition rate of **100-200 Hz**, **2.8 GHz** RF
 - Maximum linac bunch intensity $\sim 2.1 \times 10^{10}$ **particles** (both species).
 - Twice as much will be needed for e-beam for e+ production
 - Injected several times (from **30 to 1525**), **@ 6 GeV** into of PBR (SPS or new ring) with 1 linac bunch to 1 ring bucket (**400 MHz** RF system), up to **3050** bunches
 - SPS ramp to **20 GeV** with **0.25 s** ramp rate and cycle length **below 11 s**
 - Transferred to main Booster (**1-20** SPS cycles), with **400 MHz** RF frequency, to a bunch structure required by the collider (from **81 to 45750** bunches)
 - Accelerated to the corresponding energy with ramp time from **2-3 s**, and total cycle length up to **126 s**
 - Transferred to the collider by accumulating current for the full filling or single injection for top-up
 - **Interleaved** filling of e+/e-
 - Full filling below **20 min** for both species
 - Top-up target time, based on **5 %** of current drop due to corresponding lifetime, always achieved
 - **80 %** transfer efficiency



Lattice for the Main Booster

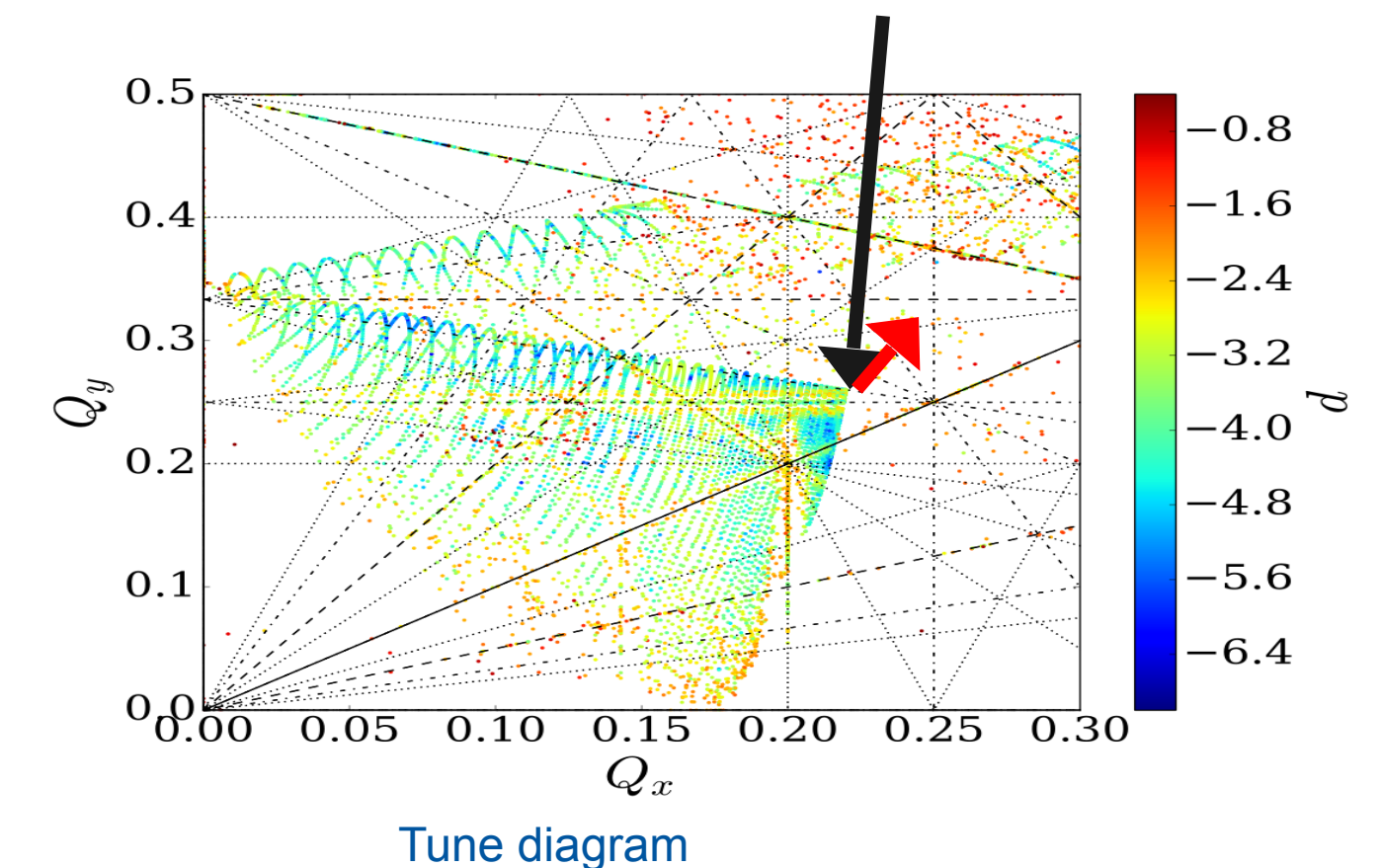
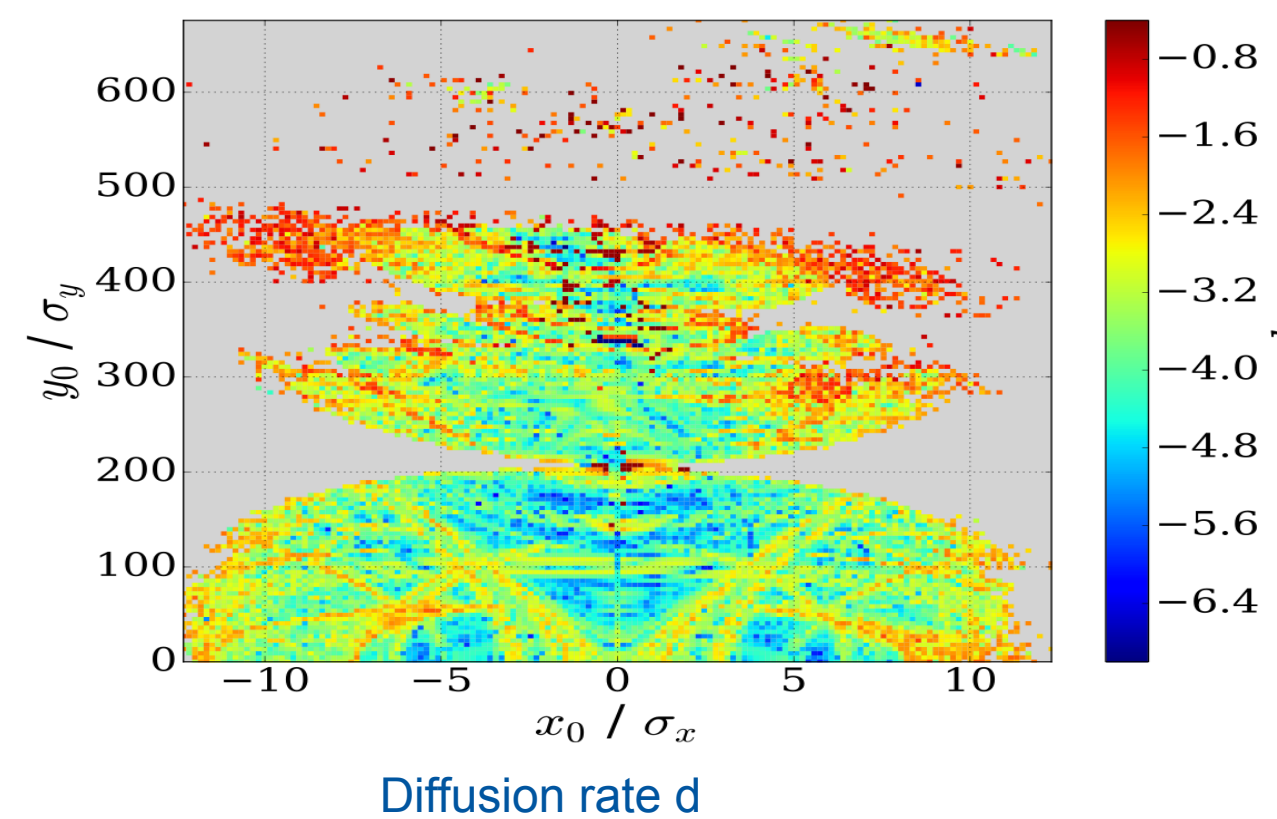
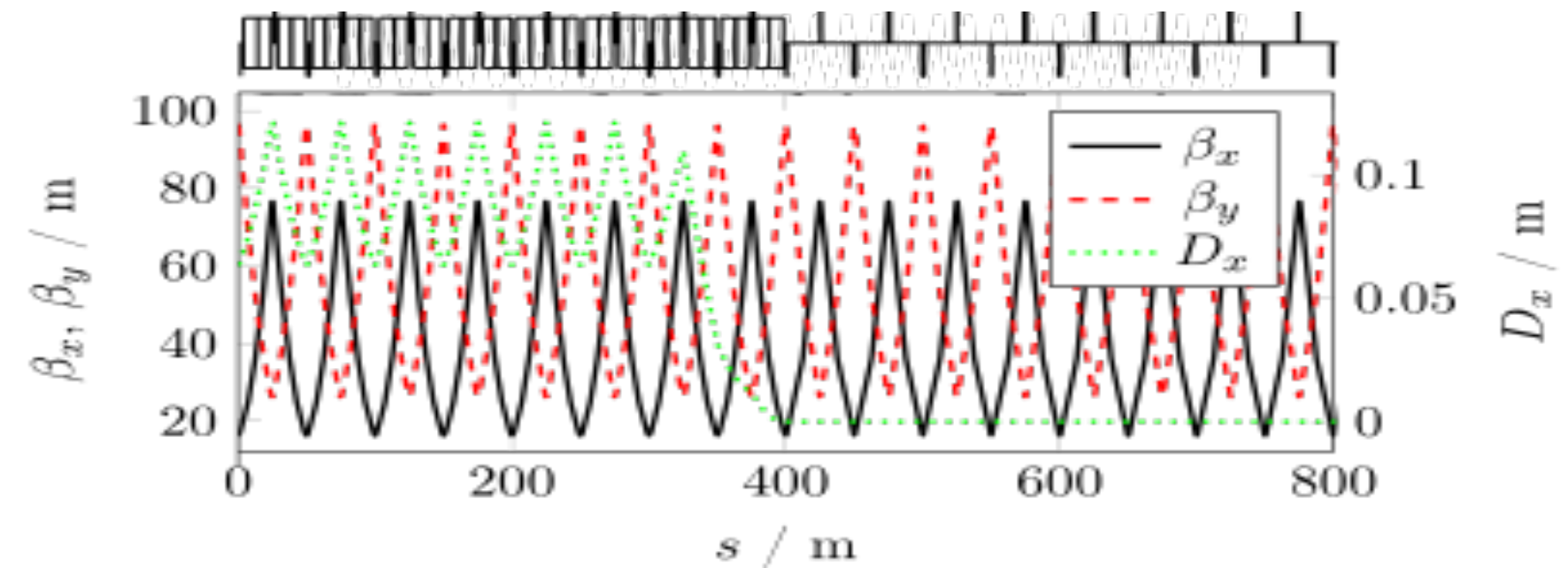
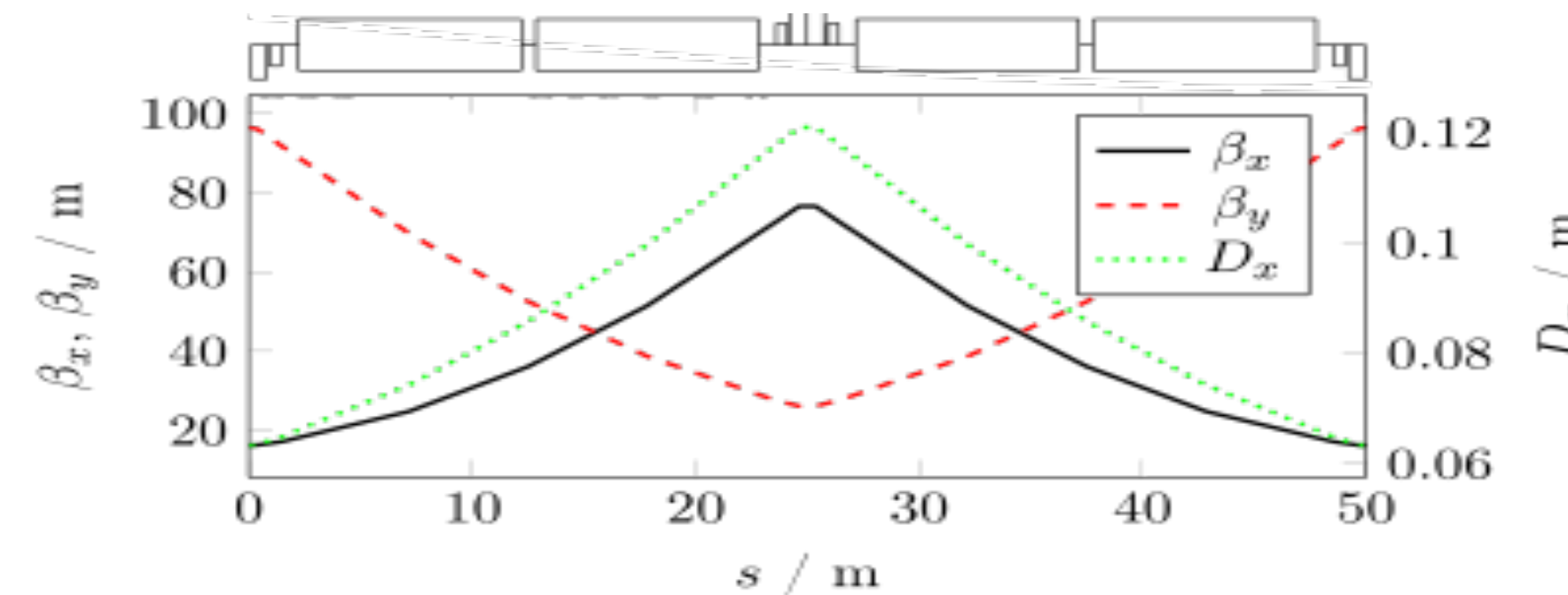
FODO cell

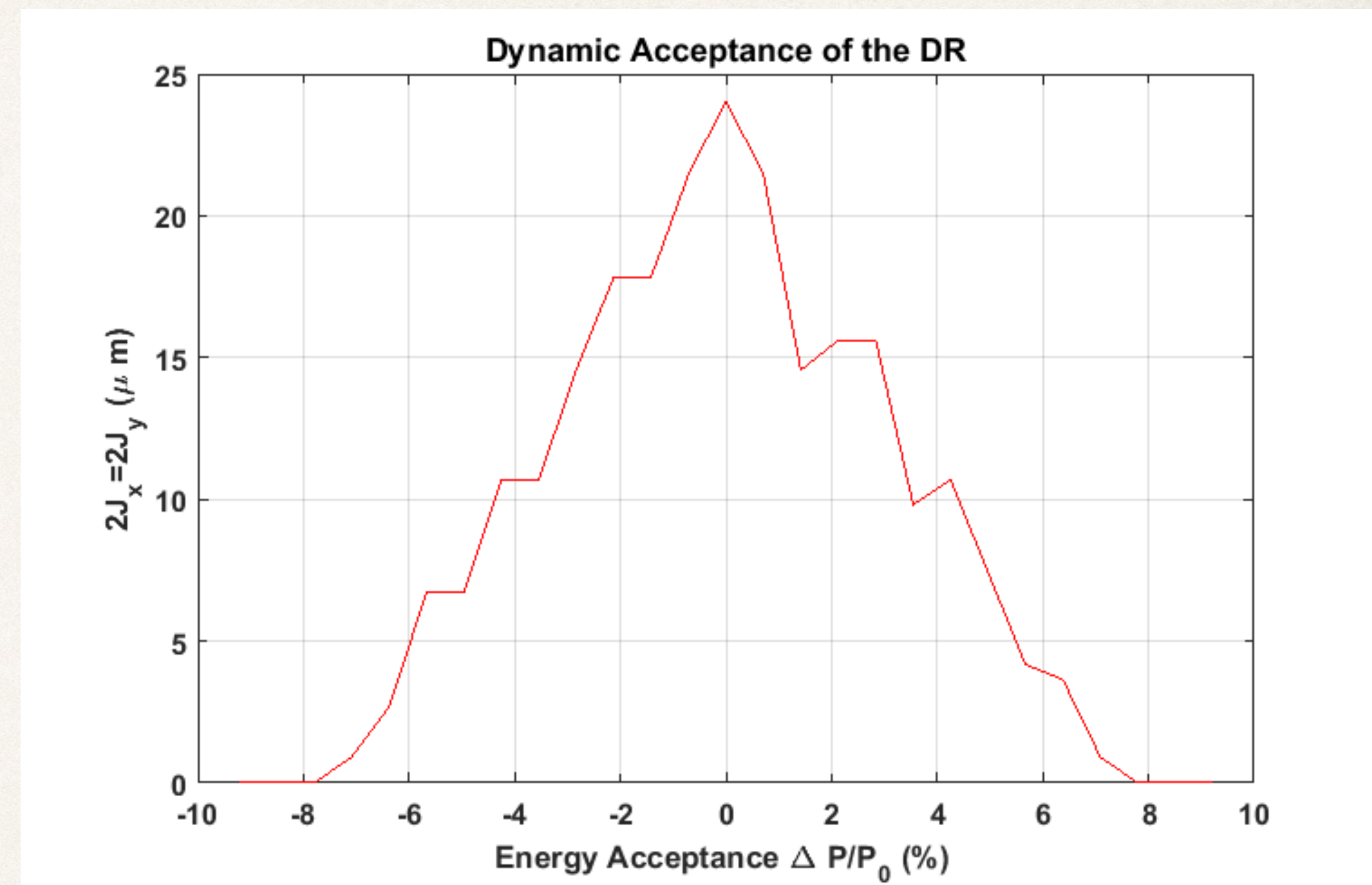
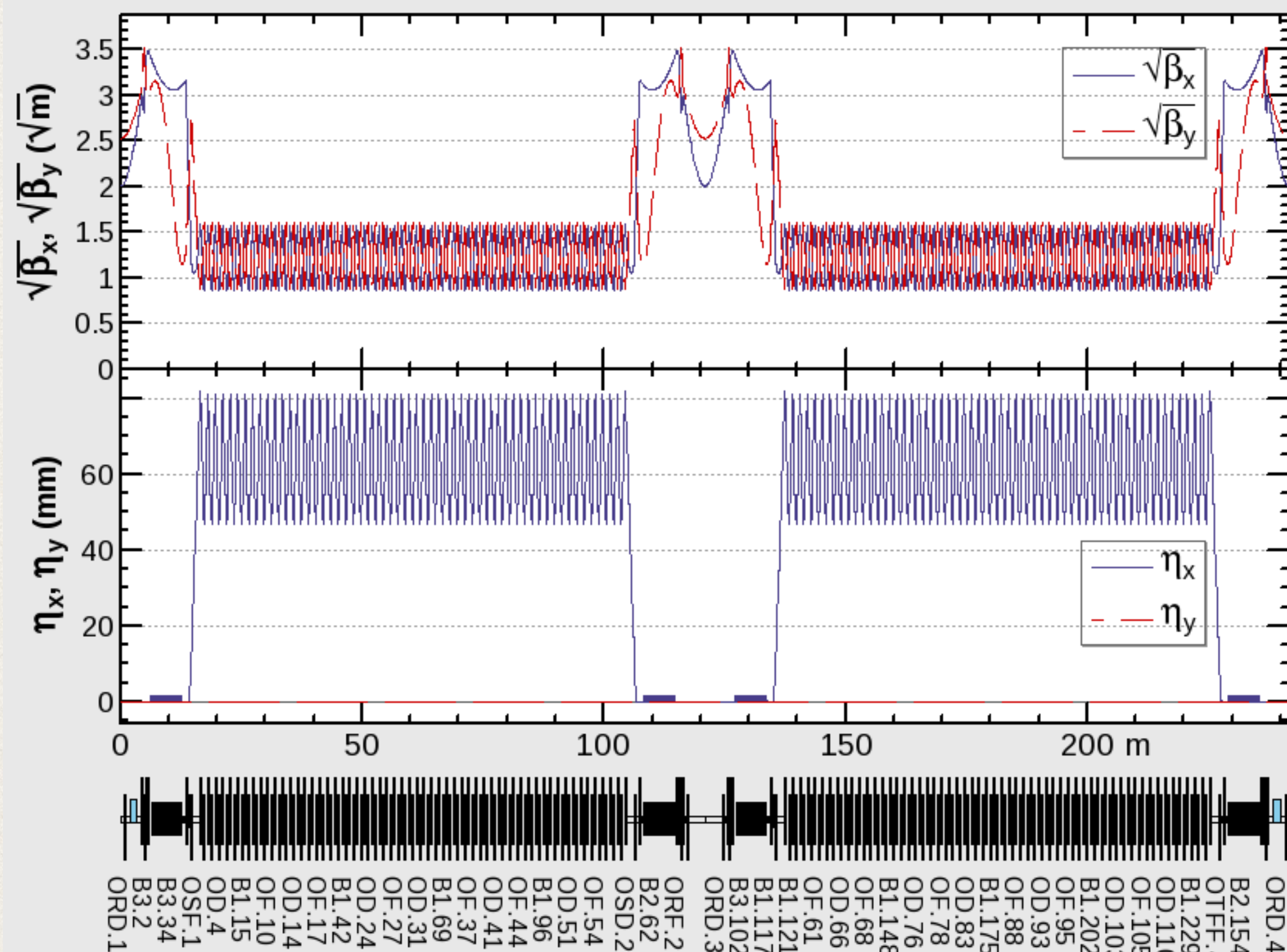
- $L = 50$ m
- $\varphi = 90^\circ/60^\circ$

Dispersion suppressor

- Two half-bend cells

Nonlinear analysis /dynamic aperture survey is going on.





- ❑ A preliminary design of the e+e- damping ring has been made at 1.54 GeV.
- ❑ It stores up to 5 trains of 2 bunches with 100 ns train spacing and 60 ns bunch spacing.
- ❑ The dynamic aperture seems enough to capture the large emittance from the e+ target.
- ❑ Further optimization will take place to match the requirements, esp. for the repetition rate of the linac.

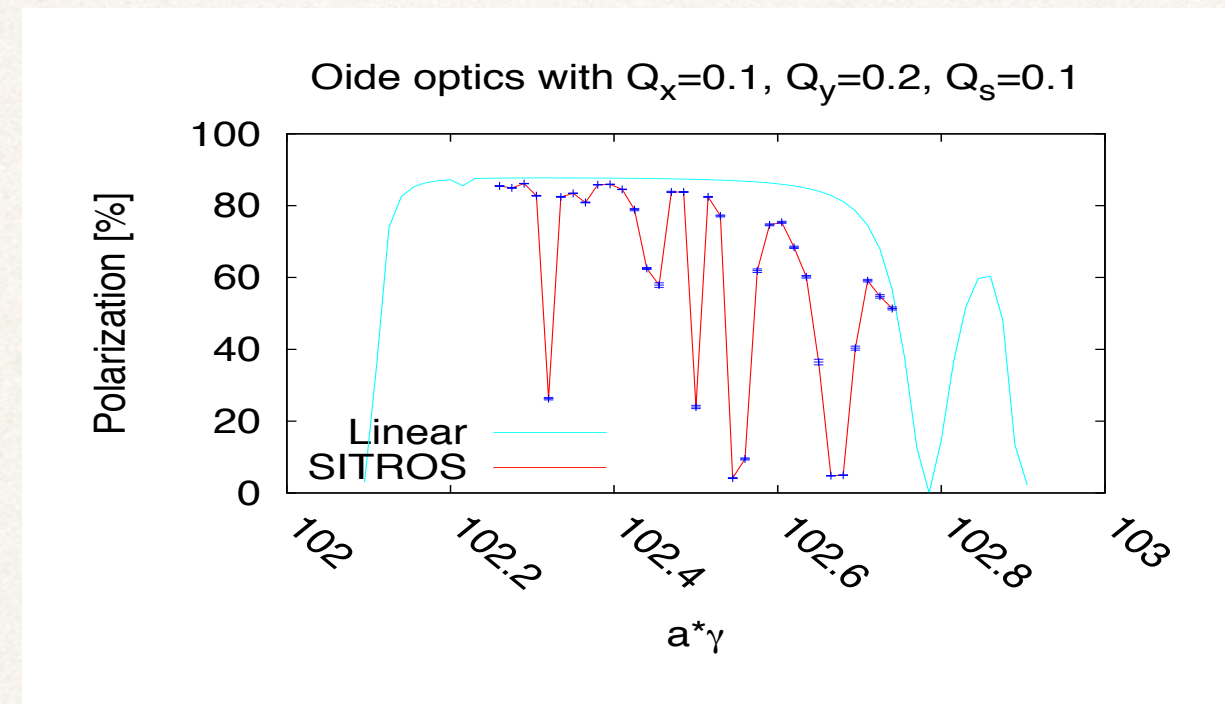
And now polarization!

45 GeV beam energy

45 GeV case with 4 LEP-like wigglers in dispersion free regions.

$\delta y_{rms}^Q = 200 \mu\text{m}$, but *no* BPMs errors: $y_{rms} = 0.049 \text{ mm}$

no harmonic bumps, $|\delta \hat{n}|_{0,rms} = 0.4 \text{ mrad}$

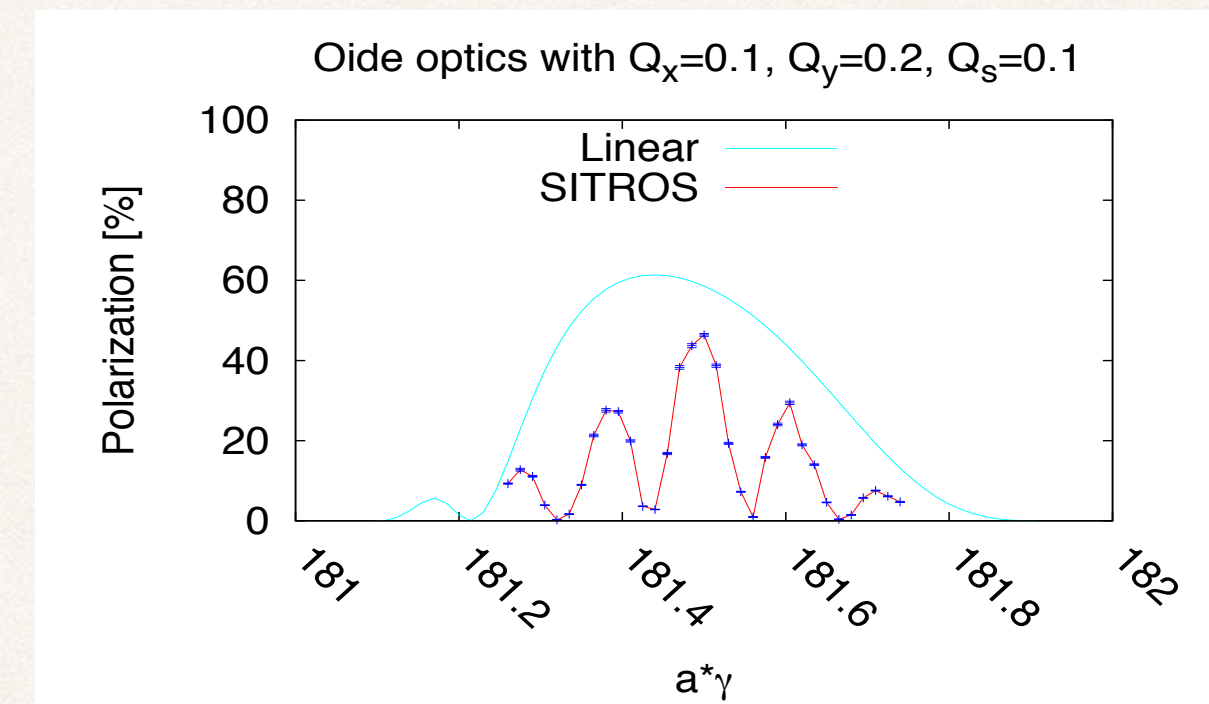


E. Gianfelice-Wendt

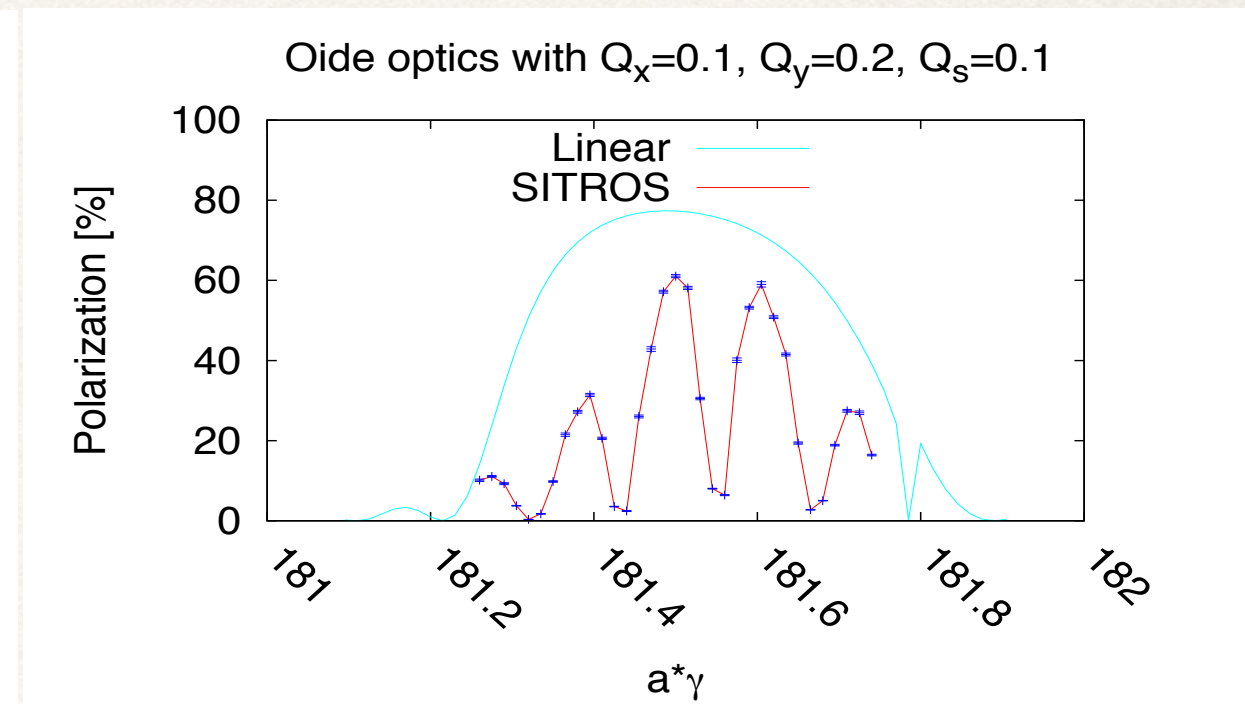
80 GeV beam energy

Same error realization as at 45 GeV: $|\delta \hat{n}|_{0,rms} = 2 \text{ mrad}$

w/o harmonic bumps



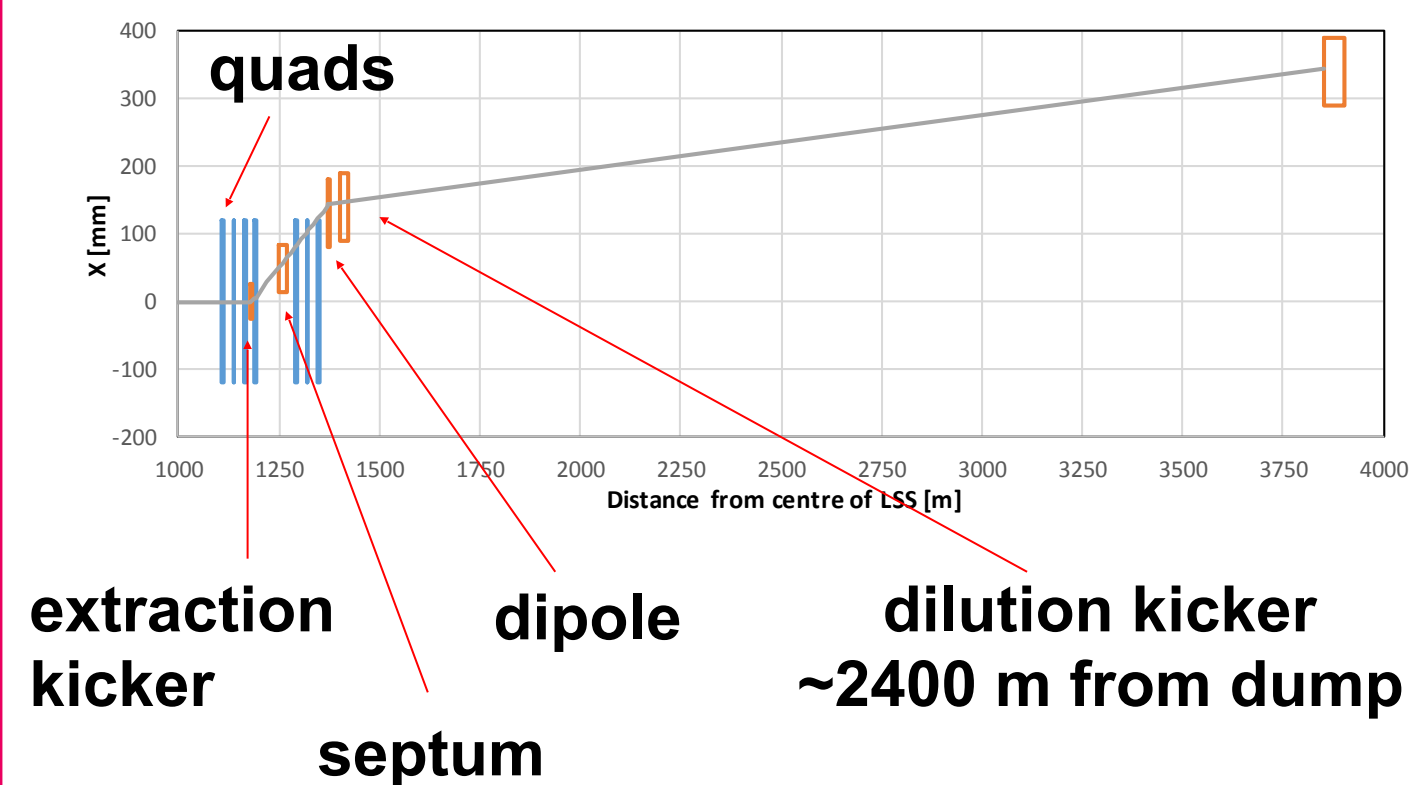
with



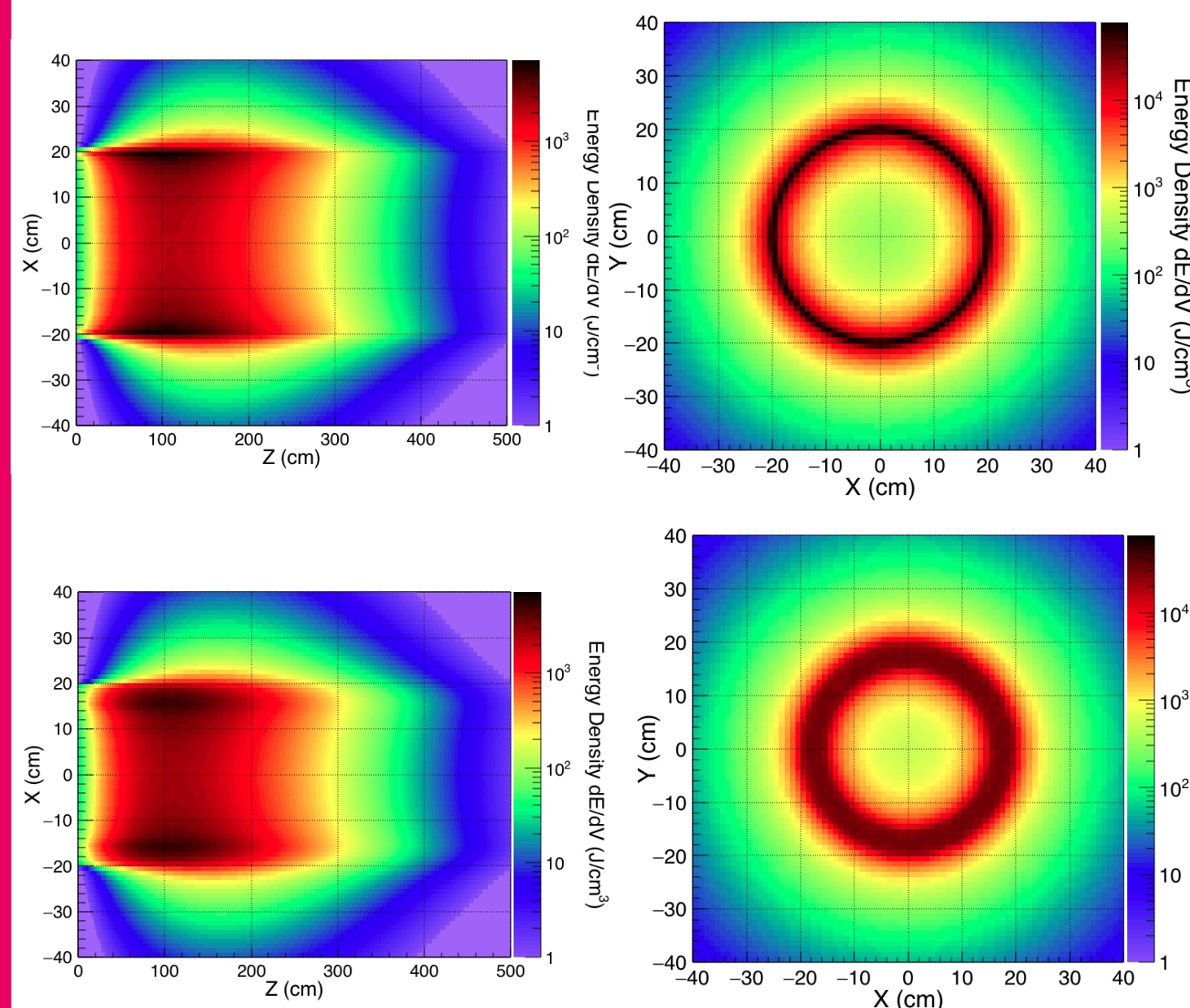
- ❑ Meaningful polarizations for energy calibration can be obtained both at 45 and 80 GeV under the presence of large misalignment of quadrupoles.
- ❑ Harmonic bumps improve the polarization.
- ❑ Possible systematic errors on the energy calibration have been studied by A. Bogomyagkov, A. Blondel.

Layout in FCC LSS

- A 99 m drift is needed after the kicker QD, containing the septum
- 3 'matching' quads are added each side of the extraction elements
- A steering dipole and dilution kickers placed at start of FCC arc
- Total length needed is 250-300 m, per beam (at ends of LSS)



Deposited Energy Density in the Graphite



Upper plots: Number of turns in spiral is 1, distance between the center of bunches is 17.76 μm .

Bottom plots: Number of turns in spiral is 57, distance between the center of bunches is 890 μm .

The energy density deposited in the graphite beam dump in the vertical-longitudinal (x-z) plane.

The energy density deposited on the graphite beam dump in the transverse (x-y) plane.

- ❑ The proposed abort system consists of abort kickers, septum magnets and a dilution kicker system.
- ❑ The dilution kickers must spread the beam evenly on the surface of the beam dump and on the vacuum chamber window, in order to prevent damages due to high energy electron and positron beams.
- ❑ Simulation studies are carried out in order to determine an operational configuration of the abort system and the required apertures of the abort beam lines

Summary (a private view, more or less)



Subject	Conceptual Design	Remaining Items
Optics/Layout	<ul style="list-style-type: none"> The baseline has been established, including the mitigation for beam-beam instability. 	<ul style="list-style-type: none"> Detailed design of sections for RF/injection/extraction.
Dynamic Aperture	<ul style="list-style-type: none"> OK without machine errors 	<ul style="list-style-type: none"> Errors and corrections top-up injection + beam-beam
Low emittance tuning	<ul style="list-style-type: none"> The goal is feasible, shown by at least four independent simulations. 	<ul style="list-style-type: none"> More realistic assumptions on the errors will be involved.
Beam-beam effects	<ul style="list-style-type: none"> Confirmed by two independent codes 	<ul style="list-style-type: none"> Evaluation of tail formation esp. at top-up injection
MDI	<ul style="list-style-type: none"> Established the baseline layout considering SR background, HOM, luminometer 	<ul style="list-style-type: none"> Realistic 3D model for the beam pipe and magnets with mechanically possible scenario for assembly. Evaluation of beam tails and collimation scenario.
IR magnets	<ul style="list-style-type: none"> A few designs have been proposed. 	<ul style="list-style-type: none"> Confirmation of the field quality via prototyping.
Arc magnets	<ul style="list-style-type: none"> Established twin aperture dipoles/quadrupoles 	<ul style="list-style-type: none"> Scheme for the sextupoles. Other dipoles, quadrupoles, wigglers
Vacuum system	<ul style="list-style-type: none"> Established the shape, size, material of the beam pipe with strategy for pumping and SR absorption 	<ul style="list-style-type: none"> Detail for e-cloud mitigation (which coating, etc.) Detailed design for the photon stop, bellows, BPMs, pumping slots, collimators, etc.
RF	<ul style="list-style-type: none"> Basic concepts for cavities, couplers, cryogenics, power sources have been proposed 	<ul style="list-style-type: none"> Actual design of individual components both for high gradient and high current versions.
Injectors	<ul style="list-style-type: none"> The Baseline scheme has been established with linac, damping ring, pre-booster (SPS), and Main Booster 	<ul style="list-style-type: none"> Detailed study of each component, incl. the gun, e+ target, beam transport lines, kickers/septa, etc. Intensity limitations at pre-booster and Main Booster. Feasibility of SPS, considering the compatibility with proton experiments.
Beam Abort / Dump	<ul style="list-style-type: none"> The basic concepts are established for the abort beam line and the dump. Utilize the FC-hh beam dump line. 	<ul style="list-style-type: none"> Incorporation into the collider optics. Detailed design of the kickers and diffusers. Further optimization of the target and diffusion scheme.
Impedance & Instability	<ul style="list-style-type: none"> Intensive evaluations have been carried out for resistive wall with coatings, bellows, BPMs, tapers, etc. Thresholds have been identified with the impedances and also e-cloud. 	<ul style="list-style-type: none"> More components such as RF cavities and collimators are to be included.
Polarization Energy calibration	<ul style="list-style-type: none"> A meaningful polarization is feasible at Z and W for the pilot bunches, under a reasonable machine errors. 	<ul style="list-style-type: none"> More systematic errors on the energy calibration are necessary.



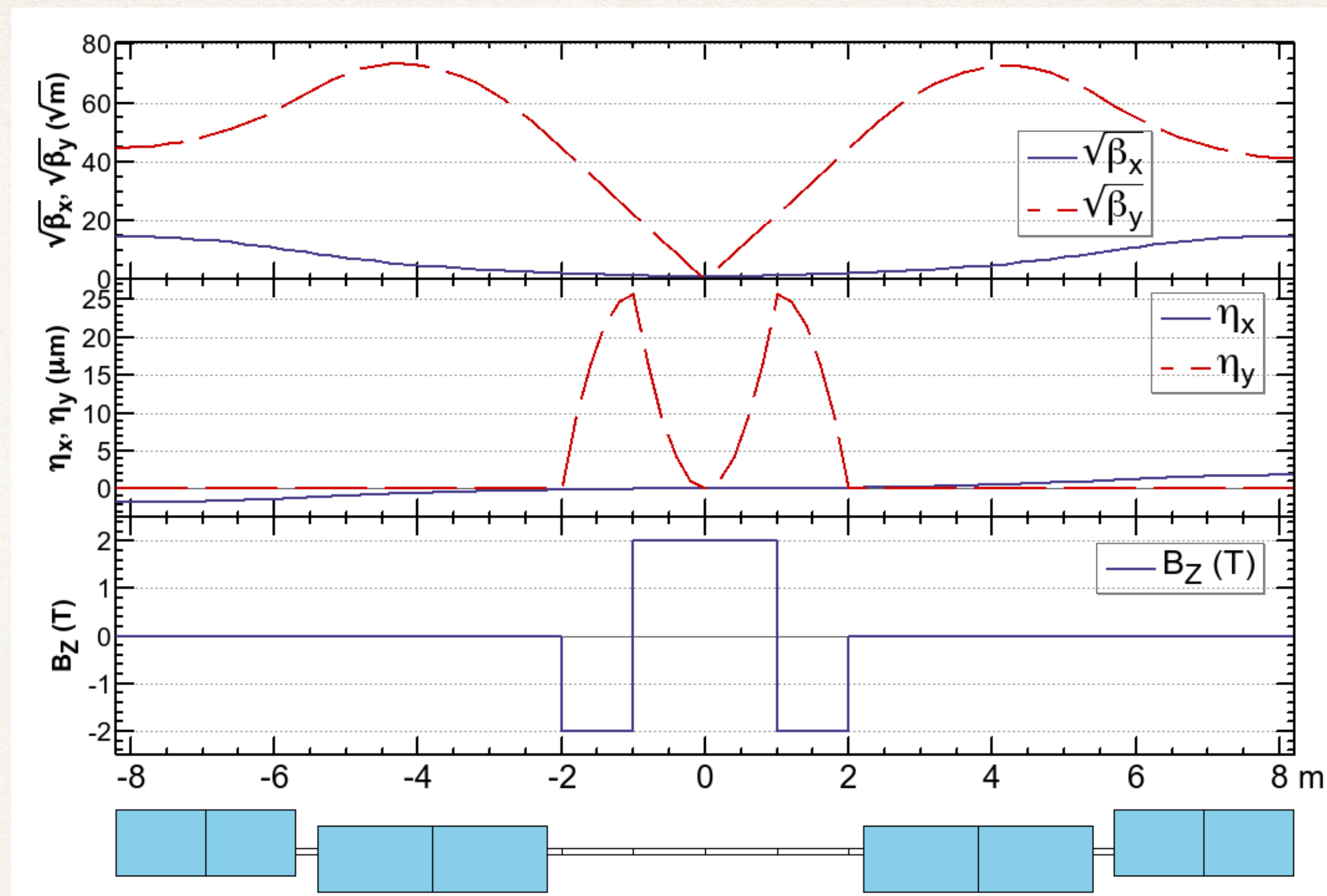
Backups

Effects included in the dynamic aperture survey



Effects	Included?	Significance
Synchrotron motion	Yes	Essential
Radiation loss in dipoles	Yes	Essential – improves the aperture
Radiation loss in quadrupoles	Yes	Essential – reduces the aperture esp. at $t\bar{t}$
Radiation fluctuation	after optimization	Essential
Tapering	Yes	Essential
Crab waist	Yes	transverse aperture is reduced by $\sim 20\%$
Maxwellian fringes	Yes	small
Kinematical terms	Yes	small
Solenoids	Evaluated separately	minimal, if locally compensated
Beam-beam effects for stored beam	after optimization (D. Zhou)	affects the lifetime for $\beta_y^* = 1 \text{ mm}$ at $t\bar{t}$
Beam-beam effects for injected beam	Not yet	
Higher order fields / errors / misalignments	Not yet	Essential , development of correction/tuning scheme is necessary

175 GeV, $\beta_{x,y}^* = (1 \text{ m}, 2 \text{ mm})$



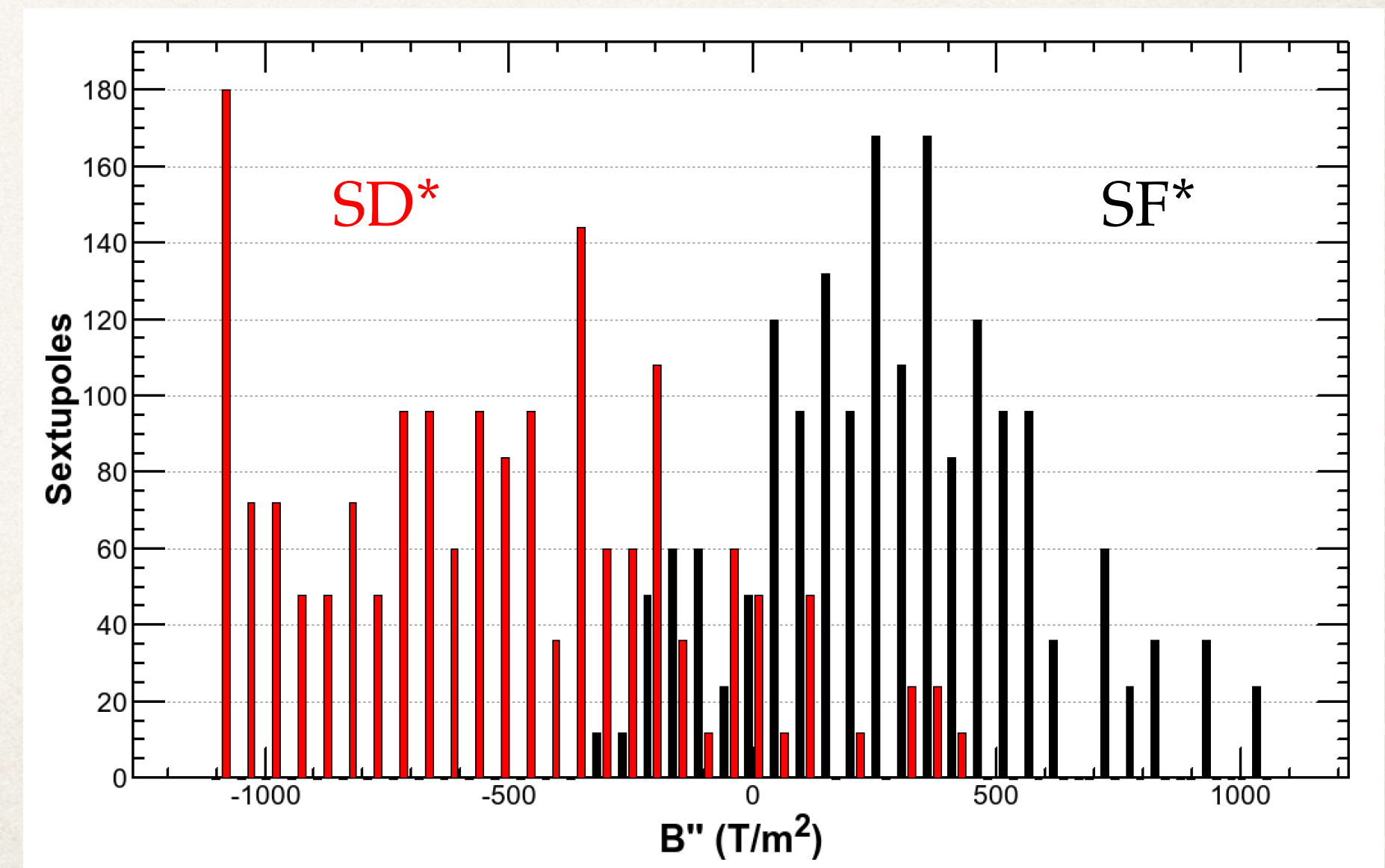
- The effect of detector solenoid field is locally compensated by counter solenoids.
- The solenoid field is shielded on the quadrupoles.
- If the compensation/shielding is perfect, their effects on the beam optics is minimal. No coupling, no vertical dispersion leak to the outside.

* The optics shown above may not be the latest one.

Parameters for Arc Magnets

Beam Energy	[GeV]	175
Cell length	[m]	55.88
Length of dipole B1 / B1L	[m]	21.94 / 23.44
Bending angle/dipole	[mrad]	2.042 / 2.183
Dipole field	[mT]	54.3
Dipole packing factor in the arc	[%]	81.7
Number of arc dipoles / ring		2900
Arc quadrupole scheme		twin aperture
Quad length, QF/QD	[m]	3.1 / 3.1
Quad gradient, QF/QD	[T/m]	9.9 / -9.9
Number of quads / ring, QF/QD		1450 / 1450
Sext. length short (long), SF/SD	[m]	0.7 (1.4) / 0.7 (1.4)
Max. sext. $ B'' $, SF/SD	[T/m ²]	1117/ 1069
Number of sexts/ring, short (long), SF/SD		588 (588) / 588 (588)

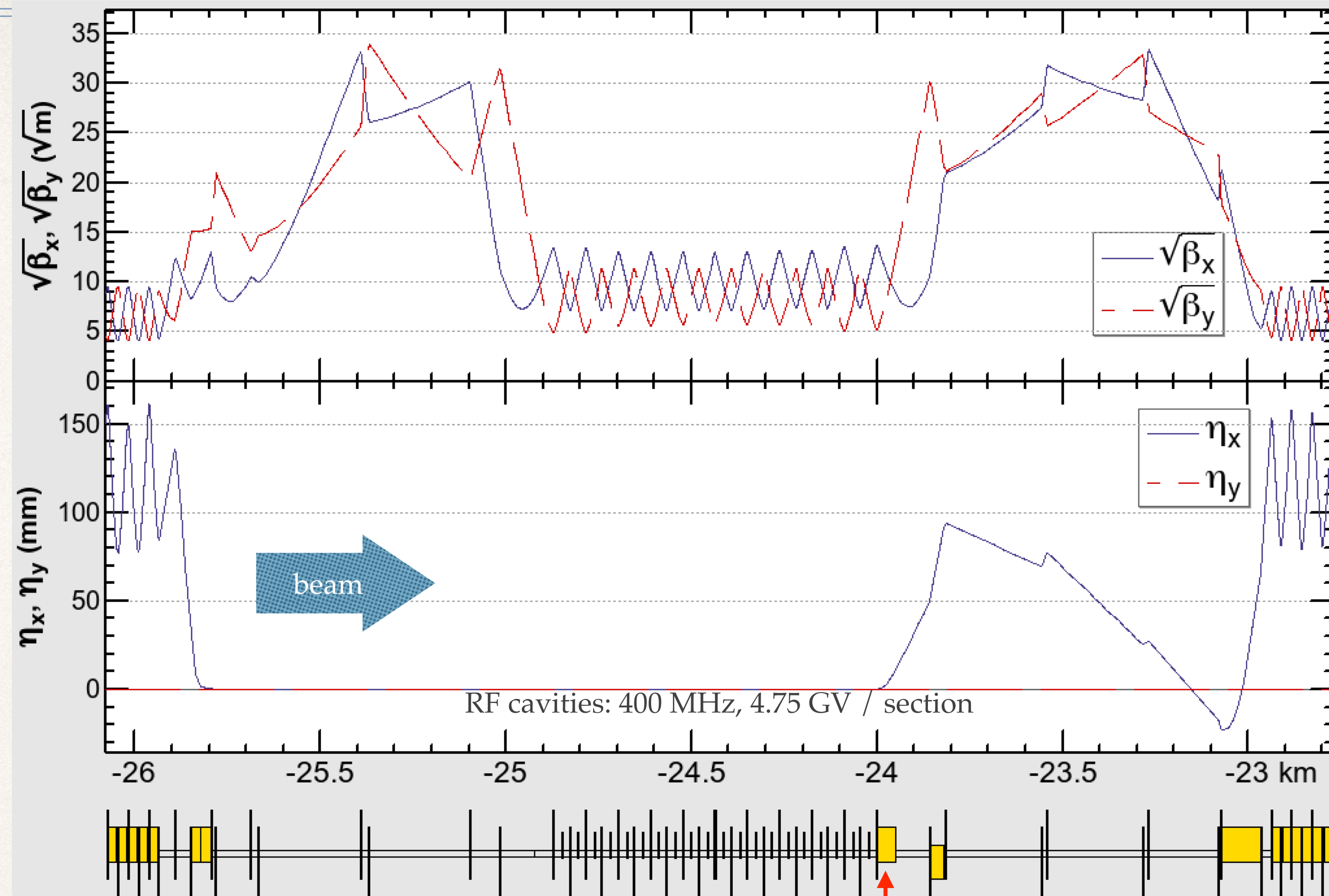
- ❖ Although the sextupoles seem very strong, the average of them is still reasonable.
- ❖ ~10% of them may need a special dedicated architecture.



The RF section (175 GeV)

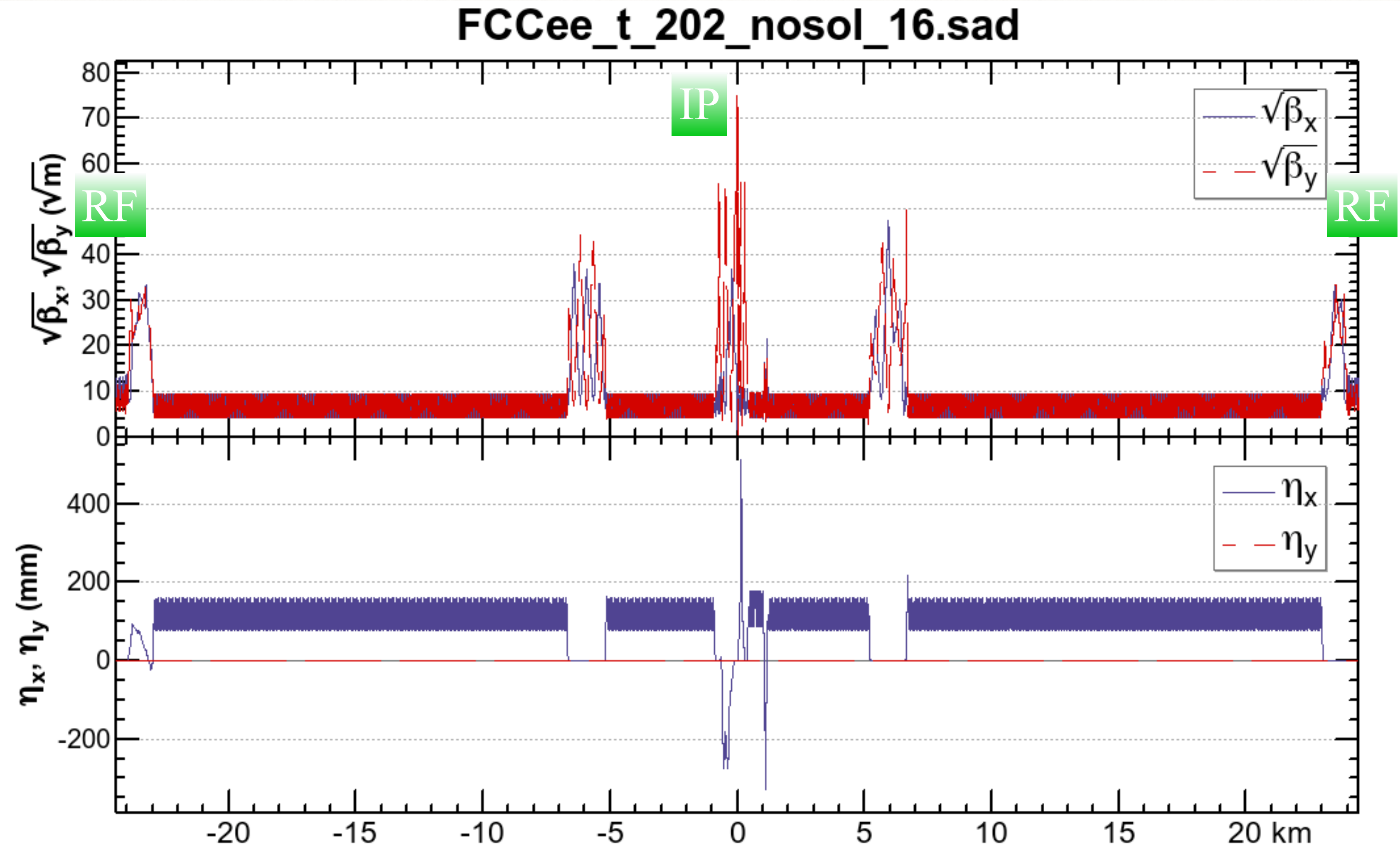
FCCee_t_202_nosol_16.sad

Beams cross over through the RF section.



An electrostatic separator, combined with a dipole magnet

- ❖ The downstream straight after RF, an extraction beam line is to be attached for each ring.
- ❖ If the nominal strengths of quads are symmetrical in the common section, it matches to the optics of both beam considering the change of local energy at their closed orbits.
- ❖ This section is compatible with the RF staging scenario. For lower energies, the common RF and cross over will not be necessary.



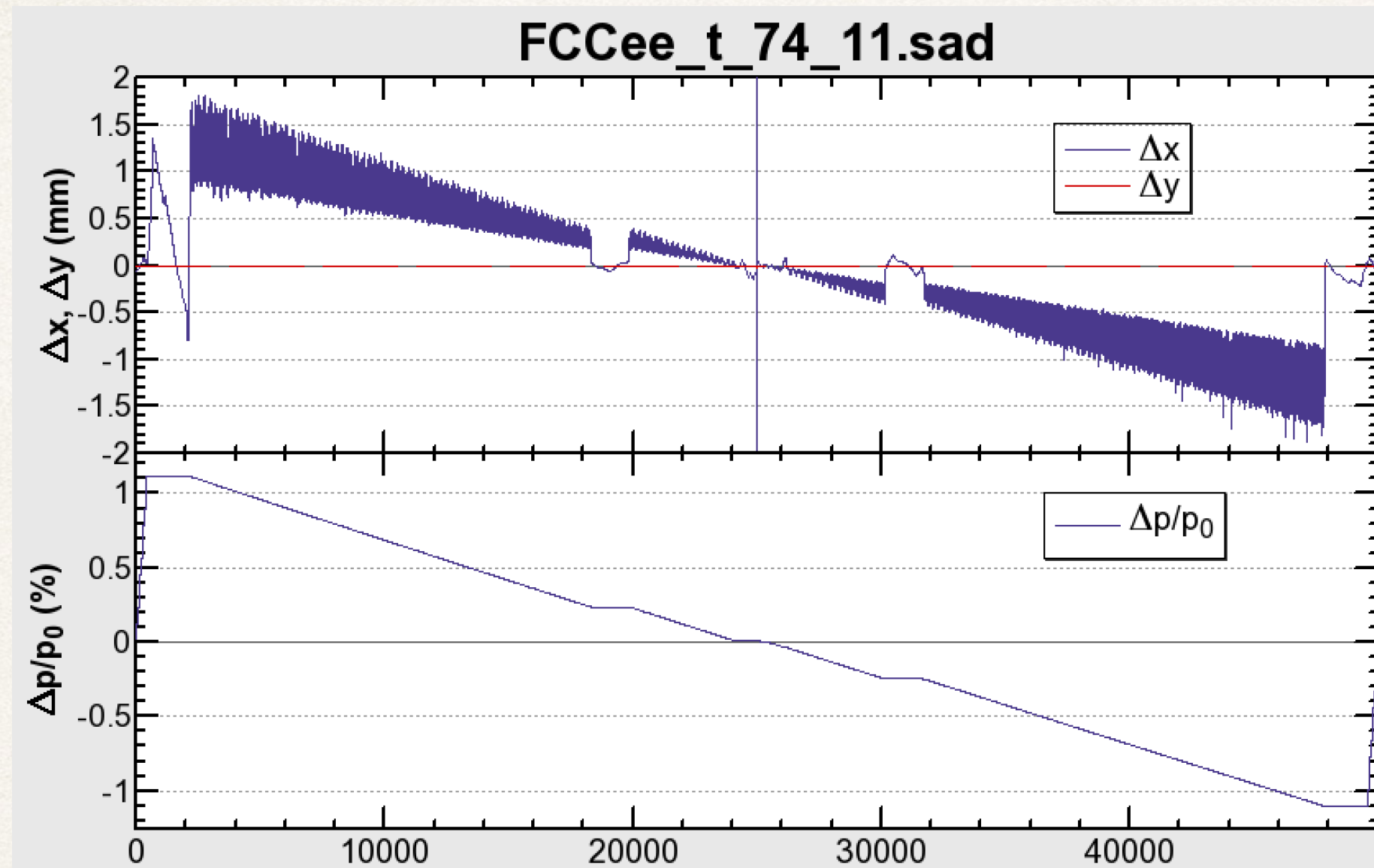
- Above are the half optics $\beta^*_{x/y} = 1 \text{ m} / 2 \text{ mm}$, for tt, Zh, & W.
- 2 IPs/ring.
- The optics for straight sections except for the IR are tentative, to be customized for infection/extraction/collimation/beam instrumentation, etc.

Parameters Comparison between 2017 and 2016

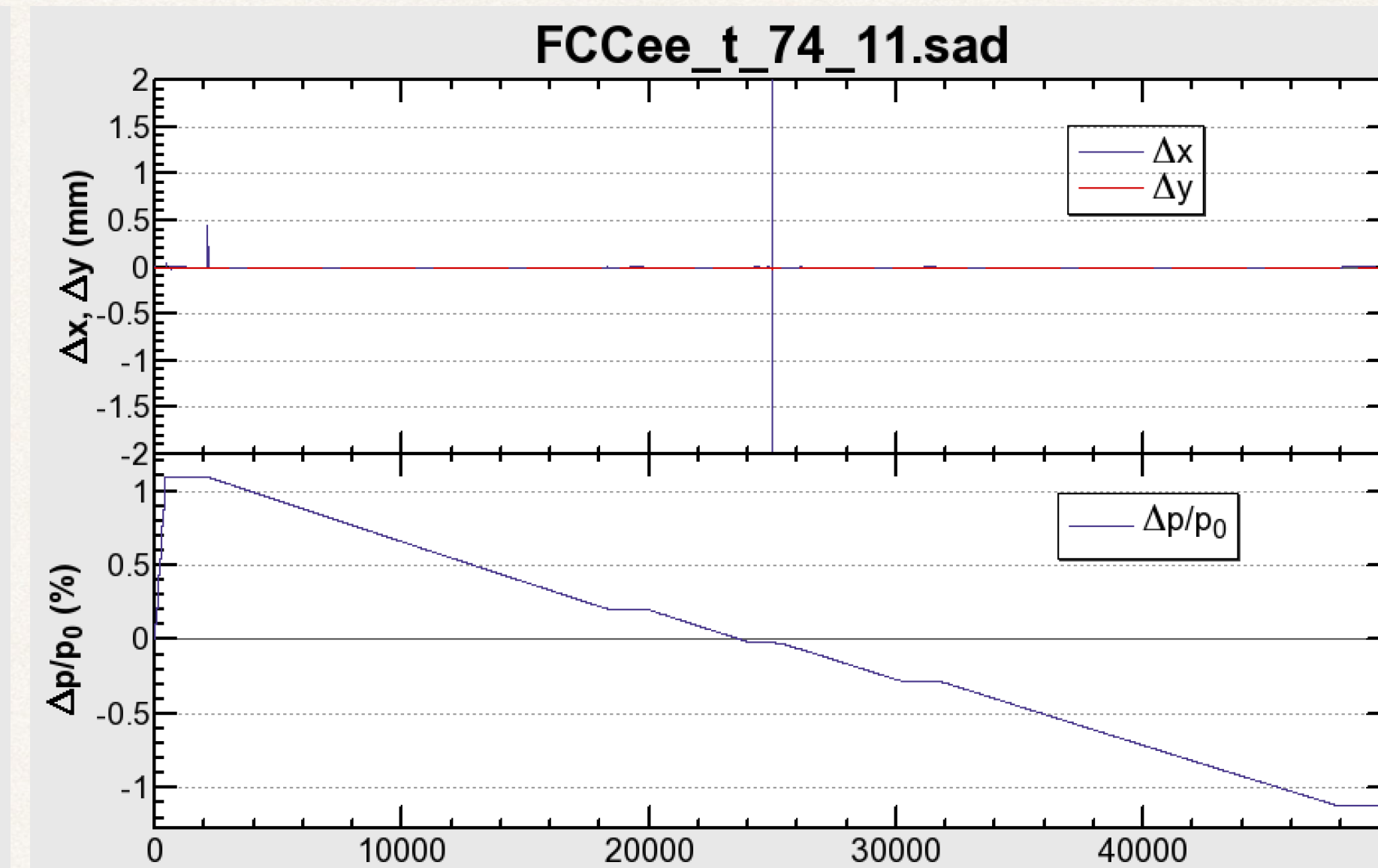


Design		2017		2016	
Circumference	[km]	97.750		99.984	
Arc quadrupole scheme		twin aperture		single aperture	
Bend. radius of arc dipole	[km]	10.747		11.190	
Number of IPs / ring				2	
Crossing angle at IP	[mrad]			30	
Solenoid field at IP	[T]			± 2	
ℓ^*	[m]			2.2	
Local chrom. correction		<i>y</i> -plane with crab-sext. effect			
RF frequency	[MHz]			400	
Total SR power	[MW]			100	
Beam energy	[GeV]	45.6	175	45.6	175
SR energy loss/turn	[GeV]	0.0360	7.80	0.0346	7.47
Long. damping time	[ms]	414	7.49	440	8.0
Polarization time	[s]	9.2×10^5	1080	9.2×10^5	1080
Current/beam	[mA]	1390	6.4	1450	6.6
Bunches/ring		70760	62	30180(91500)	81
Particles/bunch	[10^{10}]	4.0	21.1	10 (3.3)	17.0
Arc cell		$60^\circ/60^\circ$	$90^\circ/90^\circ$	$90^\circ/90^\circ$	
Mom. compaction α_p	[10^{-6}]	14.79	7.31	6.99	
Horizontal tune ν_x		269.14	389.08	387.08	
Vertical tune ν_y		267.22	389.18	387.14	
Arc sext. families		208	292	292	
Horizontal emittance ε_x	[nm]	0.267	1.34	0.086	1.26
$\varepsilon_y/\varepsilon_x$ at collision	[%]	0.38	0.2	1.2	0.2
β_x^*	[m]	0.15	1	0.5 (1)	1 (0.5)
β_y^*	[mm]	1	2	1 (2)	2 (1)
Energy spread by SR	[%]	0.038	0.144	0.038	0.141
RF Voltage	[MV]	255	9500	88	9040
Bunch length by SR	[mm]	2.1	2.4	2.6	2.4
Synchrotron tune ν_z		-0.0413	-0.0684	-0.0163	-0.0657
RF bucket height	[%]	3.8	10.3	2.3	11.6
Luminosity/IP	[$10^{34}/\text{cm}^2\text{s}$]	121	1.32	210 (90)	1.3 (1.5)

No Taper

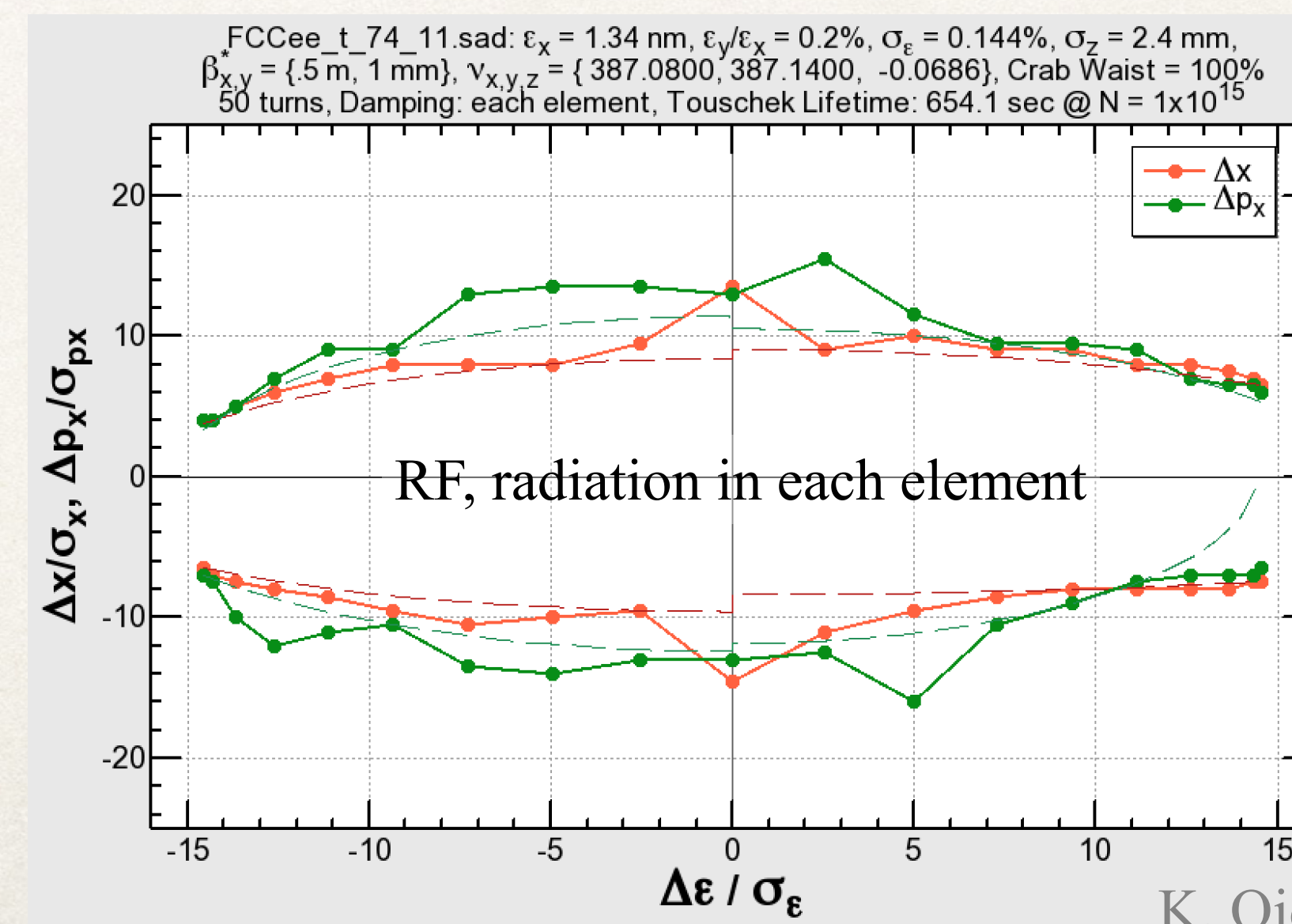
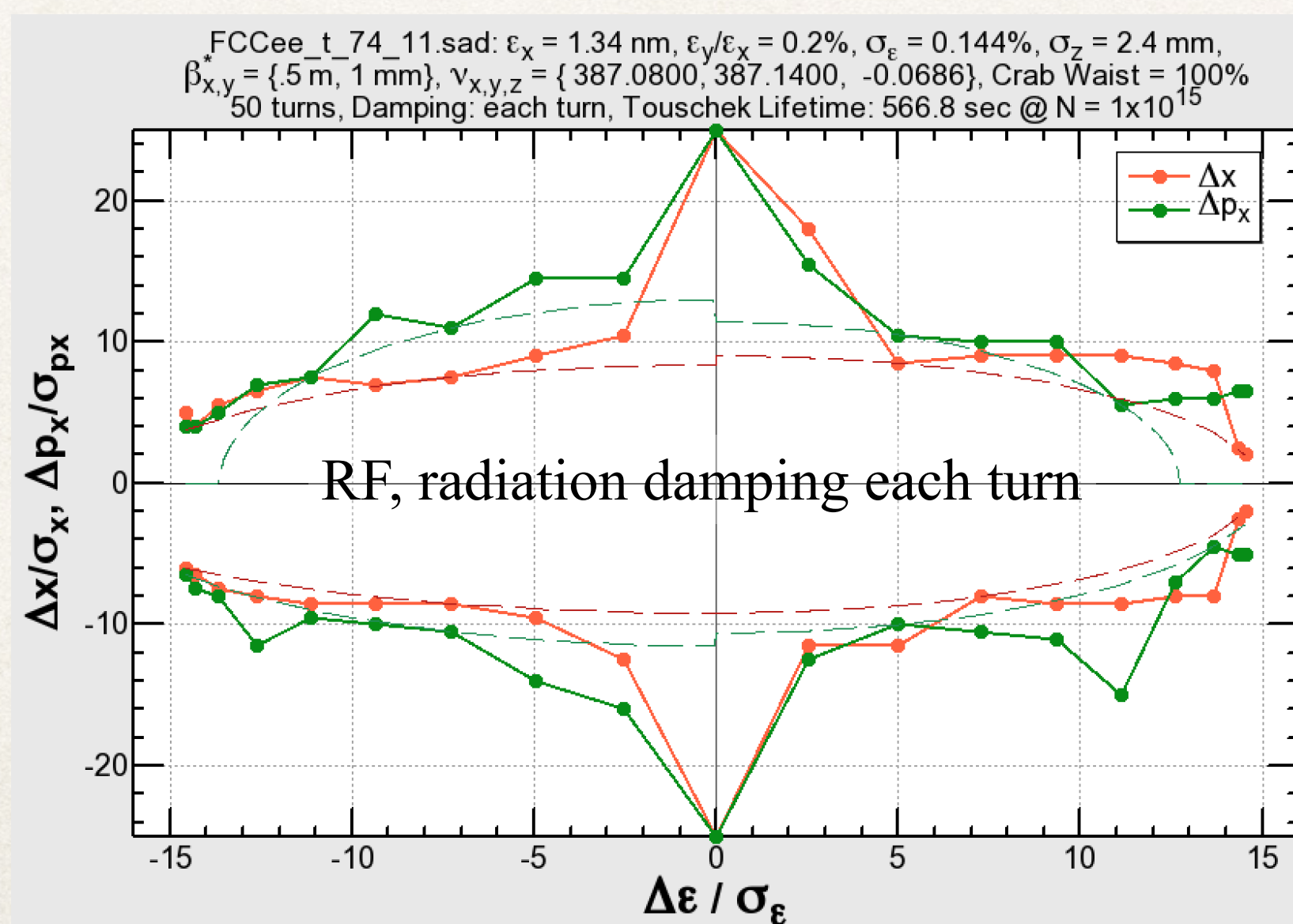
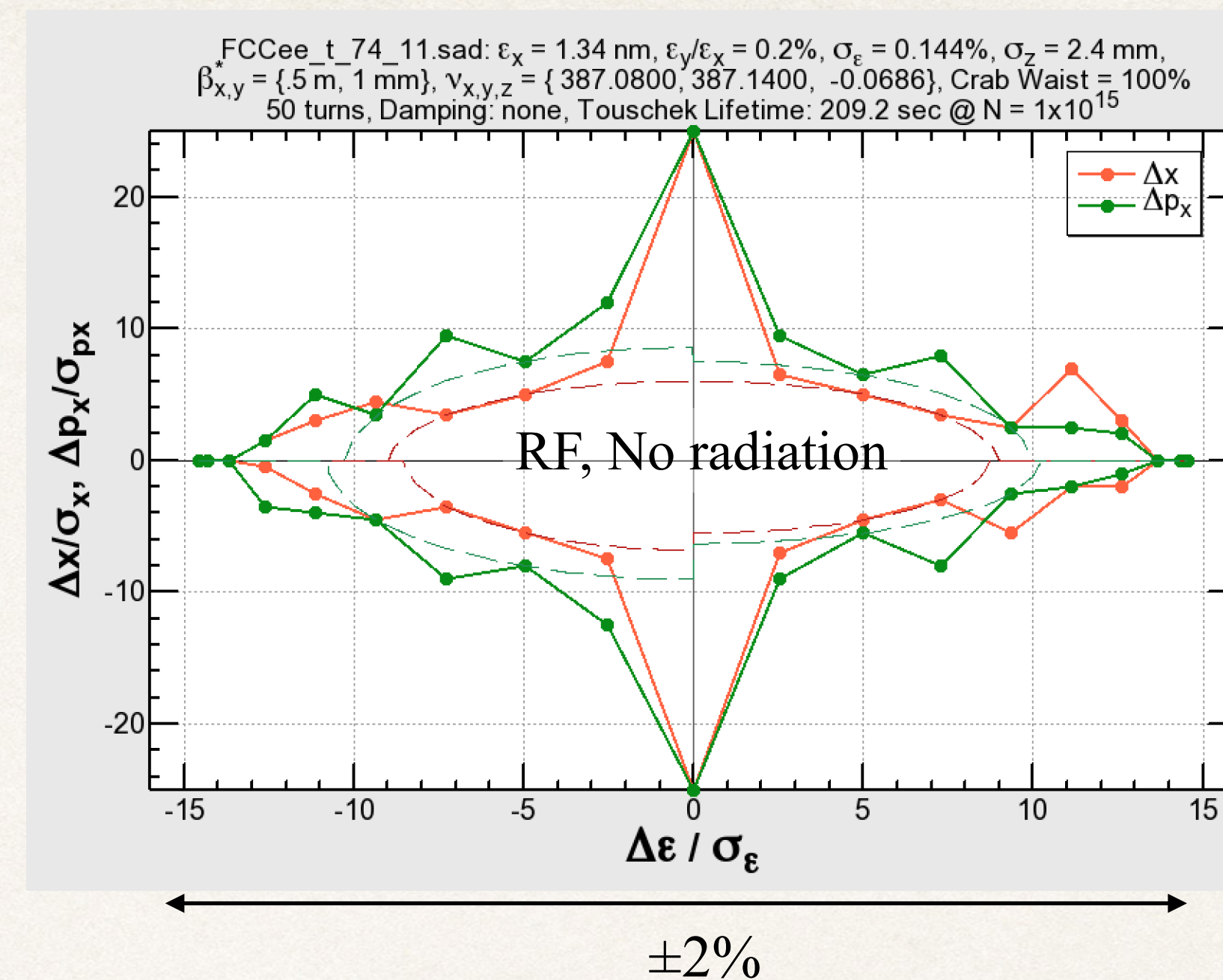
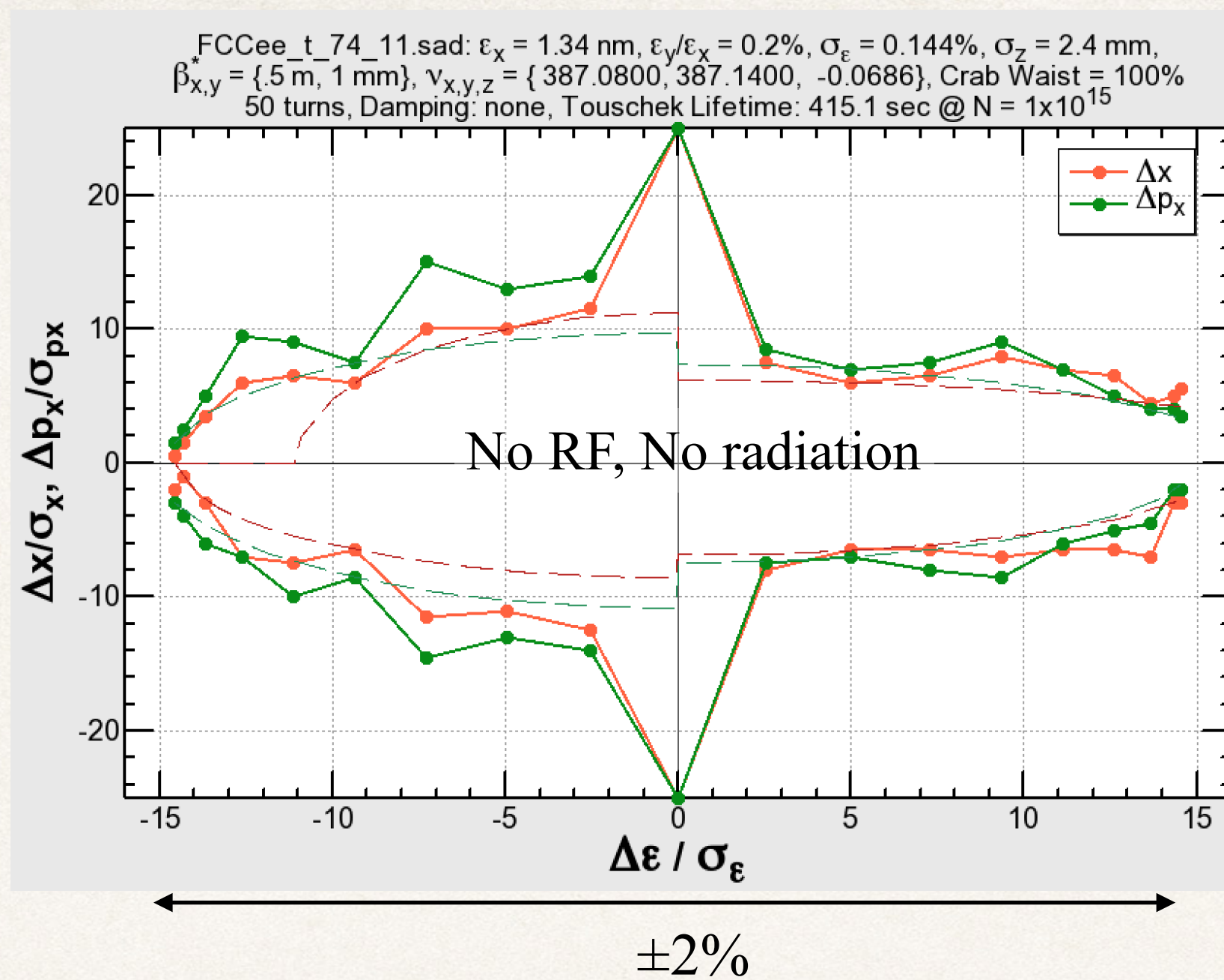


Tapered

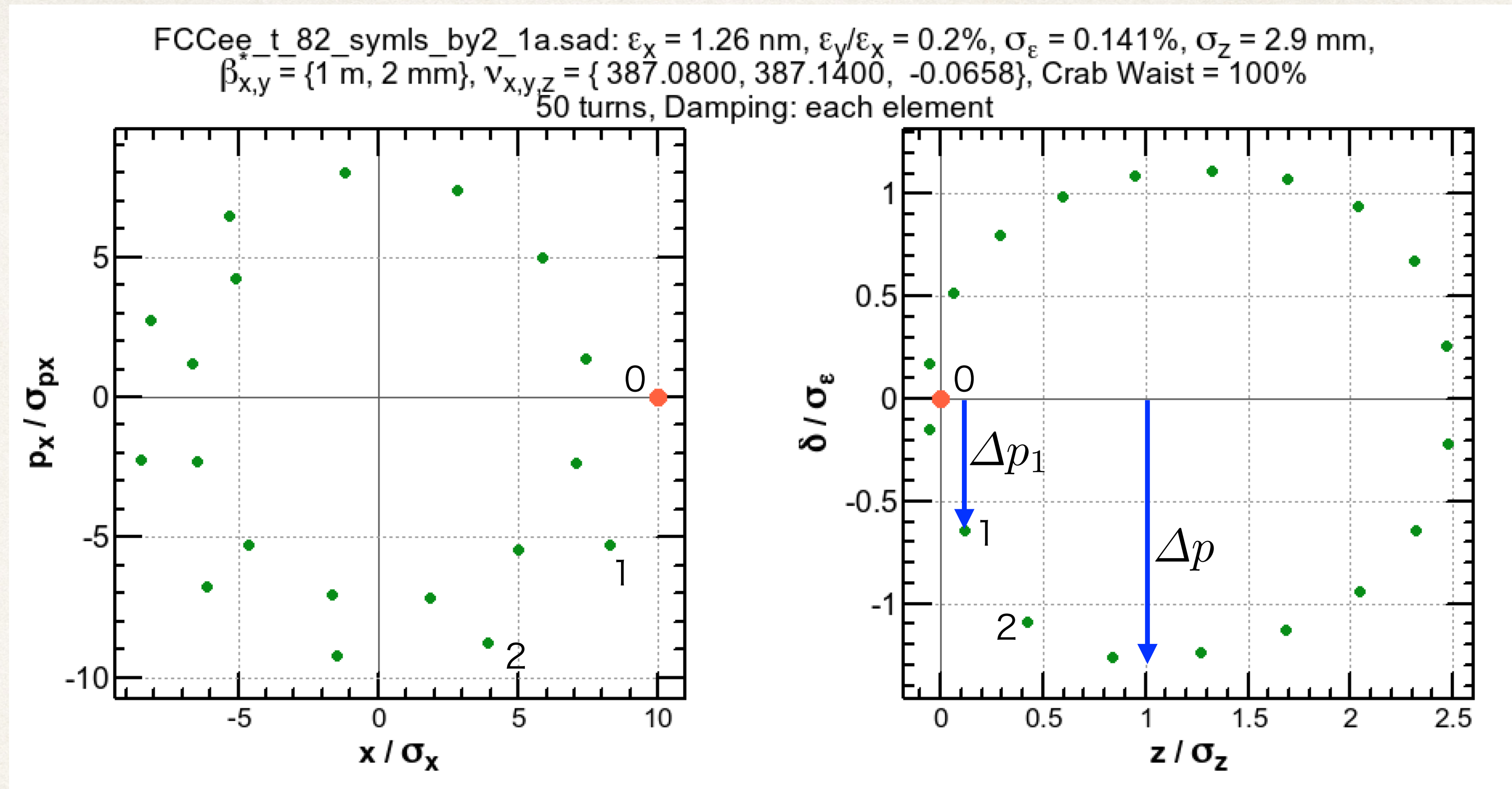


- ❖ The change of the orbit due to energy loss along the arc causes serious deformation on the optics, causing the loss of the dynamic aperture.
- ❖ Everything can be cured almost completely by “tapering”, i.e. scaling the strengths of all magnets along the local energy of the beam: this is one of the best merits of a double-ring collider (F. Zimmermann).

Several effects on the dynamic aperture



Synchrotron radiation in quadrupoles



- ❖ Horizontal betatron oscillation (left) causes a synchrotron motion (right) due to the energy loss by the synchrotron radiation in arc quadrupoles.

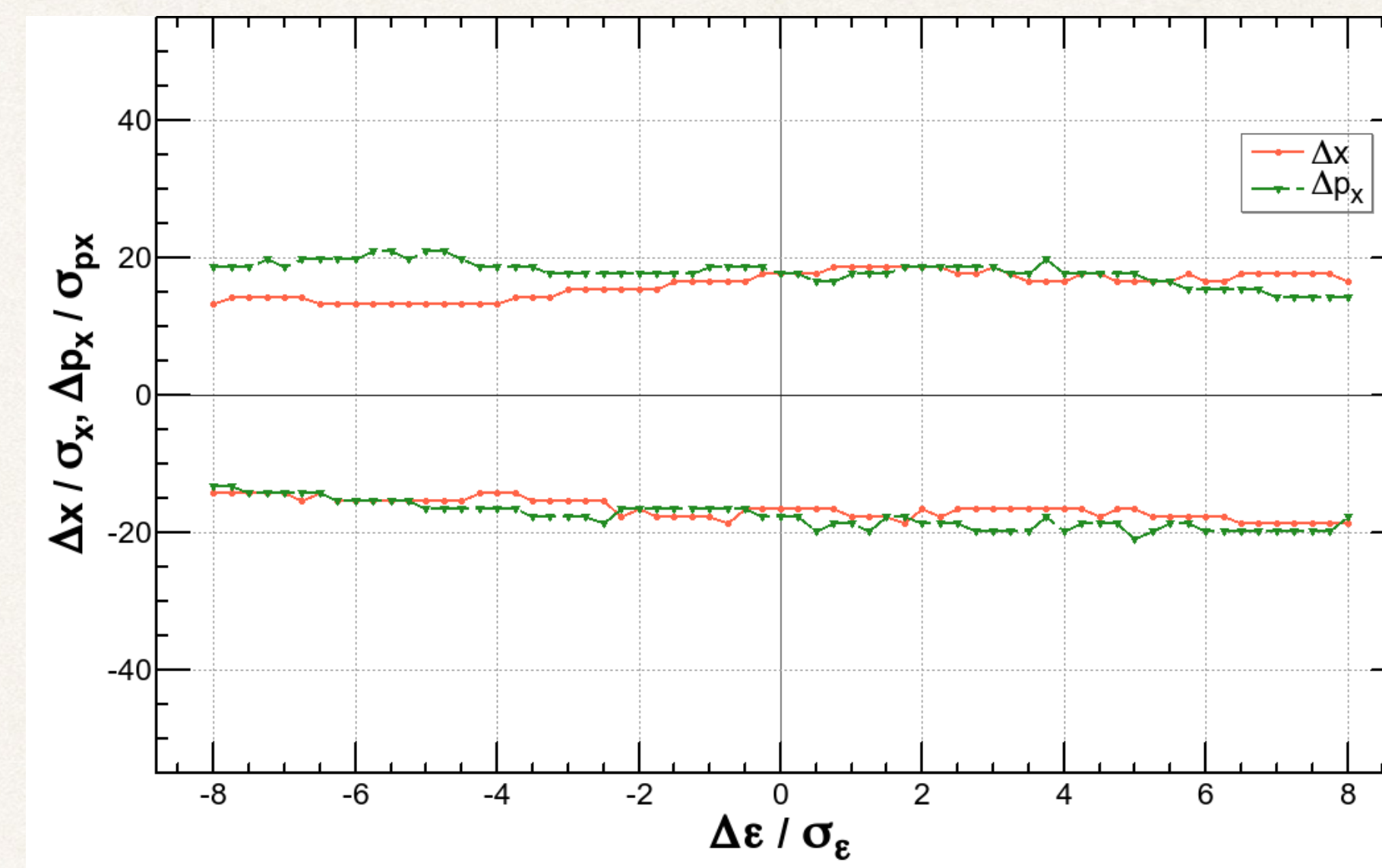
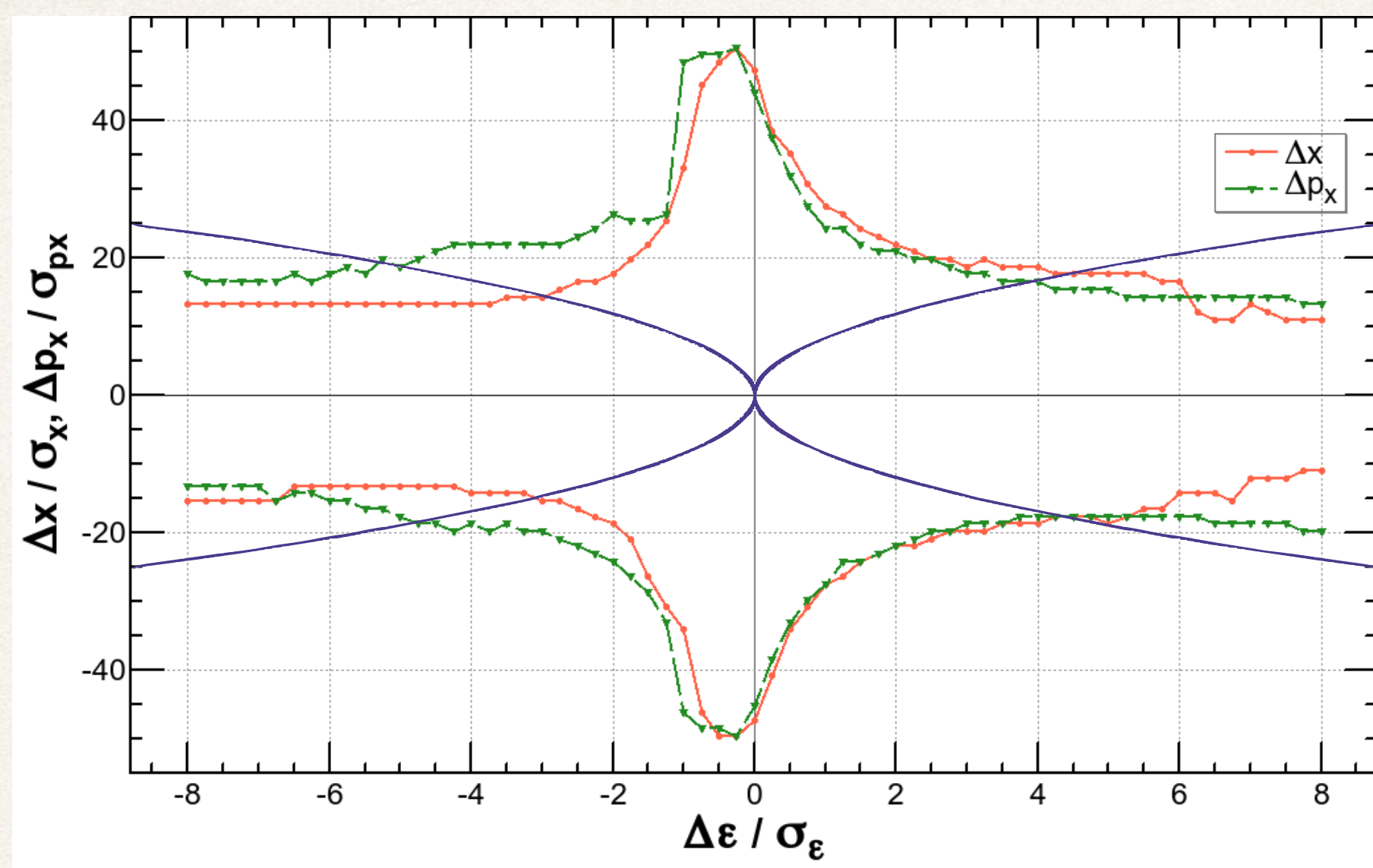
$$\Delta p = \frac{\Delta p_1}{2\pi\nu_s} \exp(-\alpha_z/4\nu_s) = \frac{\alpha_z}{\pi\nu_s J_z} R_Q n^2 \epsilon_x \exp(-\alpha_z/4\nu_s) ,$$

$$R_Q = \frac{2\sqrt{2}}{\theta_c^2} \left(\frac{\sqrt{2} + 1}{l_{QF}} + \frac{\sqrt{2} - 1}{l_{QD}} \right) \quad (90^\circ \text{ FODO})$$

- ❖ Such particles can not stay on momentum: reduction of the dynamic aperture.

Synchrotron radiation in quadrupoles (cont'd)

$E = 175 \text{ GeV}, \beta_{x,y} = (1 \text{ m}, 2 \text{ mm})$

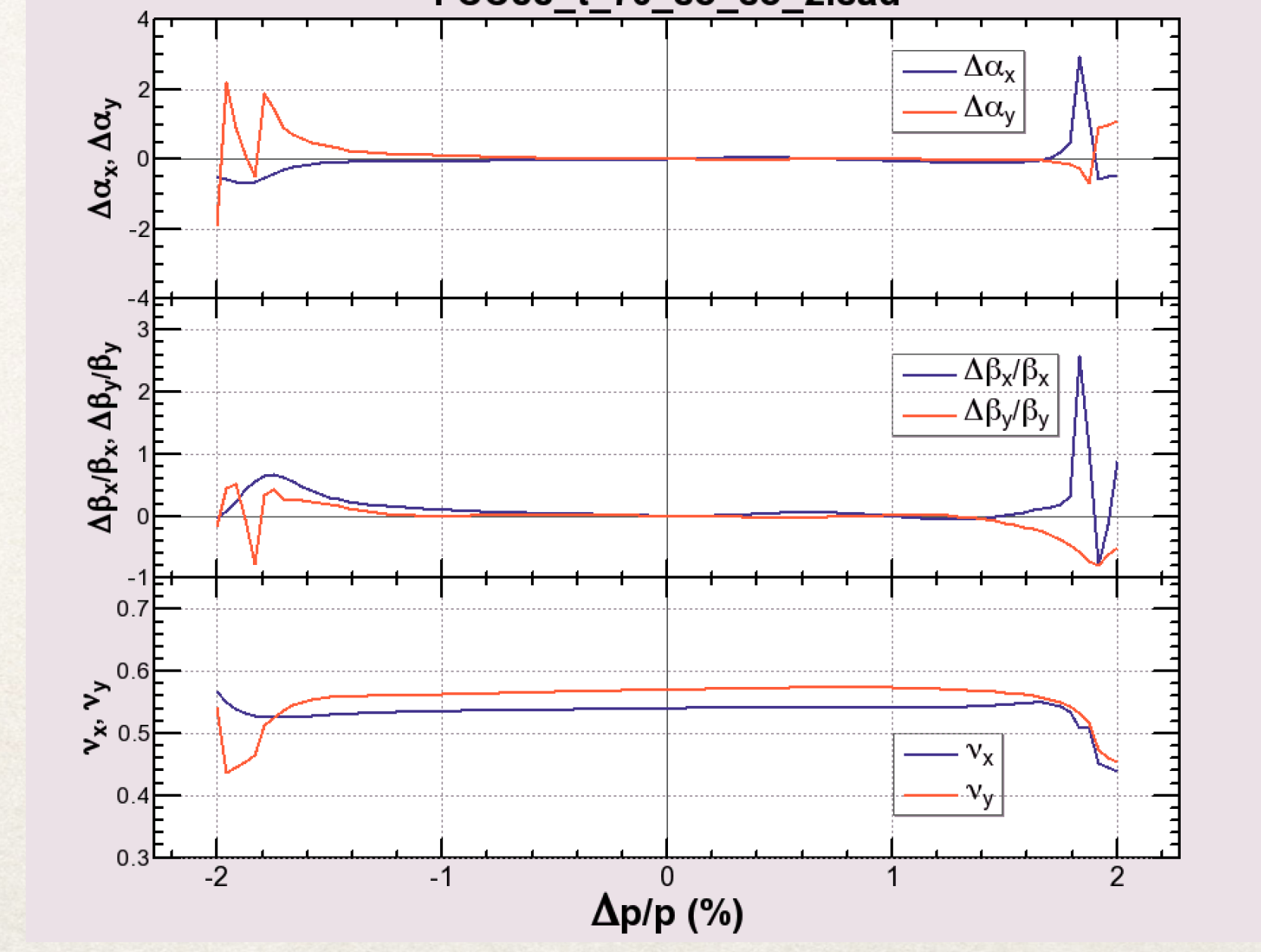
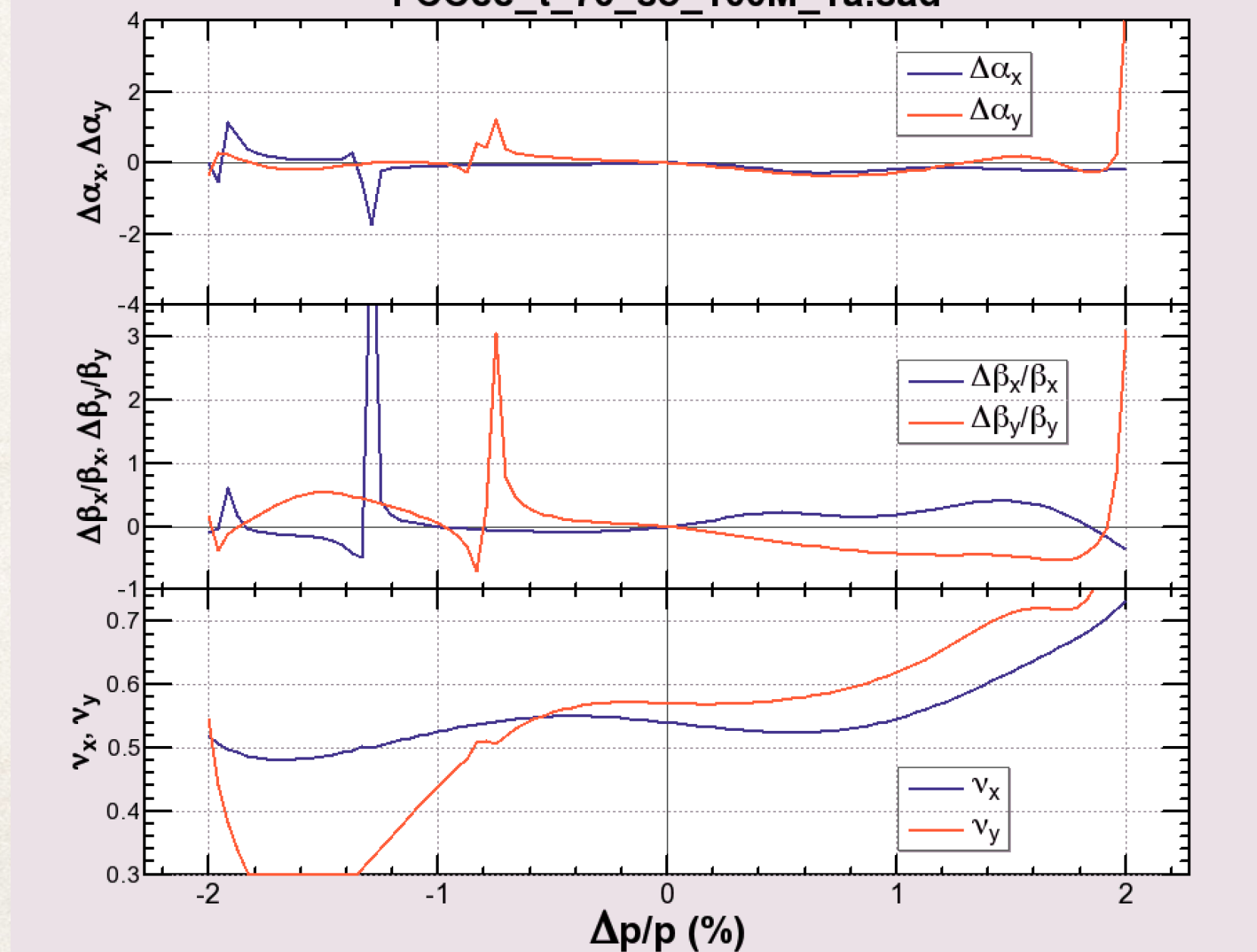
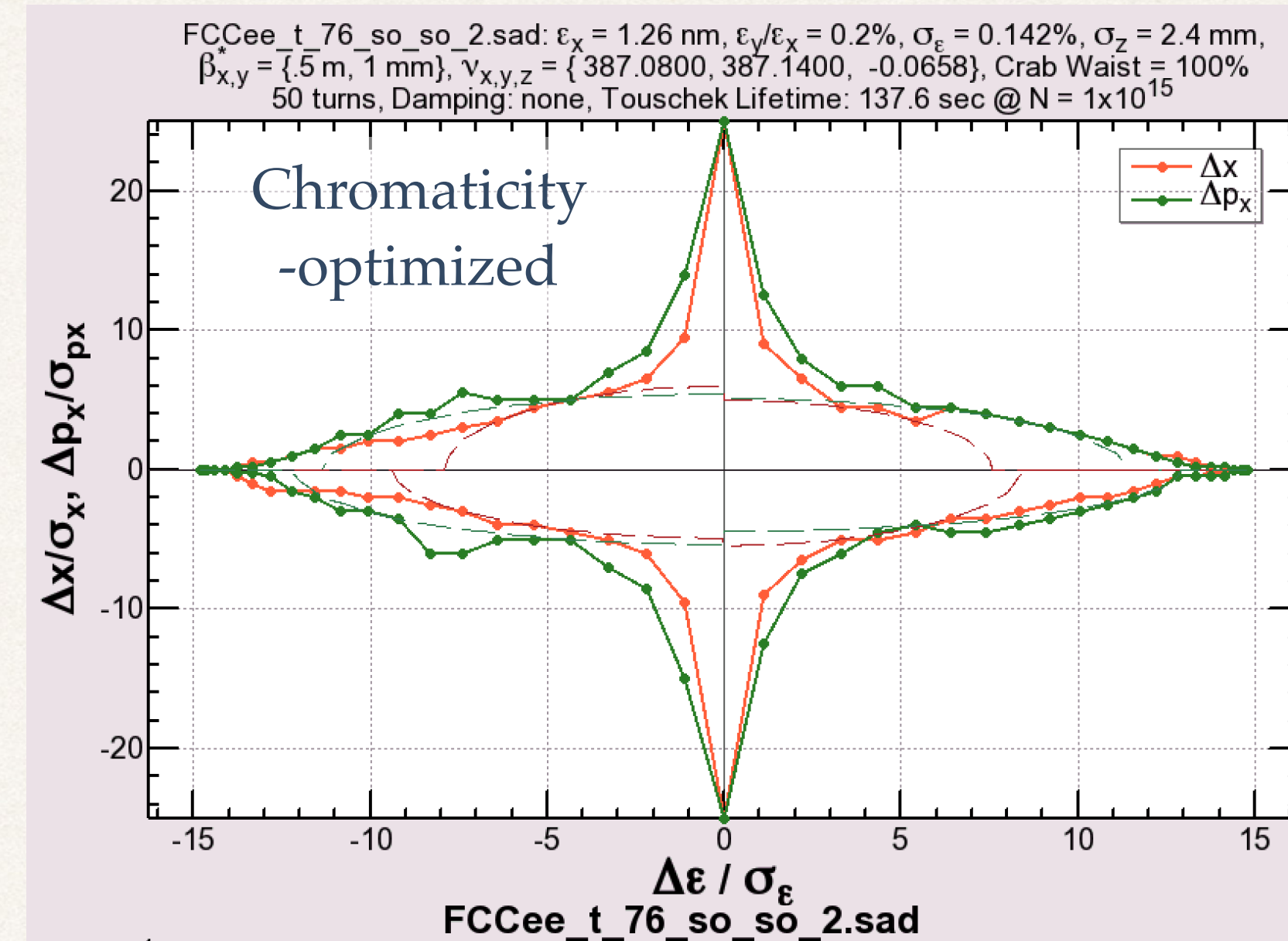
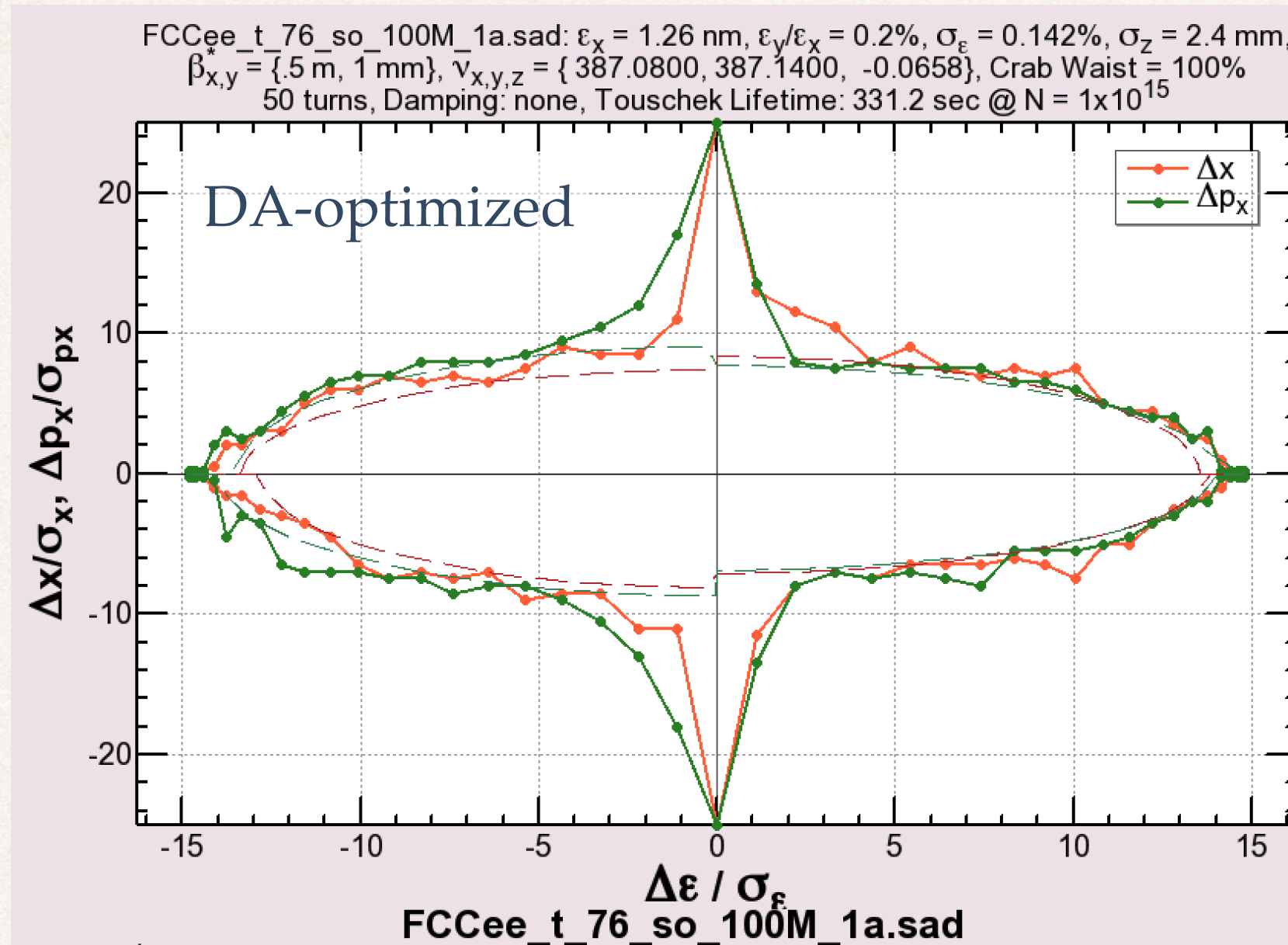


- ❖ The dynamic aperture without radiation loss in quadrupoles (left) has a sharp peak at on momentum.
- ❖ The peak is destroyed if the radiation in quads is turned on (right).
- ❖ The parabolas on the left show the amplitude of the synchrotron motion due to the radiation in the quadrupole. For a given transverse amplitude, if the parabola is beyond the DA, the particle with that amplitude will be lost.

Less chromaticity \neq better dynamic aperture



$\beta^*_{x,y} = (0.5 \text{ m}, 1 \text{ mm}), \text{ no radiation damping}$

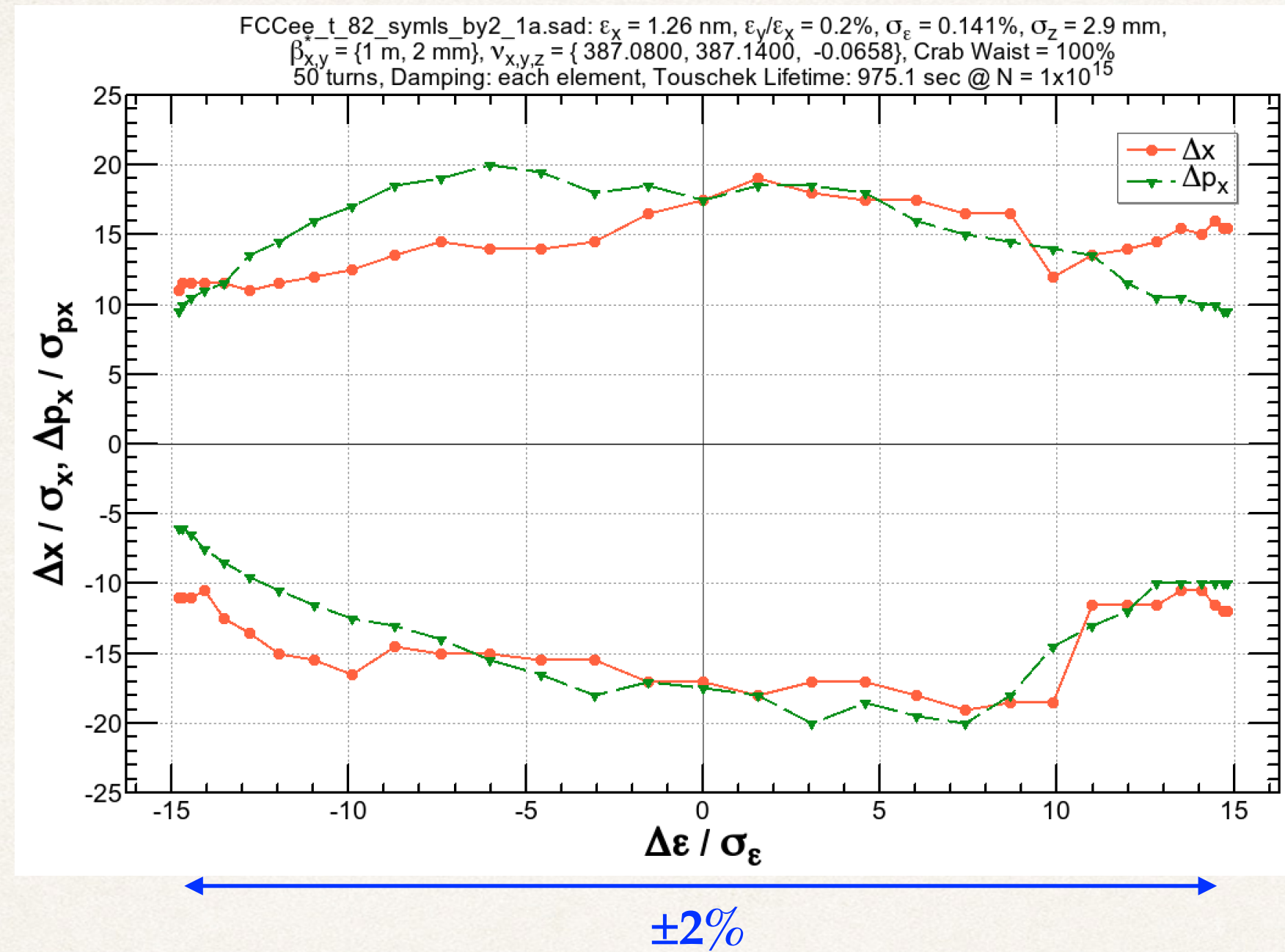


Effect of Radiation Fluctuation

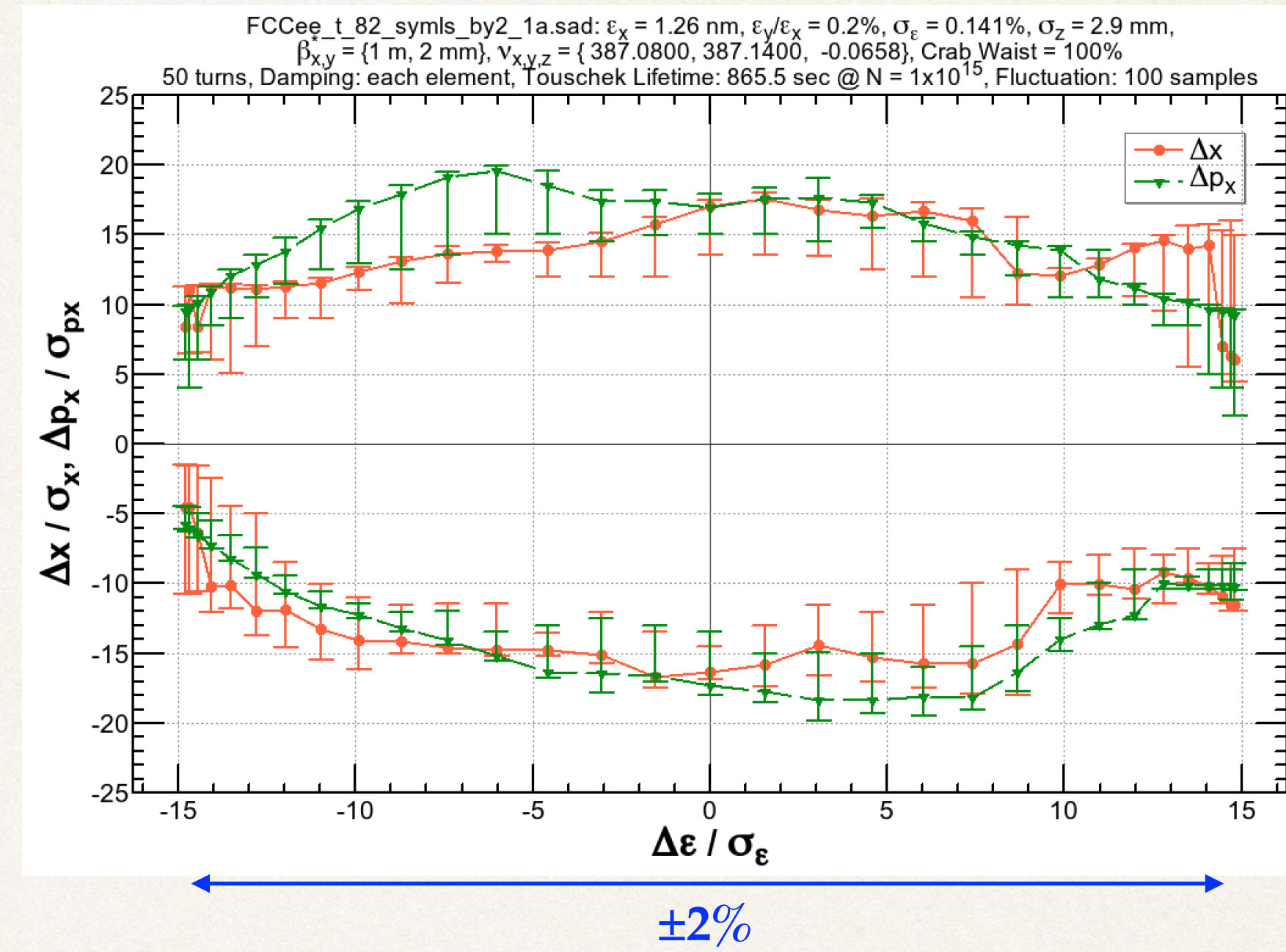


$E = 175 \text{ GeV}, \beta_{x,y} = (1 \text{ m}, 2 \text{ mm})$

Radiation damping only



Radiation damping + fluctuation



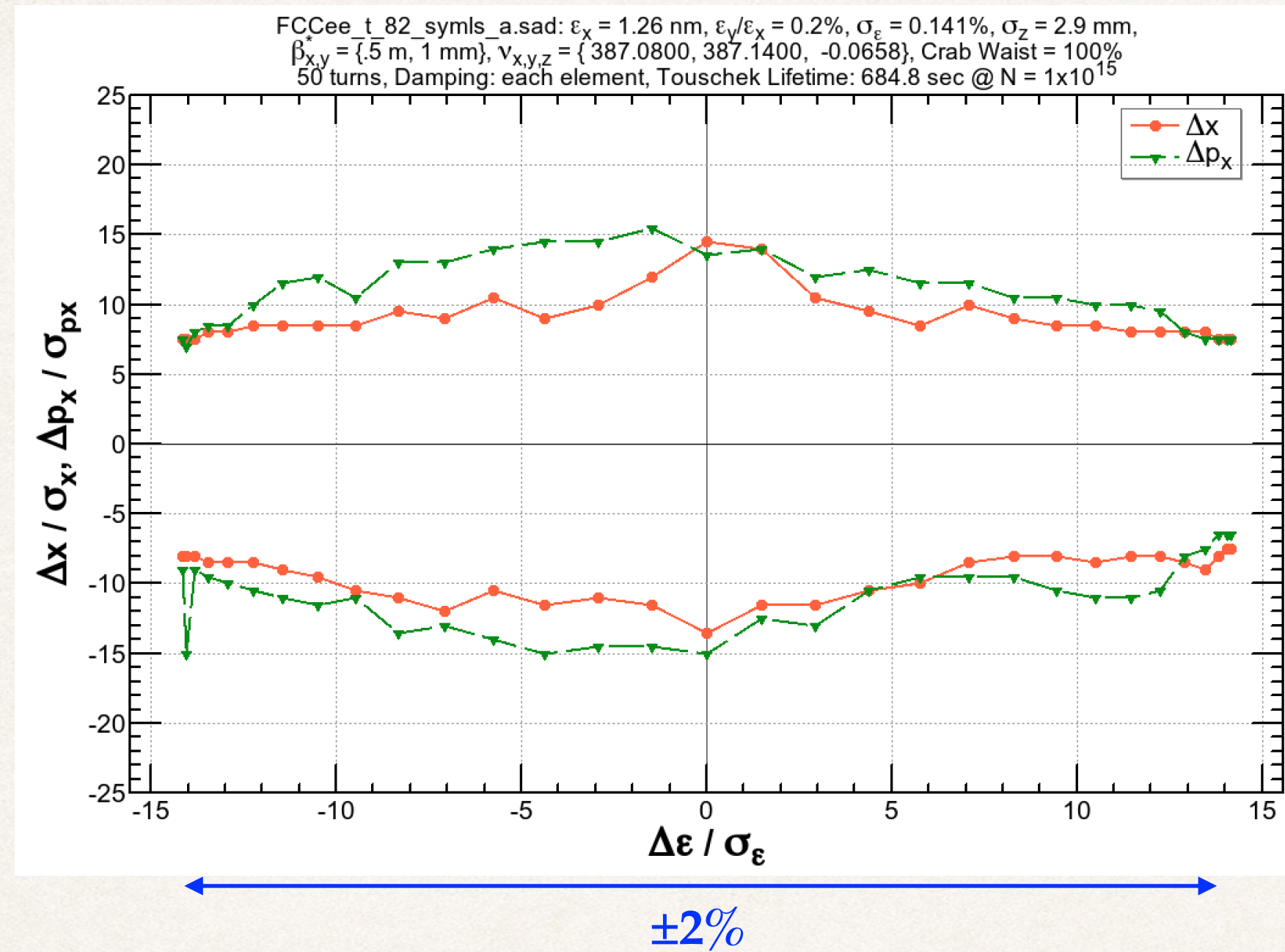
- (Right figure) 100 samples are taken to evaluate the dynamic aperture with radiation fluctuation.
 - Within the lines: particles survive for 75% of the samples.
 - Error bars correspond to the range of survival between 50% and 100% of the samples.
- It may reasonable that the 50% loss corresponds to the original aperture.
- The thickness between 50% and 100% survival can be attributed to the fractal structure of unstable orbits or resonances in the phase space.

Effect of Radiation Fluctuation (2)

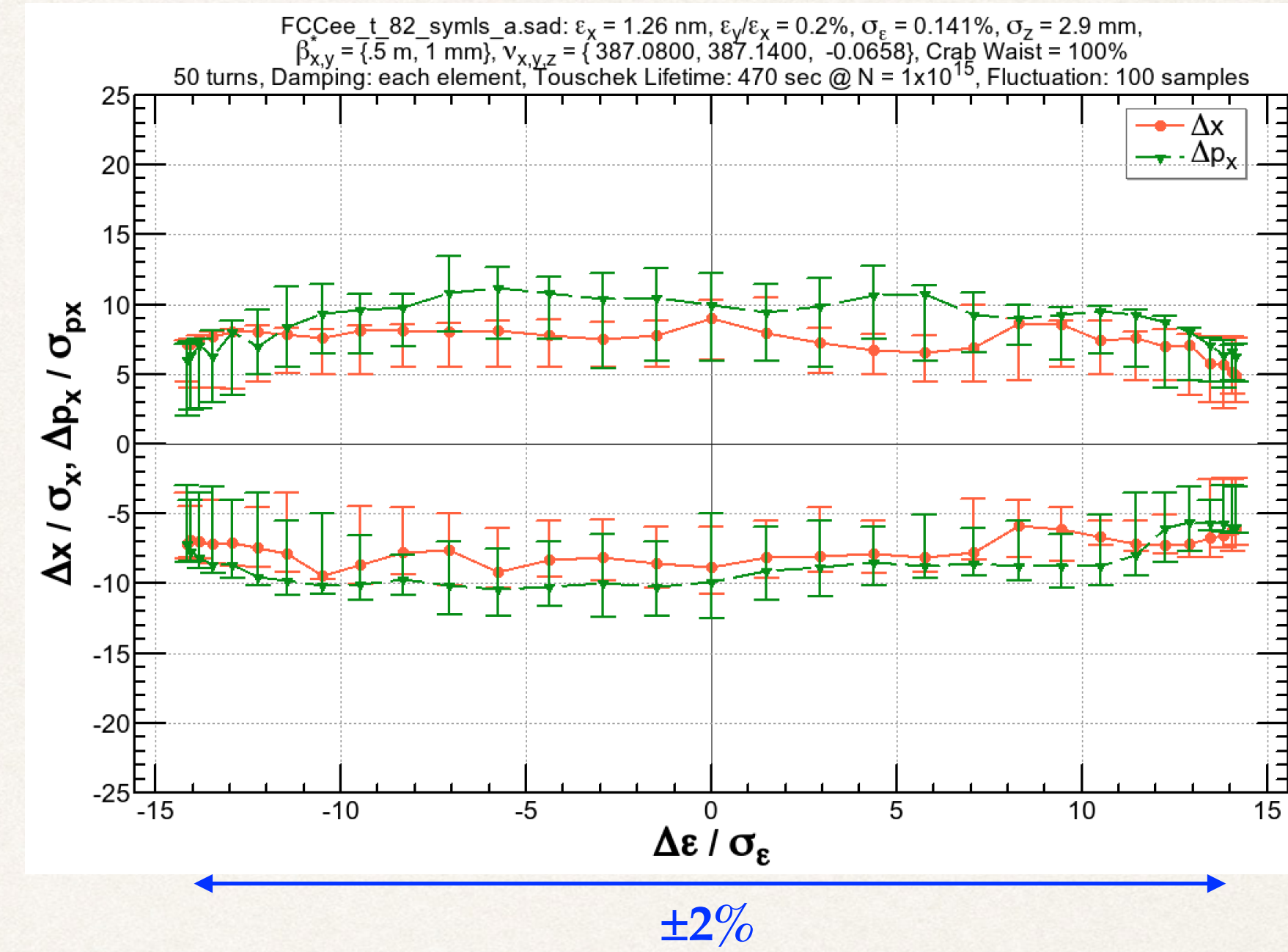


$E = 175 \text{ GeV}, \beta_{x,y} = (0.5 \text{ m}, 1 \text{ mm})$

Radiation damping only



Radiation damping + fluctuation



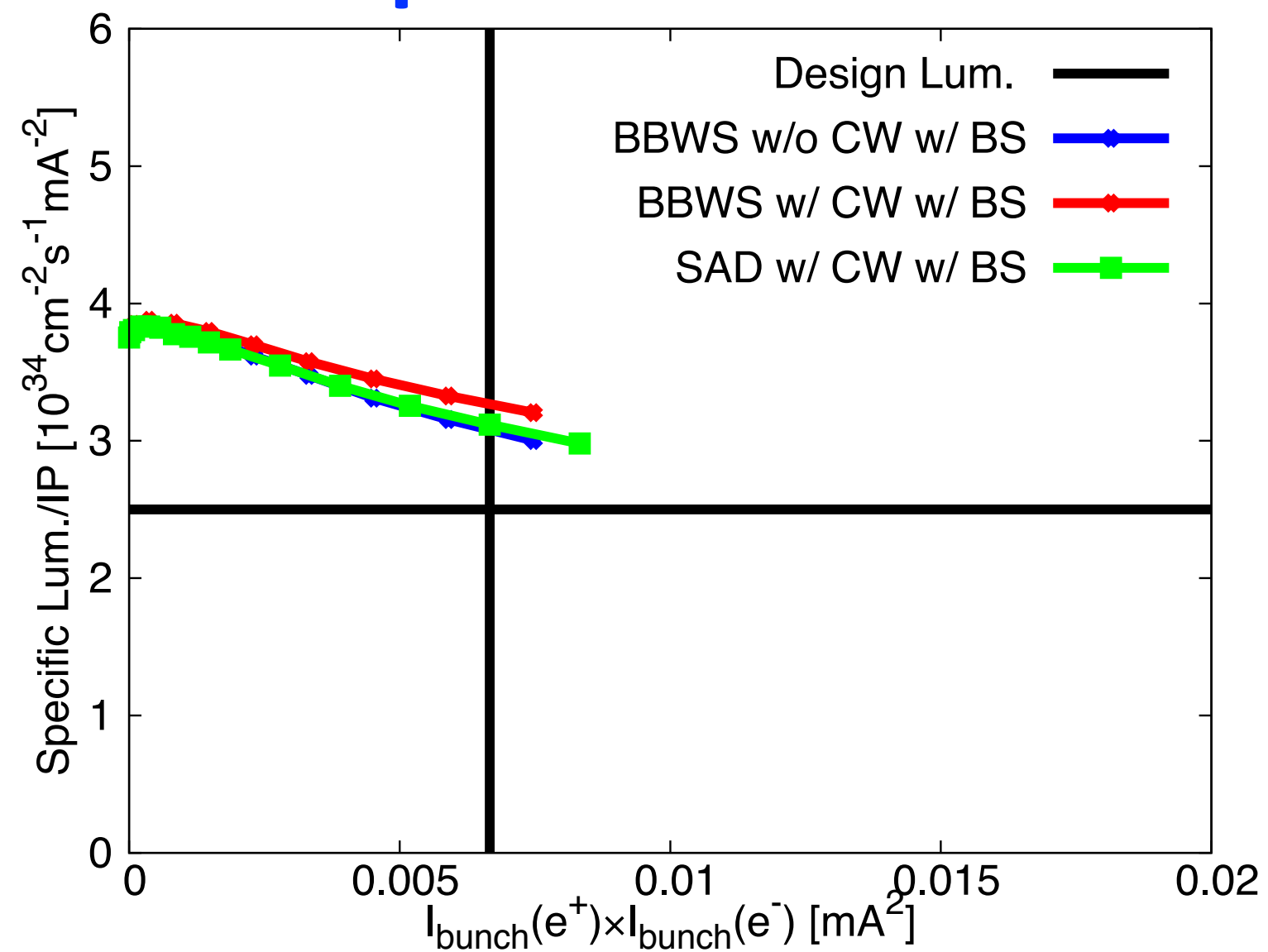
- (Right figure) 100 samples are taken to evaluate the dynamic aperture with radiation fluctuation.
 - Within the lines: particles survive for 75% of the samples.
 - Error bars correspond to the range of survival between 50% and 100% of the samples.
- The reduction of the 100% survival aperture is more significant than $\beta_{x,y} = (2 \text{ m}, 2 \text{ mm})$. However, it still maintains $\pm 2\%$ momentum acceptance.

2. Simulations: SAD: tt_{bar}

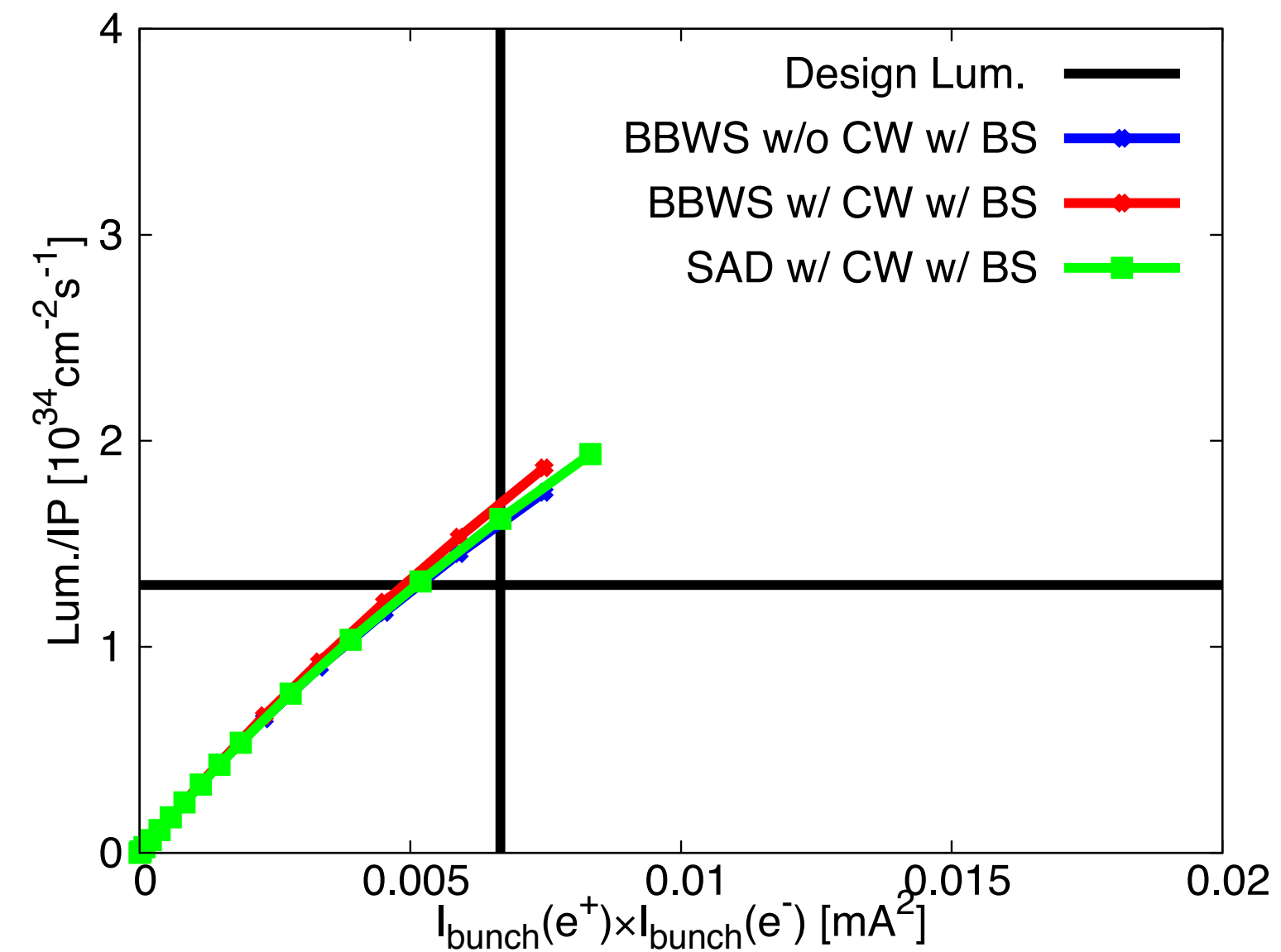
► Luminosity for $\beta_x^* = 0.5\text{m}$, $\beta_y^* = 1\text{mm}$

- Lattice ver. FCCee_t_65_26
- Small gain from CW
- Small loss (order of a few percents) due to BB+LN
- Allow lower beam current to achieve the same lum.

Specific lum.



Total lum.



FCC-ee talks later:
 Emittance tuning: S. Aumon
 Tolerance/misalignment: S. Sinyatkin

Low Emittance Tuning Simulation

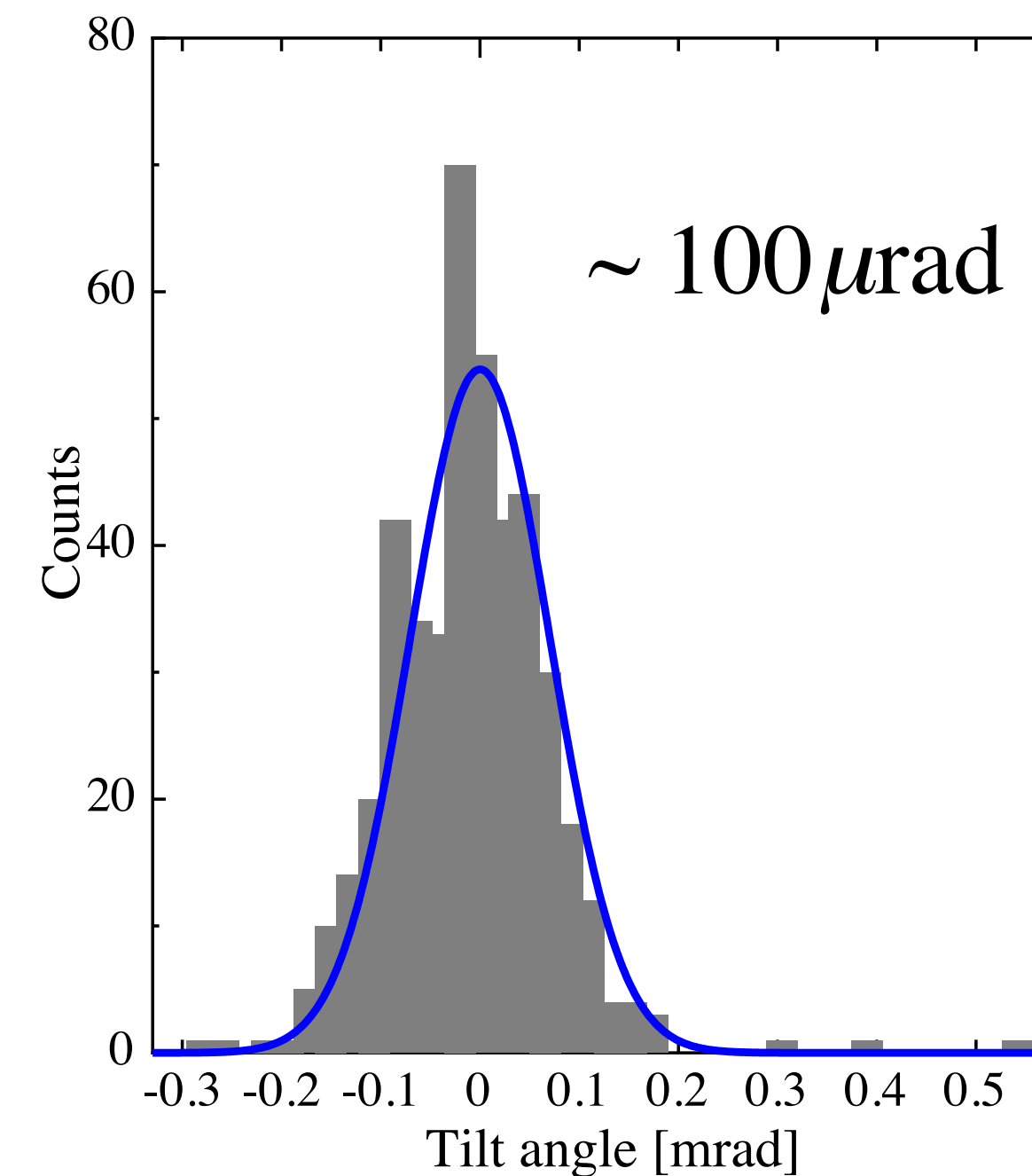
- Assumed machine errors
 - All errors are static in time.
 - Bearing KEKB alignment level in mind.
 - All errors are Gaussian distributed.

	$\sigma_x = \sigma_y$ [μm]	σ_θ [μrad]	$\Delta K/K$
Normal Quad	100	100	2.5×10^{-4}
Sext	100	100	2.5×10^{-4}
Bend	0	100	0
QCS	100	0	0

BPM jitter : $2 \mu\text{m}$

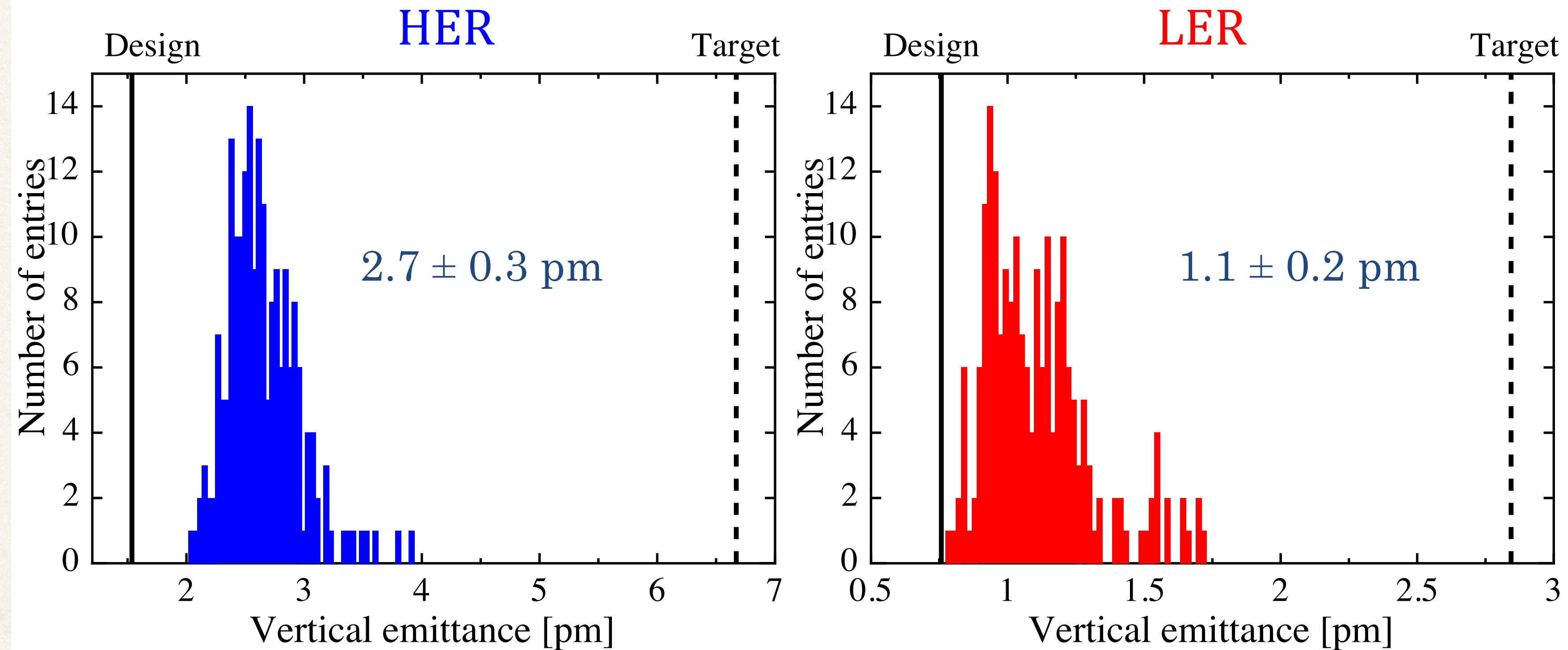
BPM tilt : 10 mrad

Quadrupole tilt angle measurement at KEKB



Vertical Emittance

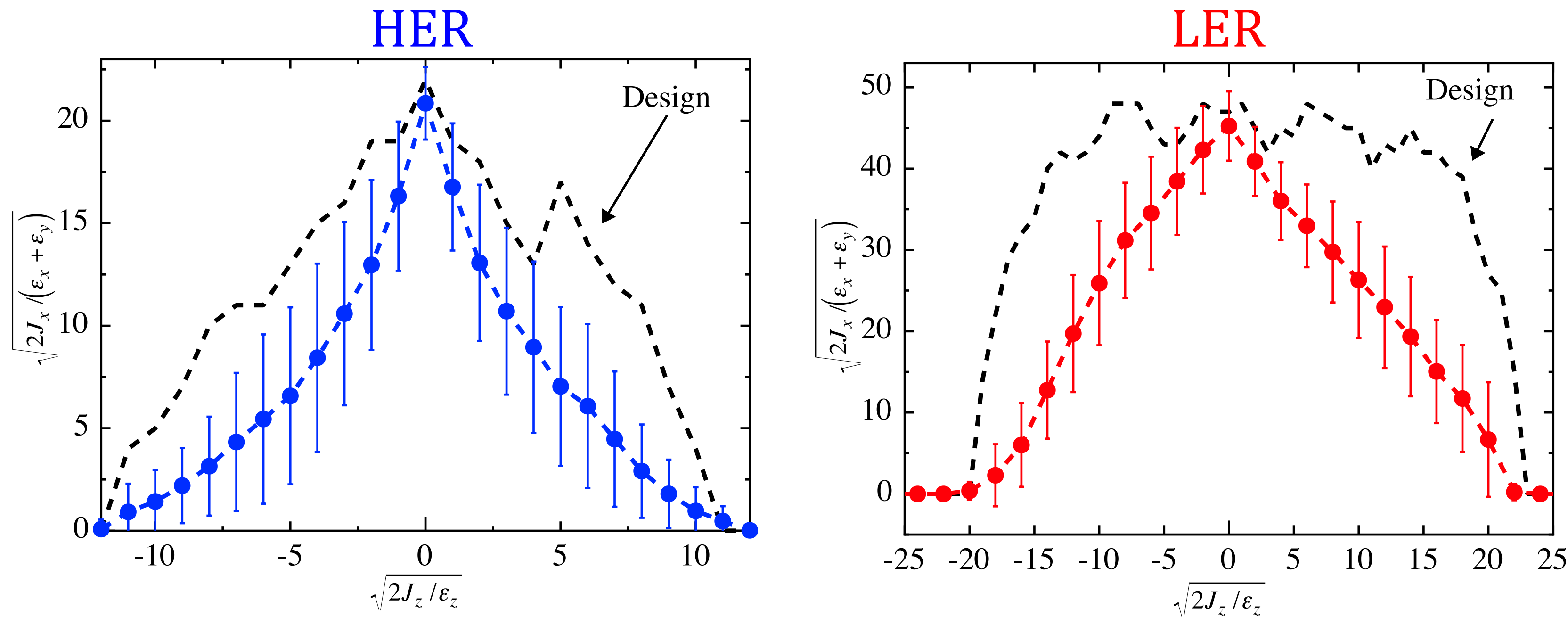
200 samples



- Vertical emittance is well below the target in both rings.

Dynamic Aperture

200 samples

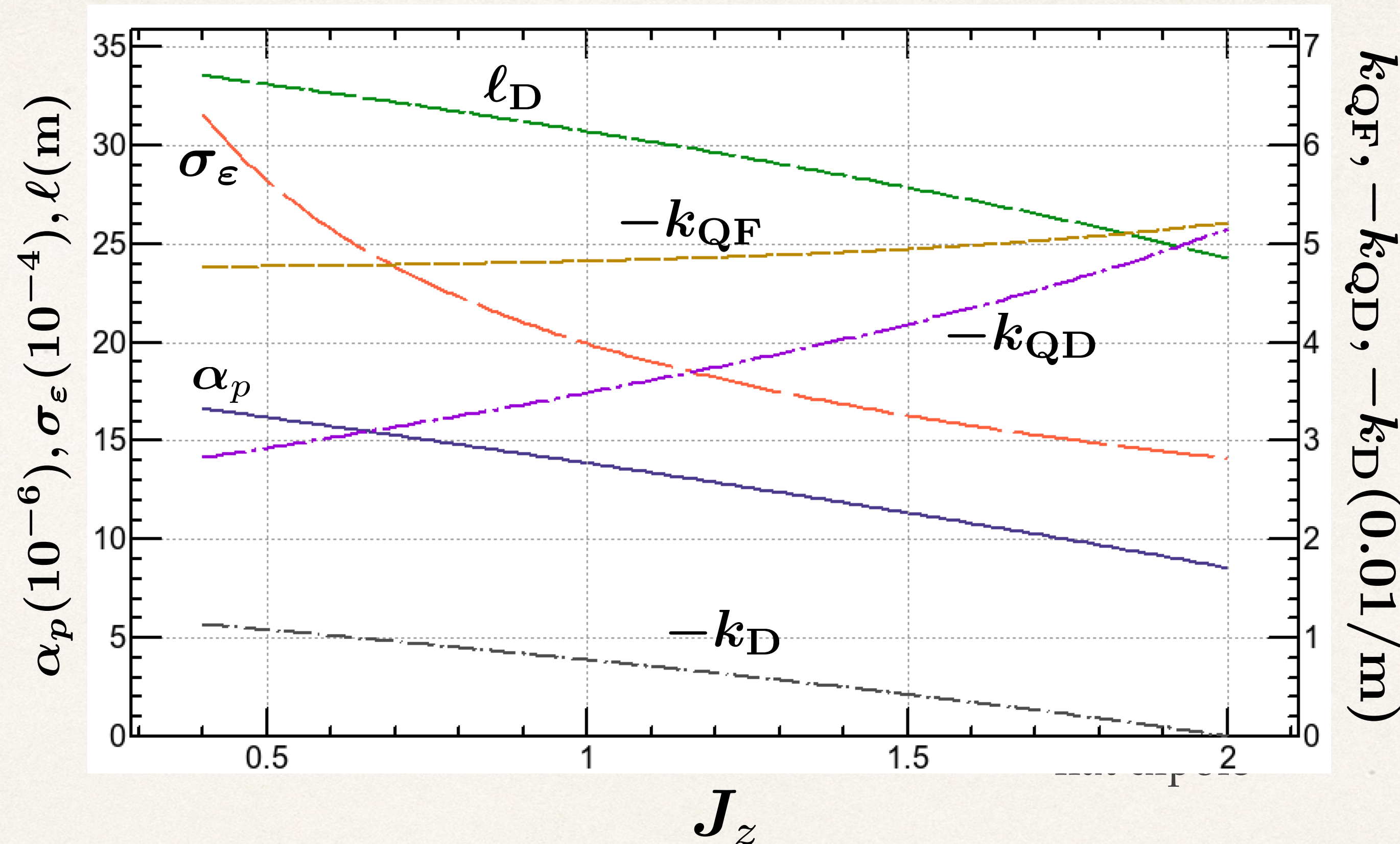


- On-momentum DA is recovered.
- Off-momentum DA is not resumed.
- Need off-momentum optics correction. (under investigation)
 - Reoptimization strategy of sextupole is not trivial because it affects vertical emittance also.

A possibility of combined function dipole in the arc



$$\varepsilon_x = 1.25 \text{ nm @ 175 GeV}$$



A negative field gradient in the main dipole of the unit cell provides:

- longer cell length for a given emittance / better packing factor
- larger momentum compaction (longer bunch length for a same RF voltage)
- larger energy spread (thus not good for polarization, esp. at WW).
- larger dispersion
- weaker sextupoles

Suggested by E. Levechev